ADDIS ABABA UNIVERSITY SCHOOL OF GRADUATE STUDIES

INVESTIGATION ON CAUSES OF LAND SLIDE IN THE BLUE NILE BASIN (GOHATSION-DEJEN ROAD AS A CASE STUDY)

A Thesis Submitted to the School of Graduate Studies of Addis Ababa University in Partial Fulfillment of the Requirement for the Degree of Master of Science in Civil Engineering

ADVISOR: MESSELE HAILE (Assist.Prof)

CO-ADVISOR: TAKASHI HARA (Mr.)

BY: ADANE AMARE

July 2013

ADDIS ABABA UNIVERSITY SCHOOL OF GRADUATE STUDIES

INVESTIGATION ON CAUSES OF LAND SLIDE IN THE BLUE NILE BASIN (GOHATSION-DEJEN ROAD AS A CASE STUDY)

ADDIS ABABA UNIVERSTY

INSTITUTE OF TECHNOLOGY

BY: ADANE AMARE BITEW

ADVISOR: MESSELE HAILE (Assist.Prof)

CO-ADVISOR: TAKASHI HARA (Mr.)

INVESTIGATION ON CAUSES OF LAND SLIDE IN THE BLUE NILE BASIN (GOHATSION-DEJEN ROAD AS A CASE STUDY)

BY

ADANE AMARE BITEW

A thesis submitted in partial fulfillment of the requirement for the degree of Master of Science in Civil engineering [Geotechnical Engineering]

Addis Ababa University Institute of Technology

Approved by Board of Examiners

1.	**Messele Haile (Assist.Prof)**	_____	_____
	Advisor	Signature	Date
2.	_____	_____	_____
	External Examiner	Signature	Date
3.	_____	_____	_____
	Internal Examiner	Signature	Date
4.	_____	_____	_____
	Chairman	Signature	Date

ACKNOWLEDGMENTS

Great appreciation is due to Dr. Messele Haile and Mr. Takashi Hara my advisor and co-advisor respectively who shared with me their long experience and deep knowledge on the field of Geo-technical Engineering and Engineering Geology starting from the selection of the thesis title to the repeated consultations they made by allocating time to the finalization of this thesis.

My acknowledgment also goes to the Ethiopian Road Authority of Alem Gena District (who supported me by providing relevant data and financial support), Addis Ababa university, ERA Highway Research Department especially Mr.Takashi HARA who supplied me with the necessary information required, for the thesis work concerning the Gohatsion-Dejen Road project. The materials he has provided includes the detail explanation for in situ test instrumentation adopted on the project and other people who helped me in material as well as by sharing their experience which greatly contributed to the finalization of this thesis work.

TABLE OF CONTENT

LIST OF TABLES

LIST OF FIGURES

ABBREVIATIONS, ACRONYMS AND SYMBOLS

JICA – Japan International Cooperation Agency

ERA _ Ethiopian Road Authority

GSE_ Geological Survey of Ethiopia

L/S – Landslide

ST – Station (Measured from Gohatsion in Km)

B05-11 = B- Borehole Drilling

= The 1st number shows station distance in Km from Gohatsion

= The 2nd number shows drilling borehole number

Fs - safety factor,

c' - cohesion,

ϕ' - shear resistance angle,

γ' - wet unit weight (wet density)

u - pore water pressure

α: inclination angle of slip surface

ABSTRACT

The Blue Nile basin is severely affected by slope failures. The characteristics of its deep gorges and rugged valley walls composed of assortment of different geological materials makes the area legitimate for study. The stretch of main road 3 that passes through the Abay Gorge steeply climbs nearly 1,500 meters from the Abay River to the plateau in 40 kilometer distance. It is plagued by landslides in the rainy season, especially from June to September, Some of the failure areas are up to two kilometers wide, putting into jeopardy this vital link road.

Work was commenced with the conception of site reconnaissance and the study area in particular provides long cliffs of sandstone, limestone, and gypsum intercalated with relatively soft units of mudstone, shale, and marl. From satellite view also the surface anomalies of the five selected priority sites shows multi block land slide mass in each station.

Interpretation and analysis of detailed borehole investigation data and different monitoring devices output data is carried out in order to grasp movements and to find the main slip surface and the geological structure. Using inverse analysis for the representative landslide blocks the shear strength parameters of the most probable slip surfaces were determined.

Finally, the study led to the conclusion that the landslides are triggered by rising ground water in the rainy season. The rising of ground water table is due to infiltration of surface run off. Therefore, controlling of the infiltration process using different remedial techniques will minimize the sub surface problem.

1. INTRODUCTION

1.1.General

Throughout history, natural hazards have caused a heavy toll and destruction, impacted the environment, and disrupted development in many countries. Engineering works and earth processes interact in two distinct and important ways:

1) Natural processes influence how structural and other development occurs. The suitability of locations for development, their design, and cost are related to the effect of natural processes.
2) Structures and development can alter natural processes, creating changes that may be undesirable. E.g. changes in stable soil mass due to road cut

The geologist develops information on earth processes that influences how development occurs and how it can avoid inducing undesirable changes in earth processes. Where this input is lacking, engineering works are likely to cost more than necessary, functions below expected optimum, or even may fail. This is not to say information on geologic factors is the only important consideration in locating, design and construction of engineering works. [Source: Tenalem, 2009]

There is an abundance of benefits for engineering works to be derived from a full understanding of geologic processes; thus geologic data cannot be safely ignored. Forecasting, or predicting, the interaction of engineering works with earth processes is necessary for safety and reliability. The point of forecasting is to ensure that the risk is at an acceptable level. This involves two activities. One is the measurement of risk. The other is judging whether that degree of risk is acceptable. [Source: Tenalem, 2009]

The engineering geologist uses existing information to predict expected risk. Long-term prediction can be a source of conflict between the Engineering Geologist and the Engineer concerned with addressing landslide and other earth processes that influence a project. The engineering geologist will define the essential conditions and characteristics of the process in largely qualitative terms. The engineer will often view this with some skepticism, wishing to have a quantitatively defined model.

Once the hazard is defined, vulnerability can be determined for the proposed or existing project. Risk is the product of the hazard and vulnerability. Specific remedies can be proposed to reduce or eliminate risk. These remedies result in different levels of risk that are then judged as to acceptability in the decision-making process.

Remedial measures generally involve:

(i) Controlling where and what types of development may occur,

(ii) Engineering-design changes, and

(iii) Distributing the losses that may result.

Each of the earth processes can pose a problem to engineering works. This ranges from the dramatic effects of earthquake caused ground motion to the subtle stresses of swelling soils. Successfully avoiding major problems will always require accommodating rather than ignoring these natural forces.

1.2. Landslides

In general, landslides are defined as the product of the rupture in the topographic surface equilibrium. Landslides can occur on any type of rock and soil and result in a movement of soil and bedrock, artificially accumulated material (such as embankments, earth dams, levees, etc.) or material that was just involved in the sliding processes. The terms *slope movement* or *failure* and *landslide* when used in a generic sense are generally equivalent in meaning. [Source: Tenalem, 2009]

The size of landslides is variable from detachments of a few cubic meters to movement of hundreds of millions of cubic meter, which may affect the entire side of a mountain or a city. In some areas the process of land slide may be so relevant to be responsible for the main morphological features of the landscape. We can therefore consider landslides as one of the major agents shaping the Earth surface.

Landslides inflict economic losses and casualties in many areas and on a frequent basis. Too often, they coincide with other natural disasters such as earthquakes, floods, or volcanic eruptions. Landslides cause damage in a number of ways. One of the most obvious is by tilting, shearing, and pulling apart of rock and soil. These results in damage to structures constructed of rock or soil and to those made of non-earth materials placed on a foundation of soil or rock. Road pavements warped and cracked by landslide movement is no longer suitable for use.

Likewise, few buildings remain fully functional and safe after their foundation is sheared by landslide movement. Impact forces, ranging from individual boulders to a debris avalanche mass, shatter or displace structures and structural elements. Debris from landslides can bury or partially bury facilities and impair their use. The blocking of roads by landslide debris is an obvious example. Damming of streams by landslides can result in later catastrophic flooding, another form of damage arising from slope movement. [Source: Tenalem, 2009]

1.2.1. Classification of landslides

Classification of landslides provides a means for comparing landslide phenomena to determine underlying causes and to identify common characteristics. Several landslide classification, based on both their genetic and morphologic features, have been proposed but attention will be focused on the main processes originating a landslide and its morphological characteristics.

A landslide involves vertical and horizontal movement of soil, rock, or some combination of the two under the influence of gravity. These slope movements are usually categorized as being either falls, topples, slides, spreads, or flows. Table 1.1 presents simplified classification of slope movements on the basis of the type of movement and nature of the materials being displaced.

Basically landslides are associated to three main types of movement; material that *falls, slides, flows* or is subjected to a combination of these types of movements. A fall or a *rock fall* is the rocky material falls from almost vertical or very steep slopes and the material moves without a continuous contact with the slope and then collapses, jump and rolls down.

A sliding occurs, instead, when an earth mass moves along a well defined shear surface and the detached material moves in an apparently unitary movement. The shear surface may be planar (more common) or concave. In the first case a slide, in the second a slump (or rotational landslide*) will occur*. When the sliding surface is just an inclined plane the moving mass may maintain its orientation and integrity or it can break up during the movement down slope. Slumps are characterized by an upward concave shear surface and by the fact that the sliding material maintains some compactness [Source: Tenalem, 2009]

Table 1-1 Simplified classification of slope movements [Source: Tenalem, 2009]

Type	Rock	Debris	Soil
Fall	Rock fall	Debris fall	Soil fall
Topple	Rock topple	Debris topple	Soil topple
Slide (rotational)	Single (slump)	Single	Single
	Multiple	Multiple	Multiple
	Successive	Successive	Successive
Slide (translational)	Block slide	Block slide	Slab slide
Non-rotational			
Planar	Rockslide	Debris slide	Mudslide
Lateral spreading	Rock spreading	Debris spread	Soil(debris) spreading
Flow	Rock flow	Debris flow	Soil flow
Complex (with run-out or change of behavior down slope)	Rock avalanche	Flow slide	Slump-earth flow

When the material slides like a viscous mass we have landslides known as flows (earth flows, debris flows, mud flows, etc.). These landslides are always made up by a mixture of solid particles and water in different proportion, with the latter commonly relatively abundant; in fact, such events are typically a direct consequence of rainfalls of extreme intensity. The flows starts as partially unconfined mass movement but become more canalized at the base of the slope.

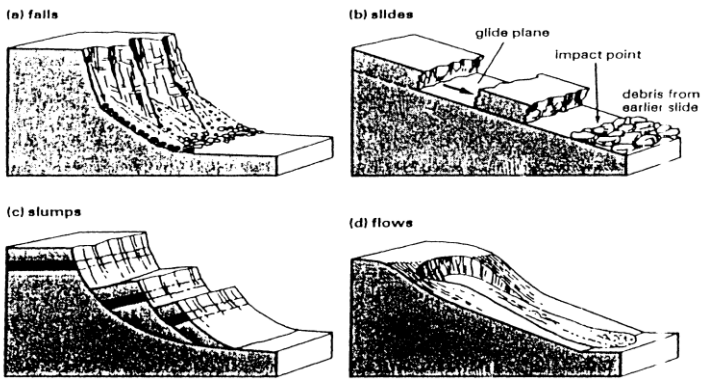

Figure 1-1 Principal mechanisms of movement in landslides. [Source: Tenalem, 2009]

Another type of mass movement, slightly different from slides but very common and important for its implication, is soil creep. The process of creeping may largely affect slope stability as well as produce a pushing action on retaining walls or other engineering structures. Soil creep is a particular process such that some stratified rocks, like clay, slate, grit, etc., have their layer margins bent in a down slope direction. Some of the causes of soil creep are:

- Alternation of heating and cooling phases in the soil
- Swelling and shrinkage in surface rocks
- Growth of ice wedges
- Alternation of aridity and humidity conditions in the soil
- Animal burrowing activity, and
- Earthquake shocks

All these effects produce some disturbance in the soil and, since gravity constantly and permanently works, soil particle are pushed down slope. Evidence of soil creep may be found on many soil-covered slopes. For example, it occurs in the form of small terracettes, down slope tilting of poles, curving down slope of trees and soil accumulation on the uphill side of retaining walls (Figure 1.2).

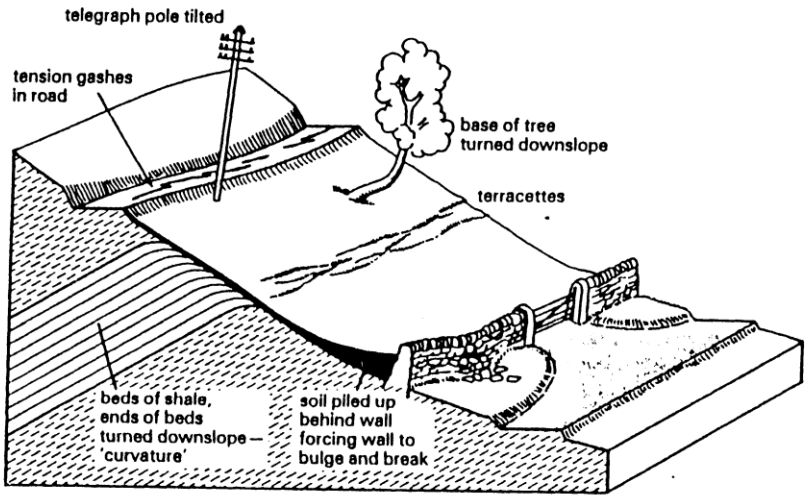

Figure 1-2 Soil creep and its main effects. [Source: Tenalem, 2009]

1.2.2. Features used for the recognition of landslides

Landslides can be active or inactive. There are certain features used for identification of landslides in the field, as listed below. [Source: Tenalem, 2009]

I. Active landslides

- Scarps and fractures possess sharp edges and open mode without secondary filling
- Main units show secondary fracture and pressure ridges
- Surfaces show polishing and striations, fresh appearance
- Deranged drainage and ponds
- No soil development and only fast-growing vegetation
- Considerable distinction between slide and non-slide areas in form, roughness, texture and vegetation cover
- Tilted vegetation and poles.

In sediments or loose deposits the following features help to identify active slide.

- Transverse ridges at the head; longitudinal ridges in track and concentric ridges at the toe running transverse to morphology
- Transverse and radial fractures at toe; radial shears at margins and crevasse-style cracking over breaks of slope
- Spreading at toe; valleys partially or wholly blocked and rivers diverted
- Materials locally derived but displaced below outcrop. Materials may include blocks of intact rock and stratigraphy can be repeated down slope.

II. Inactive landslides

- Scarps and fractures weathered and indistinct, cracks in filled
- No secondary failures of pressure ridges (often subdued)
- Surfaces weathered, vegetated
- Integrated drainage but may have irregular pattern and sudden in filled depressions.
- Soil cover and well vegetated or cultivated
- Difficult to distinguish margins and textures except on air photographs
- New growth on trees and vertical growth of post-slide trees

1.3. Background of the study

Road construction in the Blue Nile basin is largely determined by geological and geotechnical factors. The area is characterized by steep slopes and has a history of land slide. The geological formations ranges from Mesozoic sedimentary to Tertiary volcanic rocks making the stratigraphic makeup sensitive to deformation and failure. It has been noticed that road construction in these area face numerous problems and the causes of the problems are not investigated in depth. The roads constructed, in the Abbay River Gorge fail before their expected design life; in some cases after few months of completion.

The aim of this study is to investigate the causes of Slope failures of roads constructed in the Blue Nile basin, Ethiopia where The Gohatsion-Dejen road is the main part of this basin which is initially constructed by Italians in 1930's and again rehabilitated by Kajima Construction and continuously maintained by Ethiopian Road Authority. But it is still susceptible to many failures that make it interesting research area. Embankment slope instability, subsidence, hill side slope instability are among the major problems of the area.

Proper understanding of the causes of failure of roads may lead to proper remedial measures, designing methods and construction methods of roads appropriate for the area. This in turn will be helpful for the people using the road in particular and the whole of the country at large by reducing the maintenance and vehicle running costs.

The entire work was supported by data from the project for Developing Countermeasures against Landslides in the Abay River Gorge of JICA research team the study focuses on Gohatsion-Dejen rehabilitated road which is highly affected by the Land slide problem.

1.4.General information about the current situation of the problem

The study area, Gohatsion-Dejen transect, is one of the areas in the country where most slope instabilities are observed frequently. The area is part of the important main Addis Ababa-Debremarkos-BahirDar-Gondar-Metema-Sudan road and Gondar-Tigray road that connects north central and north western part of the country with the capital of Addis Ababa and port of Sudan.

Nearly all slope failures occur during rainy season. The frequent occurring landslides have damaged the road sections, bridges and farmlands almost every year. ERA has been looking for

remedies and had spent a lot of money for road maintenance every year. However, there has not been any permanent solution that can reduce or avoid the problem for various possible reasons. During the previous studies, rock fall, toppling, debris slide and rotational failure of colluvial material were some of the land instability manifestations identified in the area. However, the main causes of slope instability identified were the huge columnar jointed basalt, uncontrolled surface run off, joints of rocks, and the presence of marl and shale within hard rock's (Almaz and Tadesse, 1994).

From previous studies and personal observation to the area landslides and rock falls had damaged the road sections, bridges and farmlands. Consequently, the former route in the vicinity of the Washa Mikael church that goes from Gohatsion to Filkilik is abandoned due to landslide problem at the foundation area of the bridge. Due to this the Ethiopian Road Authority (ERA) was forced to reroute this road and built a new one. However, this route is also affected by landslide problems. Currently around five extrimly damaged sites which need priority for immediate solution is observed. These problems are severe particularly in the rainy season and it is very common to see slope failure events that hinder traffic movements in the rainy period.

Table 1-2 Five selected priority sites susceptible to landslide

No.	Location	Name	Station
1	0+800~1+100	L/S00	ST-1
2	4+800~5+500	L/S05	ST-05
3	21+850~22+100	L/S22	ST-22
4	27+500~27+900	L/S27	ST-27
5	28+000~28+700	L/S28	ST-28

These issues need to be well addressed and their spatial distribution clearly be indicated in order to design short-term and long-term solutions for the safety of the road, the population and the natural environment, as well.

As cited in JICA project, the surface anomalies of the five selected priority sites shows multi block land slide mass in each station

A) Surface anomalies of the landslide in L/SOO (ST.0+200 to 1 + 100)

In this area, several small landslide blocks which can be classified as shown in Figure 1.3 are observed.

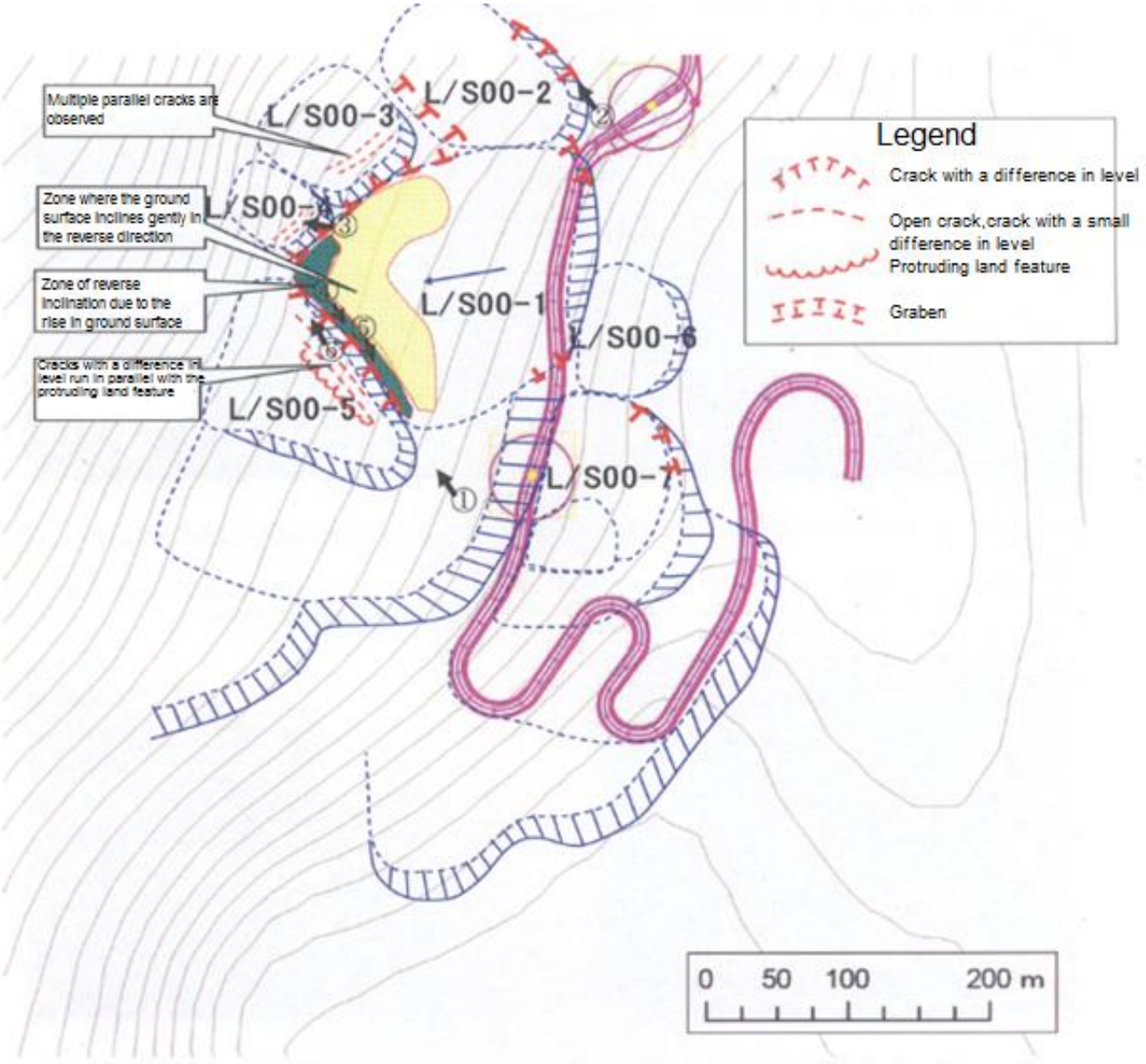

Figure 1-3 Surface anomalies in L/SOO (ST.0+200 to 1 + 100) (3)

Figure 1-4 View of the land slide at ST-1

B) Surface anomalies of the landslide in L/SO5 (ST.4+800 to 5 + 600)

In this area huge volume of debris flow from the hill side makes the road risky. The sliding in the hill side is aggravated by seeping water which may result from percolation of rain water. The retaining wall constructed is incapable to control sliding since the sliding covers large area and deep cited in its nature.

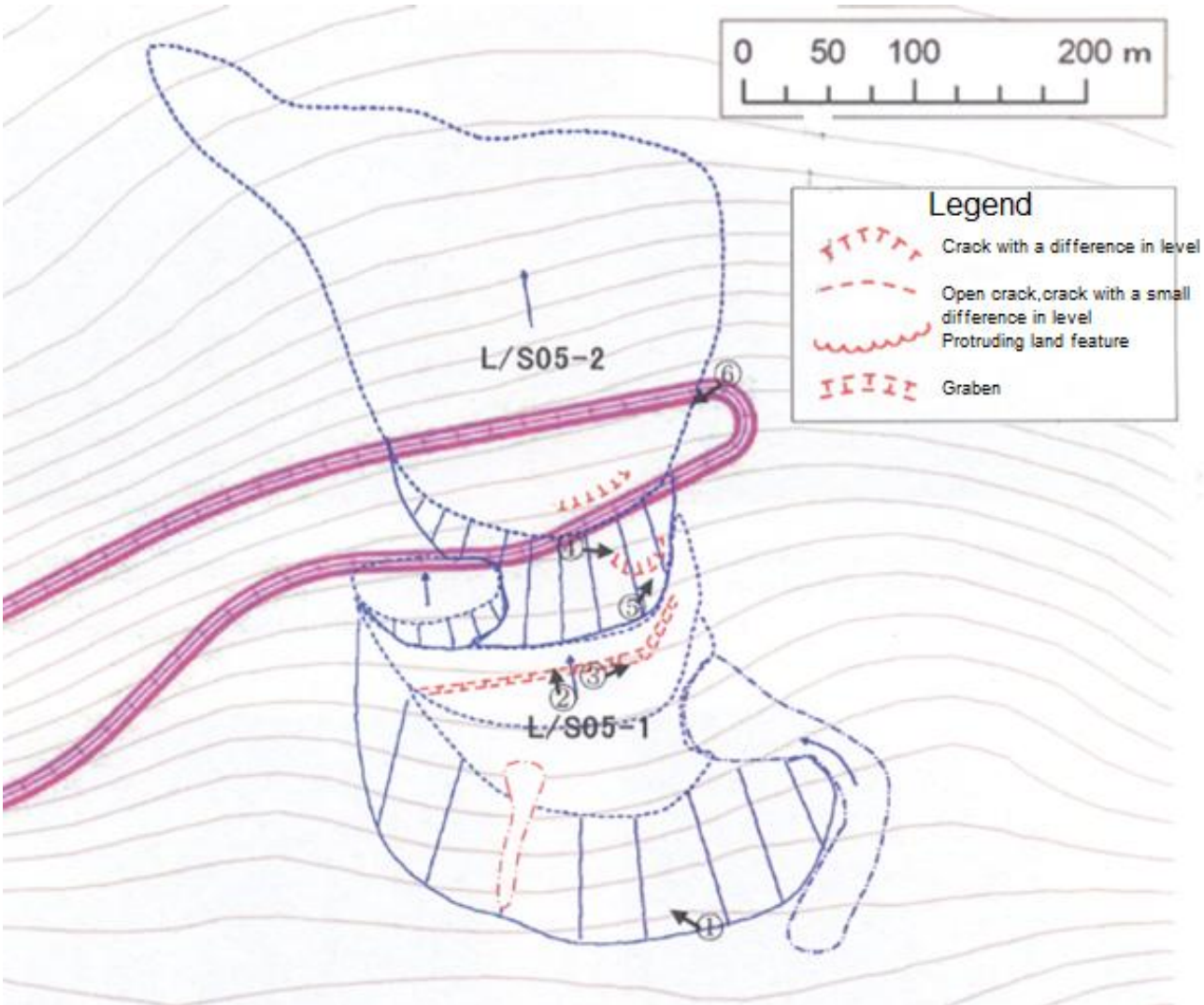

Figure 1-5 Surface anomalies in L/SO5 (ST.4+800 to 5 + 600) (3)

Figure 1-6 View of the land slide at ST-05

C) Surface anomalies of the landslide in L/S22 (ST.21+600 to 22 + 300)

In this area, there are two blocks that are believed to have been active in recent years; a predominant displacement is the L/S22-1. This block could have resulted from events that Occurred when the toe of the block has been eroded by surface water. The initial Italian Route is washed away by erosion and reroute by Kajima construction but still the new route is just on the sand stone cliff and it is under extreme damage state.

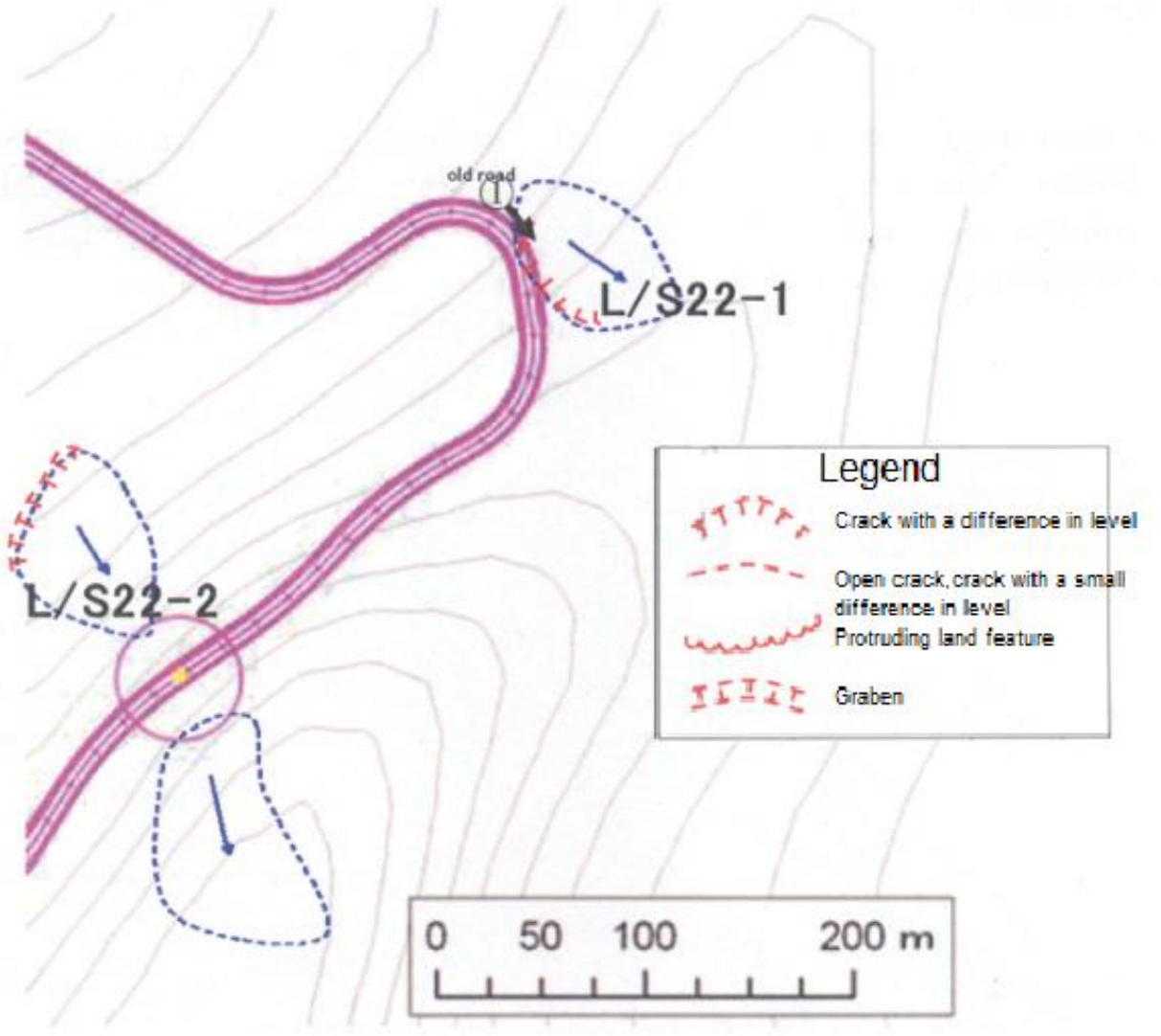

Figure 1-7 Surface anomalies in L/S22 (ST.21+600 to 22 + 300) (3)

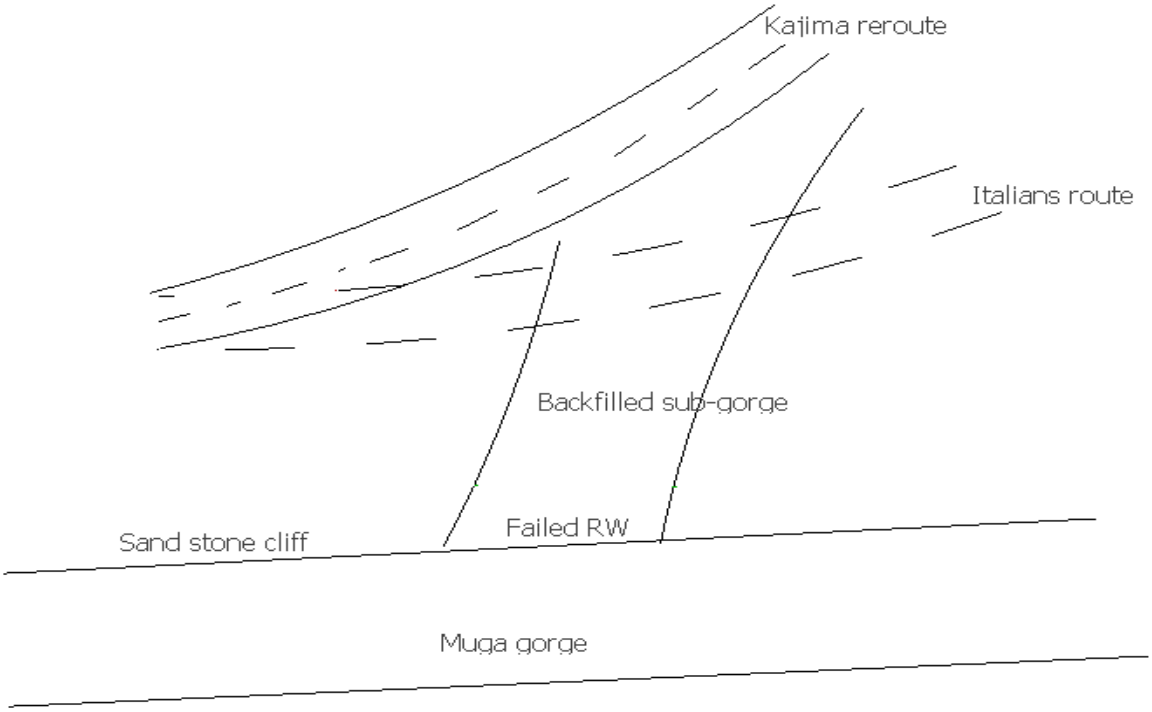

Figure 1-8 View of the land slide at ST-22

D) Surface anomalies of the landslide in L/S27(ST.27+200 to 28 + 400)

In this area, multiple landslide blocks overlap. As indicated by the significant subsidence of the road in recent years, the activities in the L/S27-2 are most conspicuous in this area In the L/S27-1, where there is a cracked church and a new church under construction, multiple displacements consisting of cracks by landslide activities are developing; however, the cracks are not new or clear. In contrast, a new continuous crack, as well as the main scarp and graben, can be observed in the L/S28-1, a subsidence on the road can also be an extension of the deformation direction. The active dip sited land slide crushes the existing retaining wall.

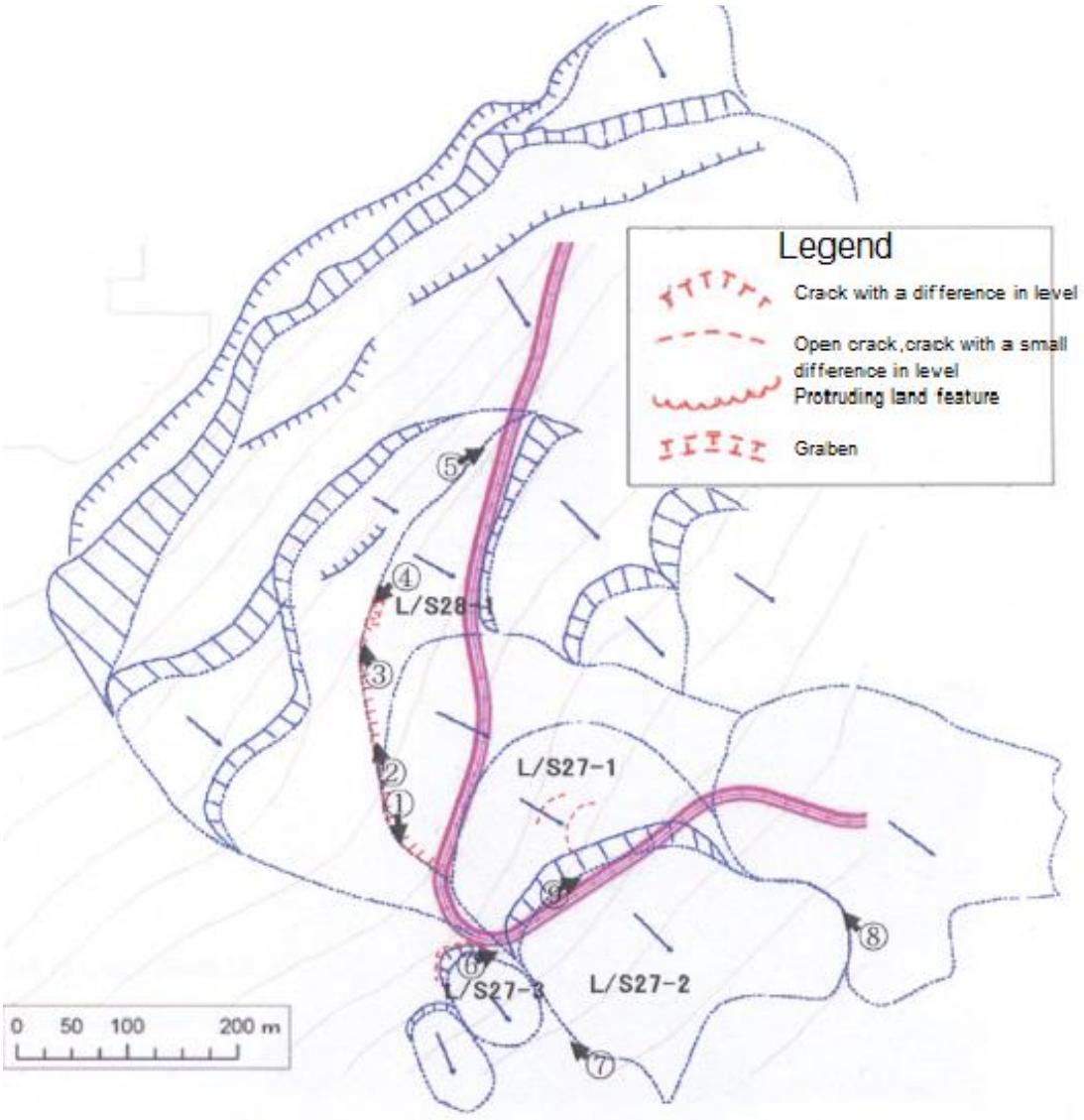

Figure 1-9 Surface anomalies in L/S27 (ST.27+200 to 28 + 400) (3)

a) Falling masonry retaining wall

b) Collapsed church

Figure 1-10 View of the land slide and its effect at ST-27

E) Surface anomalies of the landslide in L/S28(ST.28+400 to 28 + 800)

This area is positioned at the head of a large landslide covering the whole region. There are continuous clear main scarps, and cracks, whose mountain side is sinking, that runs roughly in parallel with the main scarps. L/S28-2 is one of the multiple landslide blocks in the area. Considering the size of the subsidence, it can be estimated that the current L/S28-3 moving block is at least 300 m wide. At this point big transverse subsidence is currently hindering the traffic movement.

This portion of the road is constructed by deep cut of lime stone which is secondary sedimentary rock and with terrace deposits.

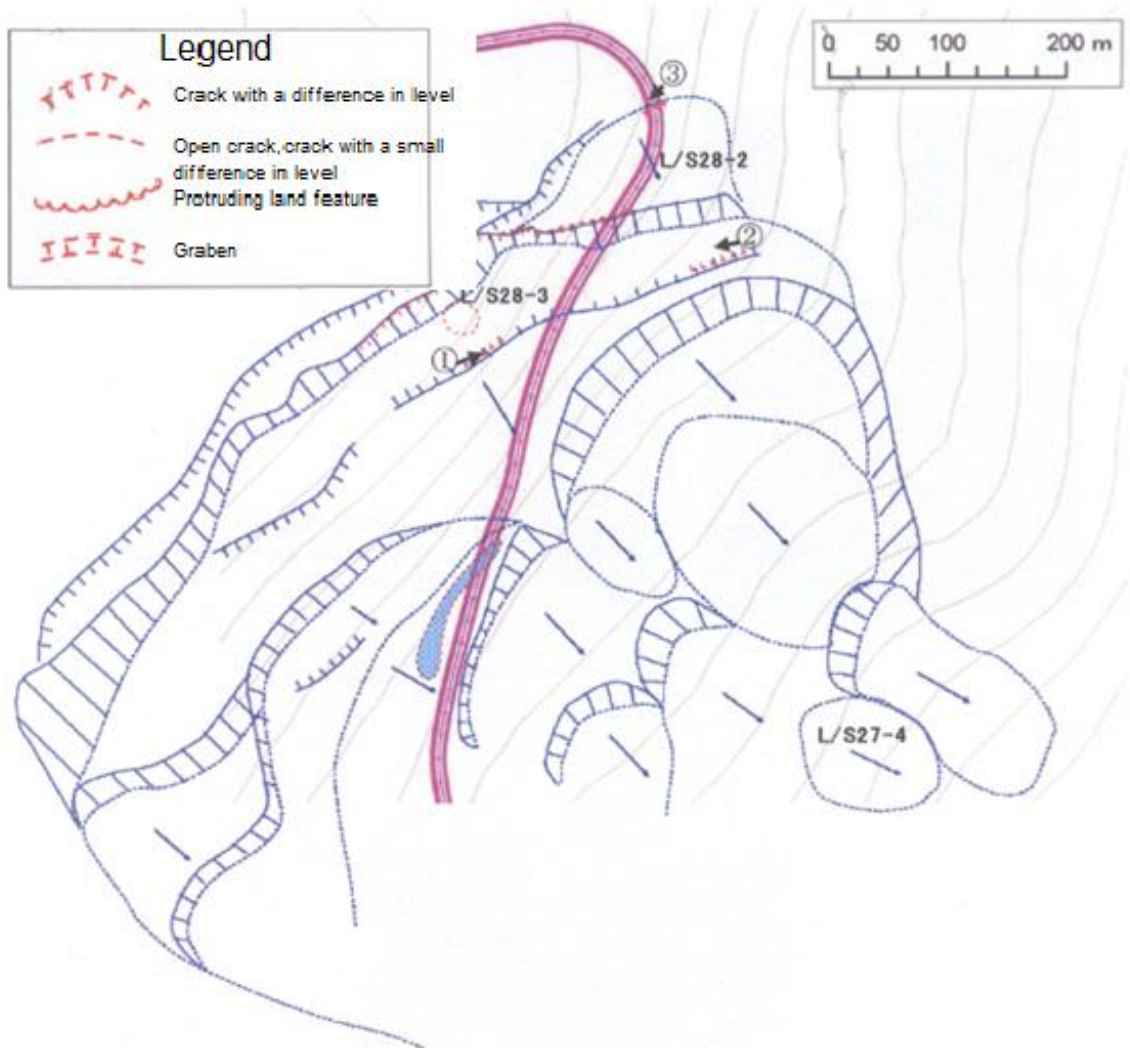

Figure 1-11 Surface anomalies in L/S28 (ST.28+400 to 28 + 800) (3)

a) Results steep slope

b) Hindering traffic movement

Figure 1-12 View of the land slide and its effect at ST-28

1.5. Objective

The objective of this research work is to undertake investigations on the causes of land slide in the Blue Nile Basin of Ethiopia and try to give remedial measures for those which have already failed.

The research attempts to study the suspected causes of failure by considering both geological and the geotechnical aspects. Appropriate field test and laboratory test data will be taken from JICA project which is the ongoing investigation on the site.

Finally based on the investigations and data analysis conclusions and recommendations with proposing proper control works have been made.

1.6. Organization of the thesis

The thesis is composed of five Chapters. In the first Chapter is a general introduction to the land slide, geology of the study area, the current situation of the road under investigation, the surface anomalies of five extremely damaged parts of the road rout and the final objective of the thesis work. The second Chapter covers previous works on landslides in the study area. The third Chapter deals with laboratory and field test results adopted from the ongoing JICA project, about insitu instrumentations and drilling log. The fourth Chapter deals with assessments of test results which were gathered from field and laboratory tests and determine the shear strength parameters of slip surfaces using back analysis. Finally in the fifth Chapter conclusions and recommendations are made.

2. LITERATURE REVIEW

2.1. Previous works on landslides in the study area

As cited in Almaz and Tadesse, 1994 the Mesozoic succession of Abay valley was studied by Jepson and Athearn and later by Mohr, but first description and paleontological determination date back to the end of the 19th Century by M. Aubry and K. Futterer. "Strata of Abay" was first introduced by Krenkel in 1926 for strata of liassic age overlying sandstones and underlying carbonates occurring in the Abay river basin. Stehanini correlated the "Strata of Abay" with similar outcrops in other parts of Ethiopia.

A number of geophysical and engineering geological investigations had been carried out in the area to recommend possible measures to the slope instability problems. The Ethiopian Roads Authority (ERA), the former Imperial Highway, Material and Research Division was the first to study the stability condition of the southern parts of the road, between Washa Mikael church and Filiklik village area, related to the failure of the viaduct (Jemal Saed, 2005). In this study, the Authority recommended certain remedial measures as diverting and draining of the springs above the viaduct etc. However, a required stability of the slope on which the viaduct rest could not be achieved. Following this, the Blue Nile Viaduct' (1967) as cited in Jemal Saed (2005) had identified the weathered basaltic rock and the colluvial moving materials under pier foundations were responsible for the failure of the viaduct, and proposed a design for realignment of the road avoiding the viaduct area.

The Geological Survey of Ethiopia (GSE), the former Ethiopian Institute of Geological Survey (EIGS), had carried out a number of geophysical and engineering geological investigations with the support of insitu and laboratory geotechnical testing of soils and rocks.

Mesfin Wubeshet et al. (1994) as cited in Shiferaw Ayele (2009) from EIGS had carried out geophysical investigations using Refraction seismic, Electrical Resistivity and Magnetics methods to determine the depth to the hard rock material and the quality of the rock defined, to locate any linear features like faults, fractures, contacts and lineaments and also to generally map the area from the engineering point of view on selected landslide-prone areas. Accordingly, the geophysical investigation carried out in the area showed that the columnar jointed nature of basaltic rock (Brodde et. al, 1989), the friableness and weak consolidation of limestone and shale

affected by water saturation being easily weathered to clayey material, in addition to the gentle slope are responsible for the instability of the area.

Almaz et al (1994) from EIGS also had conducted a detailed engineering geological mapping along the road Gohatsion to Dejen and proposed an alternative route for the upper part of the gorge (Gohatsion to Filklik) where most of the landslide problems are concentrated. During this study, a total of 7 test pits and 5 bore holes were drilled so as to identify the overburden material thickness, the depth to the bedrock at different locations, and to have an idea on the geotechnical properties of the subsurface geology. The results from these drilled boreholes revealed that on an average, the top 20m thick overburden is described to be mixture of gravel to cobble size basaltic rock fragments and fine sandy silt and clay including black cotton soils (Almaz et al, 1994). Moreover, the laboratory test results for black cotton soil indicated high to very high plasticity, plasticity index values ranging from 38.2 to 56.68 and high degree of free swelling, 95-155%.

Further, Almaz et al (1994) identified rock fall, toppling, debris slide and rotational failure of colluvial materials as the main form of landslides; and huge columnar jointed basalt, uncontrolled surface run off, joints of rocks, and the presence of Marl and Shale within hard rocks as the main causes of slope instability in the area.

Luleseged and Hiromitsun (2003) assessed on the relationships between topography and the process of land sliding and rock falling. By taking nine types of landforms on the basis of a one-to-one combination of lateral and vertical slope profiles the determination of the effect of these landforms on the occurrence of slope failures is tried to identify. Observations showed that topographic surfaces with concave lateral profiles shelter mudflows and some retrogressive rotational slumps while slopes characterized by planar lateral profiles are sites mainly for translational slides. Landslides are rare in convex-shaped slopes but when they occur, they are big and deep-seated. This paper also deduces that slope failures were part of the mega-forces that shaped the entire Blue Nile basin, and in fact, played the dominant role in landscape evolution.

As cited in Shiferaw Ayele (2009) In December 2003 Transport and Construction Design Share Company (TCDSCo) in collaboration with Oriental and Japan Engineering Consultants carried out geotechnical investigation for the Gohatsion-Dejen-Debre Markos road project to evaluate subsurface material through drilling boreholes and trial pit excavations. In this study TCDSCo identified black cotton soil supposed to be one of the causes and responsible for the instability of section in the south part of the road at about Km 3+000 (Henok, 2008)

Jemal Saed (2005) has made an inventory for landslide evaluation that mainly exists on the road section starting from Gohatsion to Dejen towns and he identified 17 critical slope sections. Of these slope sections, 9 slope sections were taken for detail slope stability studies. This study had indicated 4 sections have planar mode of failures, 2 wedge modes and 3 soil sections having a circular mode of failures

Henok (2008) as cited in Shiferaw Ayele (2009) had made landslide hazard zonation mapping in southern part of Blue Nile Gorge using a Land Hazard Evaluation Factor (LHEF) to characterize the different land elements existing in the study area. Based on his field observations, a total of 6 critical slope sections were identified along the road and its corridors in the southern parts of the study area. Out of these critical slope sections, 5 slope sections fall within rock mass whereas one slope section falls within soil slope. In this zonation mapping, the result had shown that 40.3% of the area falls in high hazard, 45.3% of the area is moderate hazard zone; whereas the rest 14.4% falls in low hazard area. During this study the author had identified that most portion of the main road falls on the high hazard zone whereas low hazard areas fall mostly on relatively flat area or low relief.

Shiferaw Ayele (2009) had prepared slope instability and hazard zonation mapping using integrated Remote Sensing (RS) and Geographic Information System (GIS) technique to classify the land surface into zones of varying degree of hazard. The author also uses a technique known as "Weighted Linear Combination (WLC)". Which is mainly based on major event controlling parameters: geology, groundwater conditions, drainage, slope, geologic structure, aspect, and land use/ land cover. This map is composed of five relative scales of landslide hazard zones, namely Very Low Hazard (VLH), Low Hazard (LH), Moderately Hazard (MH), High Hazard (HH) and Very High Hazard (VHH). The landslide hazard zonation map of the study area was verified with field observed data /event observational data. The result has shown that out of 21 critical slope failures, 7 (33.33%) occurs in very high, 7 (33.33%) in high, 5 (23.81%) in moderate and 2 (9.52%) in low hazard zones, respectively.

According to the findings of the previous works, the main causes aggravating the instability problem were the surface runoff on steep slopes, the presence of black cotton soil below the surface of the ground, the deposition of thick unconsolidated colluvial soil mass including black cotton soil, and the presence of Marl and Shale within the limestone and gypsum, and columnar jointing of rocks (Jemal, 2005)

2.2. Physiographic of the Study area

The study area, the Abay Gorge is characterized by 1400 - 1500 m deep gorge, which is made of stratified sedimentary rocks capped by basaltic plateau. The present physiographical setting of the study area is a result of various processes. Uplifting which is believed to be responsible for the formation of the deep canyon, erosional leveling, weathering and mass wasting have played a major role in creating the present landform (Almaz et al, 1994).

2.2.1. Topography

Main road 3, a major arterial road in Ethiopia, connecting the capital Addis Ababa with Sudan, is part of the Trans-African Highway Network, and is vital to its economy and the livelihoods of its citizens. The stretch of main road 3 that passes through the Abay Gorge steeply climbs nearly 1,500 meters from the Abay River to the plateau in 40 kilometers distance. It is plagued by landslides during the rainy season from June to September. Some of these are up to two kilometers wide, putting into jeopardy this vital link. To fundamentally solve this problem it is necessary to implement appropriate countermeasures after clarifying the mechanisms that trigger landslides in this stretch of road. The Gohatsion-Dejen trunk road which is the part of Main road 3 is subject of this study.

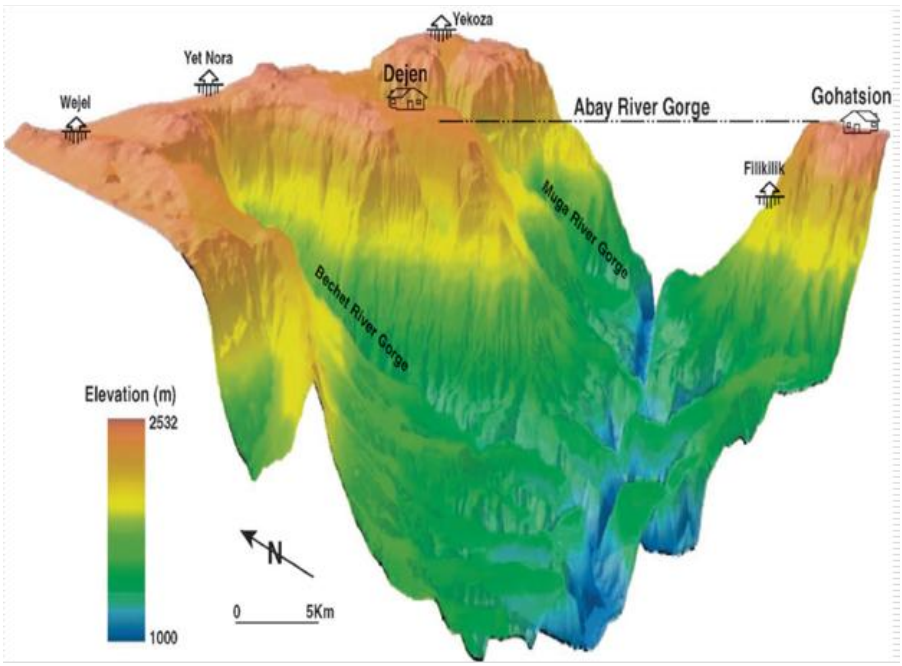

Figure 2-1 Relief map of the study area (8)

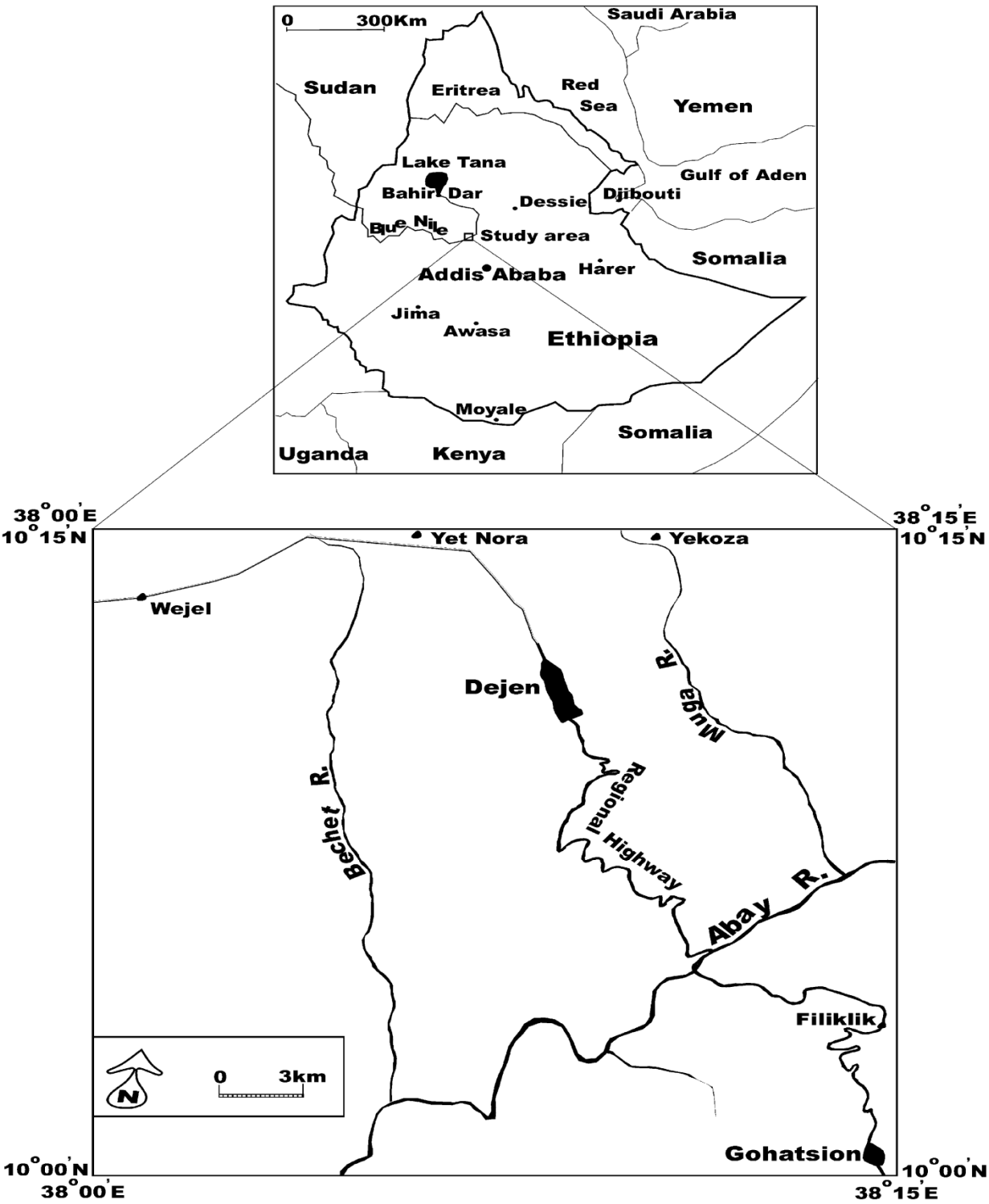

Figure 2-2 Regional setting of the study area (8)

2.2.2. Geology

Much of the Blue Nile basin is covered by Mesozoic sedimentary rocks and Trap Series basalts of Middle Tertiary (Jespen and Athearn, 1961; Mohr, 1983; Mohr and Zanettin, 1988). The study area in particular provides long cliffs of sandstone, limestone, and gypsum intercalated with relatively soft units of mudstone, shale, and marl (Getaneh, 1991; Russo et al., 1994) capped by a succession of lava outpourings which stand out in relief along gorges and depressions (McDougall et al., 1975). The Abay River and its tributaries cut deep into these rocks (Fig. 1.5) to form what is known as "Africa's Grand Canyon" in the study area and further downstream. The river drains west while collecting water and sediments from perennial streams originating from the highlands. Its major tributaries are usually characterized by steep-sided valleys with V-shaped cross-sections. In some places, frequent rapids and waterfalls are not uncommon in these tributaries especially at times when summer rains are high. (As sited in Ayalew and Yamagishi, 2003)

According to Jepson and Athearn (1961) and Tefera et al. (1996), the geology in the area is mainly classified into four formations. Table 1.1 shows the table of the geological classification in the area.

Table 2-1 Geological classification in the Abay Gorge (Tefera et al., 1996) as cited in JICA project

Era	Name	Geology/ Descriptions
Tertiary (Paleogene)	Ashangi Formation	Deeply weathered alkaline and transitional basalt flows with rare intercalations of tuff
Jurassic	Antalo Formation	Limestone
	Abay Formation	Middle Jurassic limestone, shale and gypsum
	Adigrat Formation	Triassic to middle Jurassic sandstone

Although the sedimentary and volcanic rocks in the area are exposed largely as symmetrical stratigraphy on both sides of the Abay River, the detailed sequences are unevenly distributed. The sequence in the area is not disturbed due to major faults and is generally horizontally deposited. However, there are a lot of minor normal faults with a down throw of 1-2 meters. Figure 1.5 shows a schematic geological cross section of the Abay area (Ayalew and Yamagishi,

2003). The characteristics of the stratigraphy on the major sequences are described from the lower unit by Almaz and Tadesse (1994) as follows.

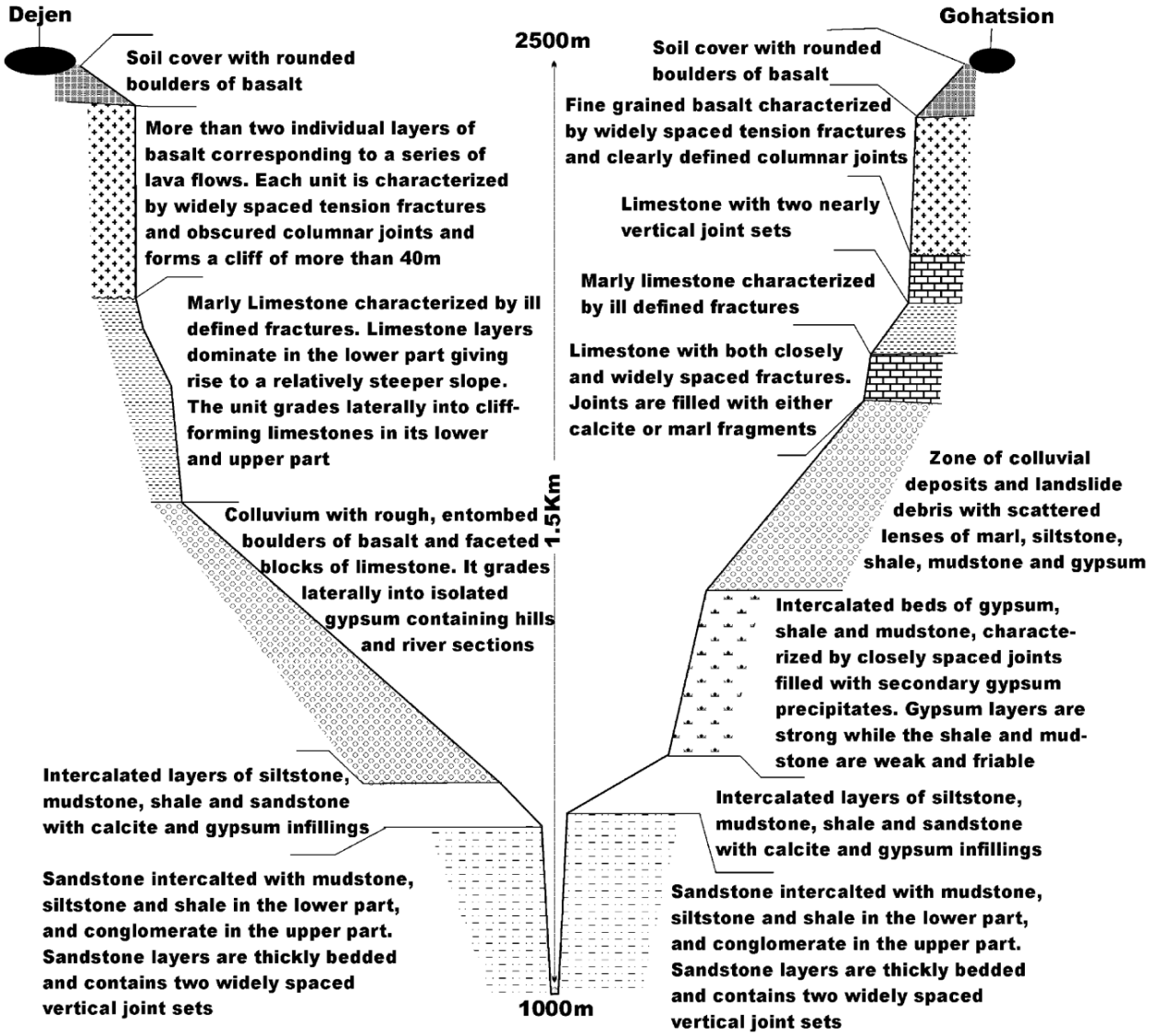

Figure 2-3 A geological cross-section along the north-south section of the Abay River Gorge (8)

2.2.2.1. Sandstone

The river bank and terrace is composed of highly consolidated sandstone, which is fine to medium grained, which belongs to the Adigrat Formation (Figure 2.4). It is intercalated with mudstone, siltstone and shale in the lower part, and conglomerate in the upper part. It is 200 - 400 meters thick near the road. The rock is brownish red in color, but varies to brownish grey, pinkish and greenish grey due to chemical weathering. No fossils are reported in the unit. This unit is underlain by upper Paleozoic sediments and has gradational contact with the overlying siltstone.

In general, they are horizontally bedded, but also locally show cross bedding which are graded. The upper part of the sandstone is thickly bedded whereas the lower part is thinly bedded. The unit has three joint sets, the bedding plane which is horizontal and other two sets trending NW and NE. It forms a vertical cliff, resulting in rock falls due to the intersection of these three joint sets.

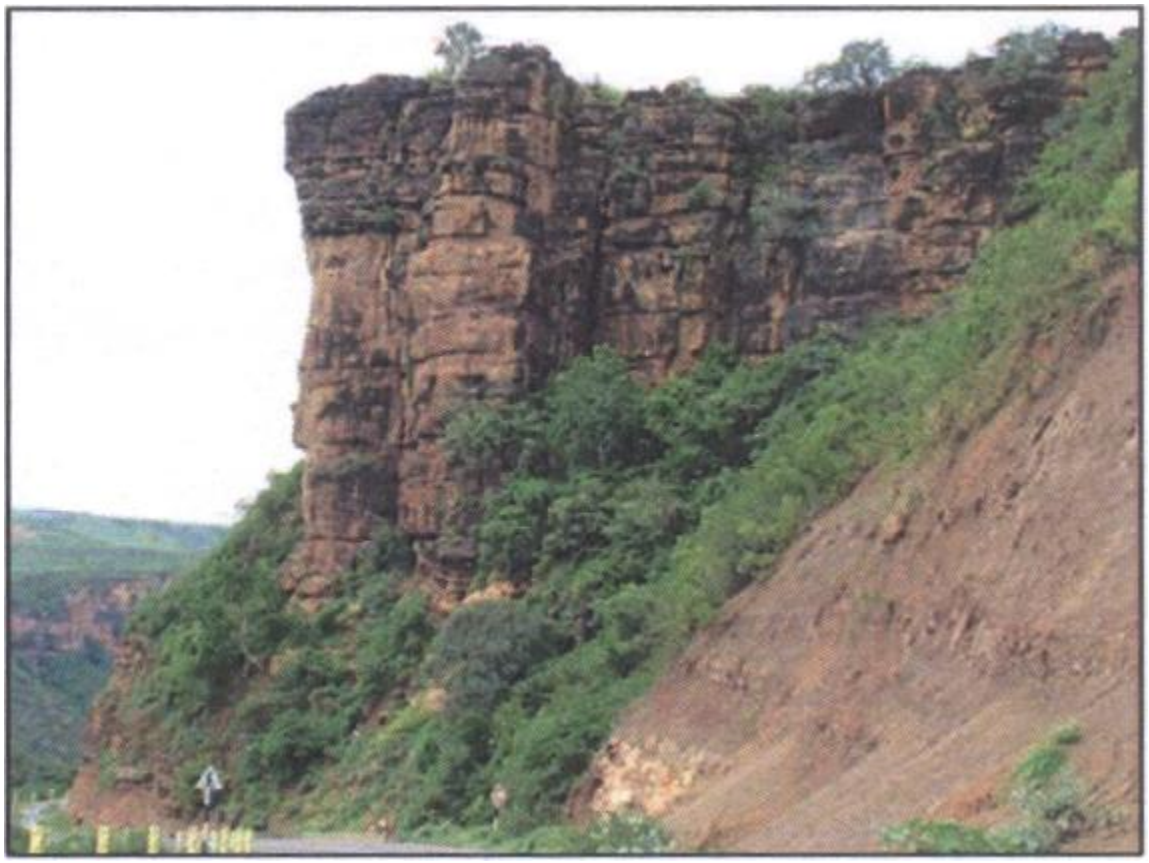

Figure 2-4 View of the sandstone

2.2.2.2. Siltstone

This siltstone unit is composed of silt/clay particles cemented together and belongs to the Abay Formation of Jurassic age (Figure 2.5). It is found intercalated with shale, mudstone and sandstone with calcite and/or gypsum veins in places which indicates a change of the depositional environment. It is mostly yellowish green to brownish grey in color. The unit has also characteristic greenish layers which are presumed to include chlorite and glauconite. The siltstone is highly consolidated and partly alternating, which is thickly laminated and cross-bedded. It is characterized by weak and friable layers. These rocks are horizontally bedded with closely spaced minor vertical joints.

Figure 2-5 View of the siltstone rocks

2.2.2.3. Shale

The argillaceous clastic sedimentary rock which contains a lot of clay minerals belongs to the Abay Formation. The shale found between the underlying siltstone and overlying gypsum is often called "the lower shale unit" and the one which is found between the gypsum and after-mentioned limestone is "the upper shale unit" in the Abay Gorge area (Figure 2.6). It is 100 - 200 meters thick near the road. The color of the layers varies from place to place, such as brown, grey, black, red, green and purple. In the study area, the lower part of the shale has been removed by weathering and erosion. Part of the shale is totally changed to clay by weathering. The shale located beneath the limestone and the gypsum is relatively soft and weak due to the exerted load of the overlying units. These rocks are characterized by closely spaced joints filled with secondary calcite and/or gypsum precipitates.

Figure 2-6 View of the Shale

2.2.2.4. Gypsum

The gypsum unit is composed of CaS04-2H20. It belongs to the Abay Formation. It also has intercalation of thinly bedded shale. It is 150 - 250 meters thick near the road. The gypsum is interbedded between the lower shale unit and the overlying upper shale unit. It is generally white in color, but varies to grey, bluish grey and black (Figure 2.7). The variation in color is attributed to several ferruginous minerals and organic impurities. Generally gypsum is susceptible to weathering and erosion, this phenomenon is evident on the Goha Tsiyon side where the gypsum is exposed along the roadside. The weathering in the gypsum contributed to the change of color on the surface and along the joint plane.

In the gypsum unit, two sets of joints which are N30W and N70E as well as a horizontal bedding plane are observed. Although the rock itself is hard and strong, the two joint sets and the bedding plane would result in huge rock failure due to the intersection.

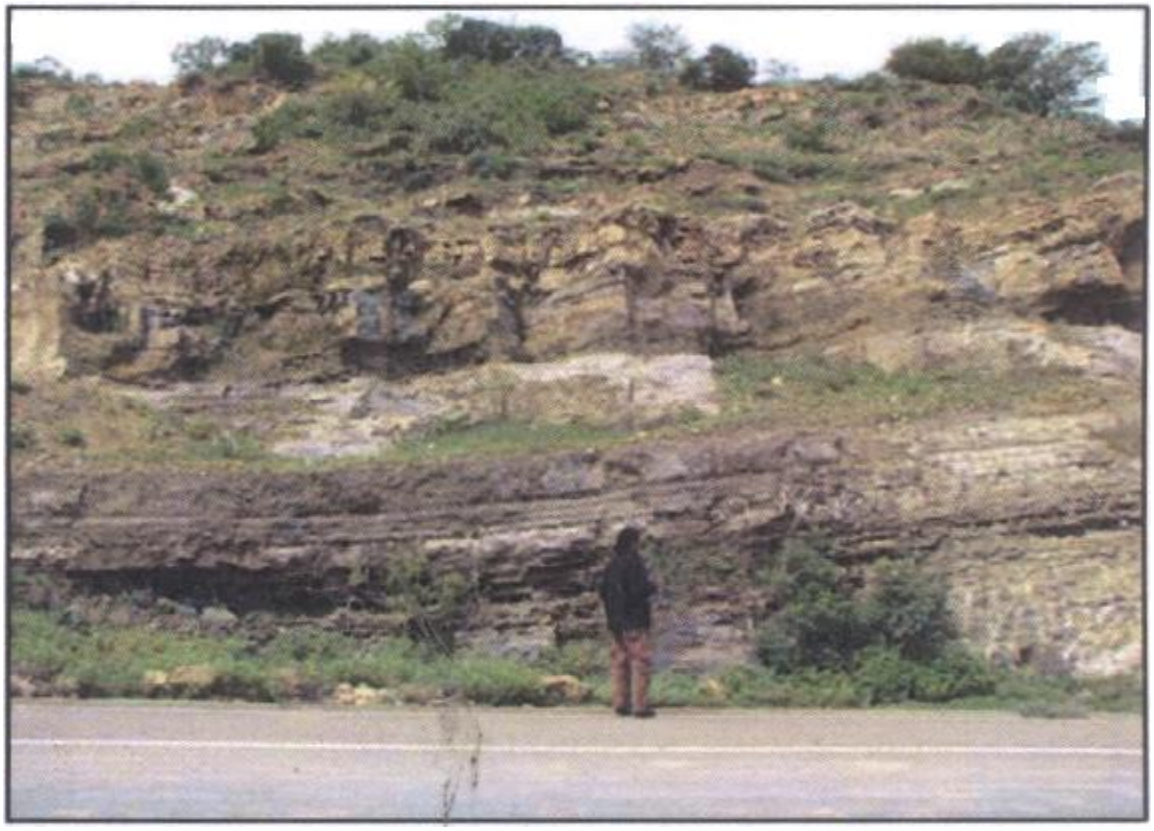

Figure 2-7 View of the gypsum

2.2.2.5. Limestone

This unit overlies the upper shale unit and belongs to the Antalo Limestone Formation (Figure 2.8). The limestone which is fine to medium grained is widely distributed in the area and is more than 400 meters thick near the road. The form of the limestone layers creates fitful steep slopes and escarpments. The unit also has shale, carbonated clay and marl, and is highly fossiliferous. The marl which means clayey carbonate is characteristically found in the area. It is generally white in color, but varies to yellowish grey, and brownish grey.

In general, this unit is horizontally bedded and has two developed joint sets trending NW and NE and a bedding plane. The joints of the limestone are filled with either calcite or marl fragments. The three joint sets with both closely and widely spaced fractures would result in huge rock failure due to the intersection. The upper part of the limestone is thickly bedded whereas the lower part of it is thinly bedded.

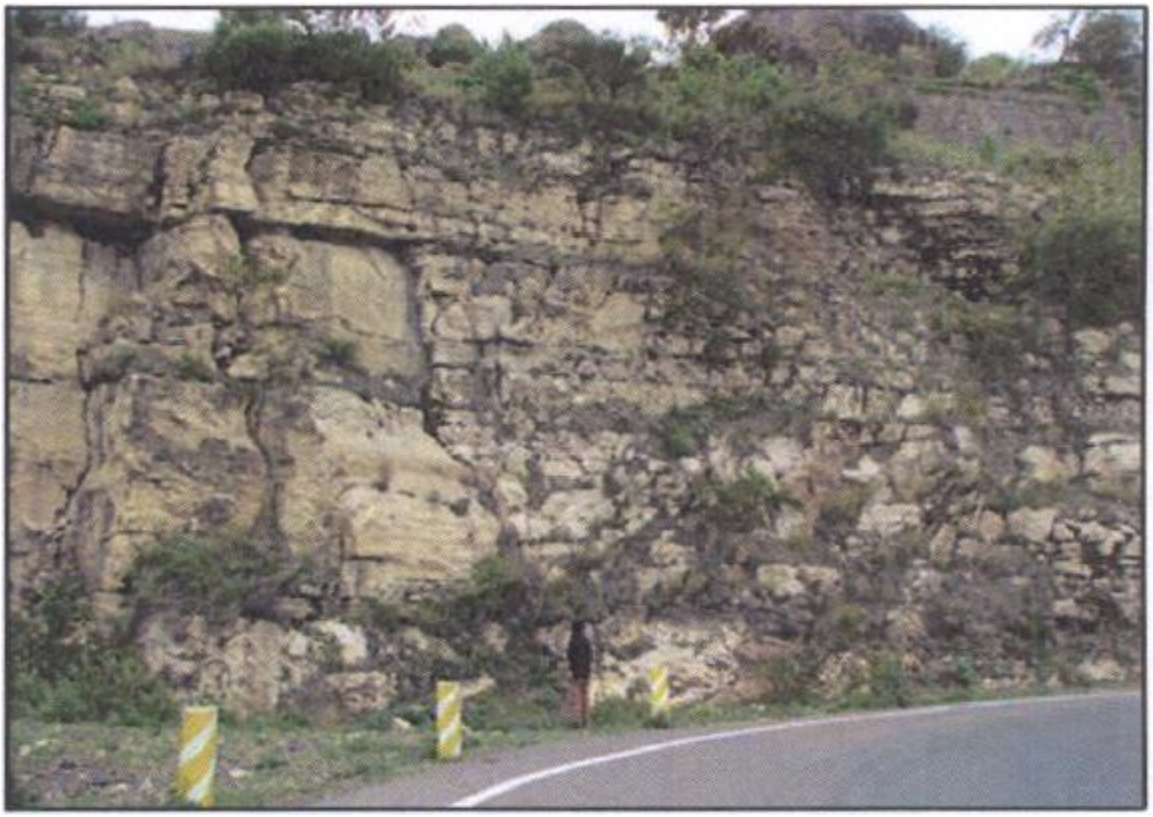

Figure 2-8 View of the limestone

2.2.2.6. Basalt

The basalt overlies unconformably on the limestone and belongs to the Ashangi Formation (Figure 2.9), which has thickly intercalation of pyroclastic rock. The pyroclastic rock is brittle brown layer and susceptible to water erosion.

The basalt unit is widely exposed and stratified with two prominent layers corresponding to a series of lava flows. It shows steep escarpments at the beginning of the Abay Gorge on both Goha Tsiyon and Dejen side. The basalt is characterized by widely spaced tension fractures and forms cliffs of more than, 40m. The basalt unit is dark grey in color, whereas a part of the surface is reddish brown due to oxidation reaction. This unit contains 10-15 m thick deeply weathered basalt which acts as impervious soft layer possibly triggering landslides

The upper part of the unit clearly develops columnar joints (20-50cm). As for the lower part, the columnar joints are partly obscured and the bottom is composed of more than 15-20 m thick massive huge blocks.

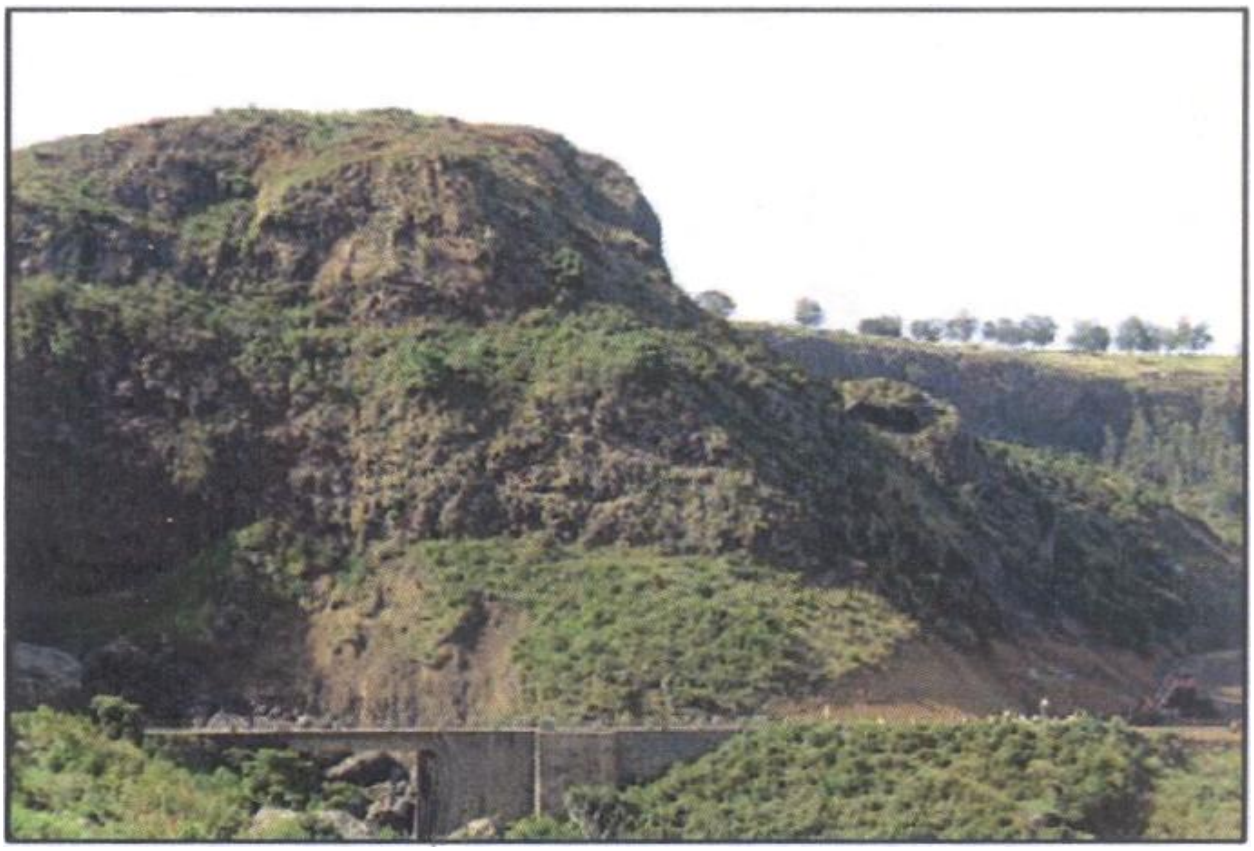

Figure 2-9 View of the basalt

2.2.3. Surface soils

In the study area, there is huge amount of surface soil covering the bed rocks. As cited in Almaz and Tadesse (1994) Soils in these areas are genetically classified into three units: namely, colluvial soil, alluvial soil and residual soil. Most of the area is covered with colluvial soil where as stream channels and terraces are covered with alluvial soils. Flat agricultural lands are covered mainly with residual soil and partly with colluvial soils. The location of the deposit depends on their source and geography. Basalt, limestone, gypsum and sandstone layers generally form steep cliffs, and pyroclastic rock, siltstone and shale form gentle slopes due to the susceptibility to weathering and erosion in the area. The pyroclastic unit and the shale unit are covered by huge amount of surface soils, has a lot of landslide forms. [1]

2.2.3.1. Alluvial soils

Alluvial soil is found mainly following all along the river channel of Abay river and also along the main tributaries of Abay such as Muga river and Ada Wedeb. Coarse grained gravels and sands are also present along major stream channels and gullies.

2.2.3.2. Colluvial soils

Colluvial soils are deposits displaced from their original location of formation or deposition by gravity forces. It is mainly composed of gravel, cobble, boulder sizes of Basalts and limestones with in silty clay matrix. It is generally poorly sorted resulting in the occurrence of voids and hence the colluvium could be categorized as very loose, weak, heterogenous and permeable unit. Most of the springs emanate from colluvial soil indicating high permeability nature of the soil. Scree deposits are also part of colluvial soil deposits.

2.2.3.3. Residual soils

Residual soil covers most of the plateau and the step like terraces formed by basalt and completely flat lands. The residual soil developed from the basalt plateau is very red in colour due to the high content of iron oxides in the clays. Whereas down the gorge it changes its colour into brownish and yellowish as the rock unit changes into limestone and shale.

2.2.4. Climate

National Atlas of Ethiopia (1981) defined five locally recognized climatic zones: "Kur" (Alpine), 3000 m and above; "Dega" (temperate), 2300 m to about 3000 m; "Weina Dega" (Sub tropical), 1500 to about 2300m; "Kolla" (Tropical), 800 m to about 1500 m and "Bereha" (Desert), less than 800 m. According to this traditional climatic zone classification, the study area lies between "Kolla" (Tropical) and "Dega" (Temperate). [1]

2.2.4.1. Rainfall

Monthly total rainfall records of three stations for the year between 1976 and 2007 is used to analyze monthly mean rainfall and annual mean rainfall. The mean monthly and annual mean rainfall of National Meteorological Services Agency (NMSA) stations at Dejen, Filkilik and Gohatsion stations are shown in Table 2.2 [1]

Table 2-2 Mean monthly and annual rainfalls in three stations

Station	J	F	M	A	M	J	J	A	S	O	N	D	Ann. mean
Dejen (mm)	9.2	14.0	62.7	75.9	79.3	149.2	352.4	343.5	170.9	83.9	20.2	7.6	1293.9
Filkilik (mm)	6.3	11.3	41.0	58.9	68.6	113.7	317.3	289.5	131.9	61.3	21.0	5.7	1014.5
Gohatio n (mm)	11. 6	18.7	55.9	58.9	85.2	121.3	316.4	303.9	116.6	53.7	16.2	7.2	1121.5

The monthly mean records of rainfall for thirty-two years shows that the mean annual rainfall at Dejen, Filklik and Gohatsion station is 1293.9mm, 1014.5mm and 1121.5mm respectively. Thus, the study area receives annual average rainfall of about 1143.3mm. Moreover, in all stations the heaviest amounts of rainfall occur in the months of July. While the minimum amount of rainfall occurs in January at Filkilik station.

2.2.4.2. Temperature

Under normal conditions, air temperature decrease with increasing altitude at a mean rate of 0.7oc for every 328 feet (Fetcher, 1998) as cited in Shiferaw, 2009. This works also in Ethiopia where temperature decreases with increasing elevations. The monthly mean maximum and minimum temperature records of Gohatsion for the years between 1976 and 2007 was used to calculate monthly and annual average. The computed average maximum and minimum temperature is presented in Table 2.3.

Table 2-3 Mean Monthly Temperatures of Gohatsion

Gohatsio n Station	J	F	M	A	M	J	J	A	S	O	N	D	Ann avg.
Avg.max. temp (oC)	23.9	24.9	25.2	25.3	25.3	23.4	19.9	19.7	21.5	22.8	23.3	23.6	23.2
Avg. min. temp (°C)	15.2	15.5	15.9	16.2	16.4	14.4	12.7	13.0	14.7	15.9	15.8	15.6	15.1

As shown in Table 1.3, the highest mean monthly maximum temperature occurs in the months of May (25.3° C) and the lowest is in the month of August (19.7° C). The mean monthly minimum temperature ranges for the lowest from 12.7 °C in July to the highest 16.4° C in the month of May. Thus, the average temperature of Gohatsion (from 32 years data, 1976- 2007) is 19.2◦C.

The monthly mean maximum and minimum temperature records of Filkilk for the years between 1976 and 2007 can be used to calculate monthly and annual average. The computed average maximum and minimum temperature is presented in Table 2.4.

Table 2-4 Mean Monthly Temperatures of Filklik

Filklik Station	J	F	M	A	M	J	J	A	S	O	N	D	Ann avg.
Avg. max. temp (^{o}C)	31.7	34.1	34.9	35.2	35.1	32.1	27.2	26.7	30.8	30.0	30.6	32.1	31.7
Age. min. temp (^{o}C)	14.7	15.4	14.8	14.8	14.5	13.7	12.2	12.2	12.8	13.5	13.3	13.3	14.7

The highest mean monthly maximum temperature occurs in the months of April (35.2◦C) and the lowest is in the month of August (26.7◦C). While the mean monthly minimum temperature ranges from 12.2 °C (the lowest) in August to 15.4◦C (the highest) in the month of February. Thus, the average temperature of Filkilik and Gohatsion (32 years data 1976- 2007) is 23.2^{0}C.

In the study area, generally the altitudes vary from 1002m to about 2548m a.s.l. and the mean annual temperature is 16.02^{0}C.

3. LABORATORY AND FIELD TEST RESULTS

3.1. General

During the time of this study a well organized research team from JICA and GSE has under taken a study with the help of detailed borehole investigation and instrumentation.

To overcome different data resource problem and to maximize the scope of this study this work is done by working closely with this study team and exploit different instrumentation technology in addition to taking any necessary row data for the analysis purpose.

During the field observation, it was found necessary to start by visual inspection of the whole stretch of the Gohatsion - Dejen road. During initial visit the whole portion of the road was covered and the failed sections which were identified visually. In the following visits five extremely damaged failed sections are identified as priority sites which need special and immediate attention. For this study these five sections are assumed to be representative sampling area for different failure conditions observed in different portions of the road route.

Detailed borehole investigation and different monitoring devices installation were carried out on these sites by JICA research team in order to grasp movements and to find the main slip surface and the geological structure.

3.2. Field test results

The monitoring devices adopted in the JICA Project are: 1) Extensometer, 2) Borehole Extensometer, 3) Borehole Inclinometer, and 4) Groundwater level meter. The devices 2) to 4) are installed with special casings and/or filling sand/gravel in each bore hole after completion of drilling to monitor condition in the ground at the landslide area, whereas the device 1) is set along the direction of landslide movement on the surface.

The number of the monitoring device installed at the selected priority sites is shown below

Table 3-1 Monitoring sites

No.	Location	Name	Monitoring			
			Extensometer	Borehole Extensometer	Borehole Inclinometer	Groundwater Level meter
1	0+800~l+100	L/S00	1	1	2	1
2	4+800~5+500	L/S05	2	1	2	2
3	21+850—22+100	L/S22	0	0	1	0
4	27+500~27+900	L/S27	1	1	2	2
5	28+000~28+700	L/S28	2	1	3	1
Total			6	4	10	6

The methods of landslide monitoring are classified into two categories: measuring movement; and measuring inducing factors. Furthermore, the methods of measuring movement are classified into two categories: monitoring under the ground, or in boreholes; and monitoring on ground surface.

Inducing factor surveys contain precipitation observation, surface water observation, groundwater observation, seismic observation, and so on, which are usually conducted landslide monitoring simultaneously.

Table 3-2 Type of landslide monitoring currently practiced in Abay Gorge

Location	purpose	Method of monitoring
Borehole	Slip surface survey	Borehole extensometer measuring
		Borehole inclinometer measuring
	Groundwater survey	Borehole water level measuring
Ground surface	Ground surface deformation survey	Ground surface extensometer survey
	Inducing factors survey	Precipitation observation

3.2.1. Horizontal Extensometer Survey

Method of ground surface extensometer based on measuring the distance between main part of extensometer and the end of the wire that is installed over the pressure mounds, cracks and steps. When the wire is installed on an active landslide, the wire expands in length by movement of the

landslide. The record of the extensometer can be obtained in real time to compare with inducing factors, such as precipitation and groundwater level. With this device one cannot obtain the macro movement of the landslide. It measures the movement of a specific part of the landslide. To identify trigger/motion mechanisms of landslides, measurements were made with extensometers. These were installed along the direction of landslide movement and along each survey line to measure the amount of expansion in cracks and subsidence.

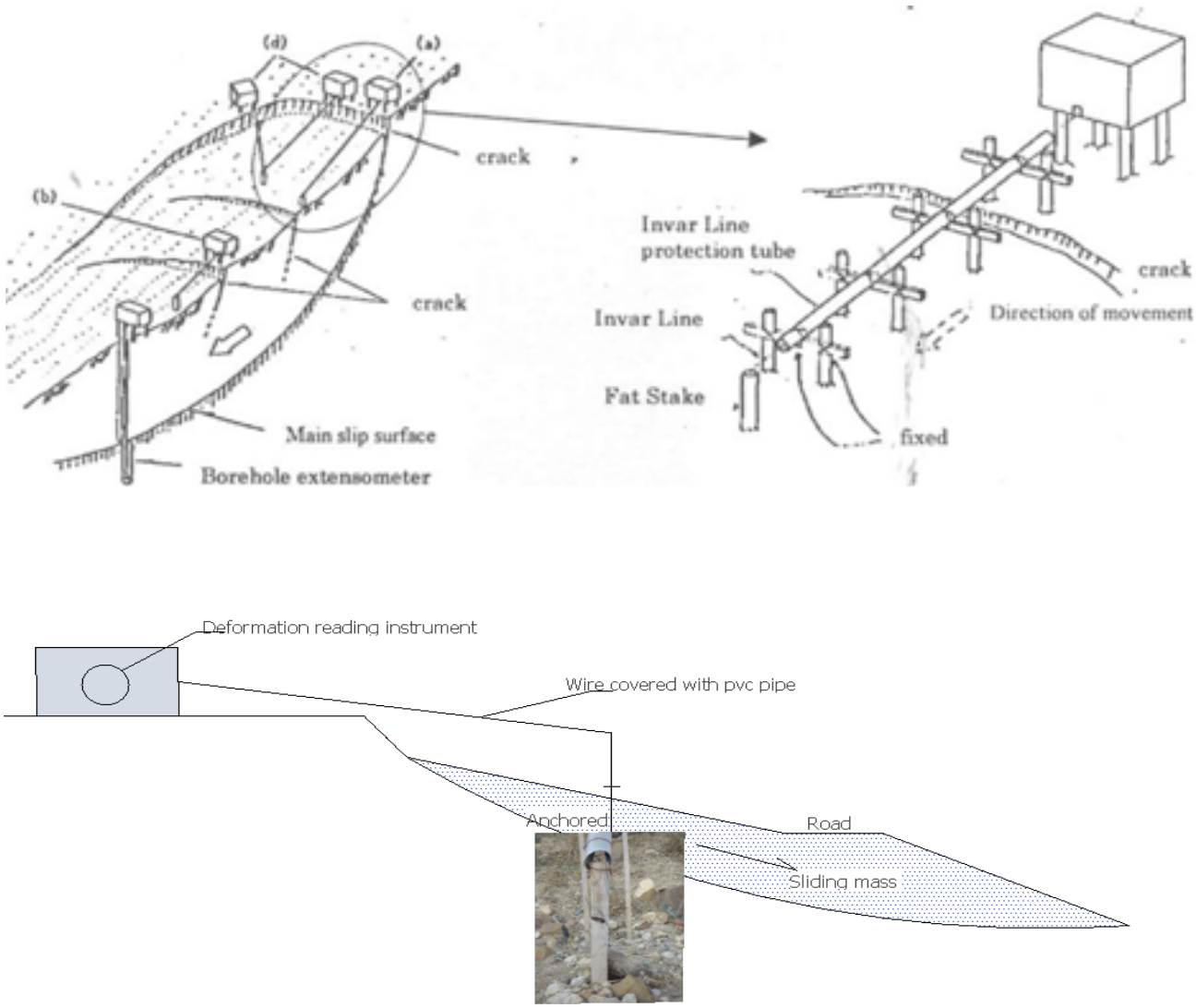

Figure 3-1 Conceptual diagram of Horizontal Extensometer

Typical horizontal extensometer reading at L/S00 is presented below for illustration and the others readings is summarized in Table 3.3

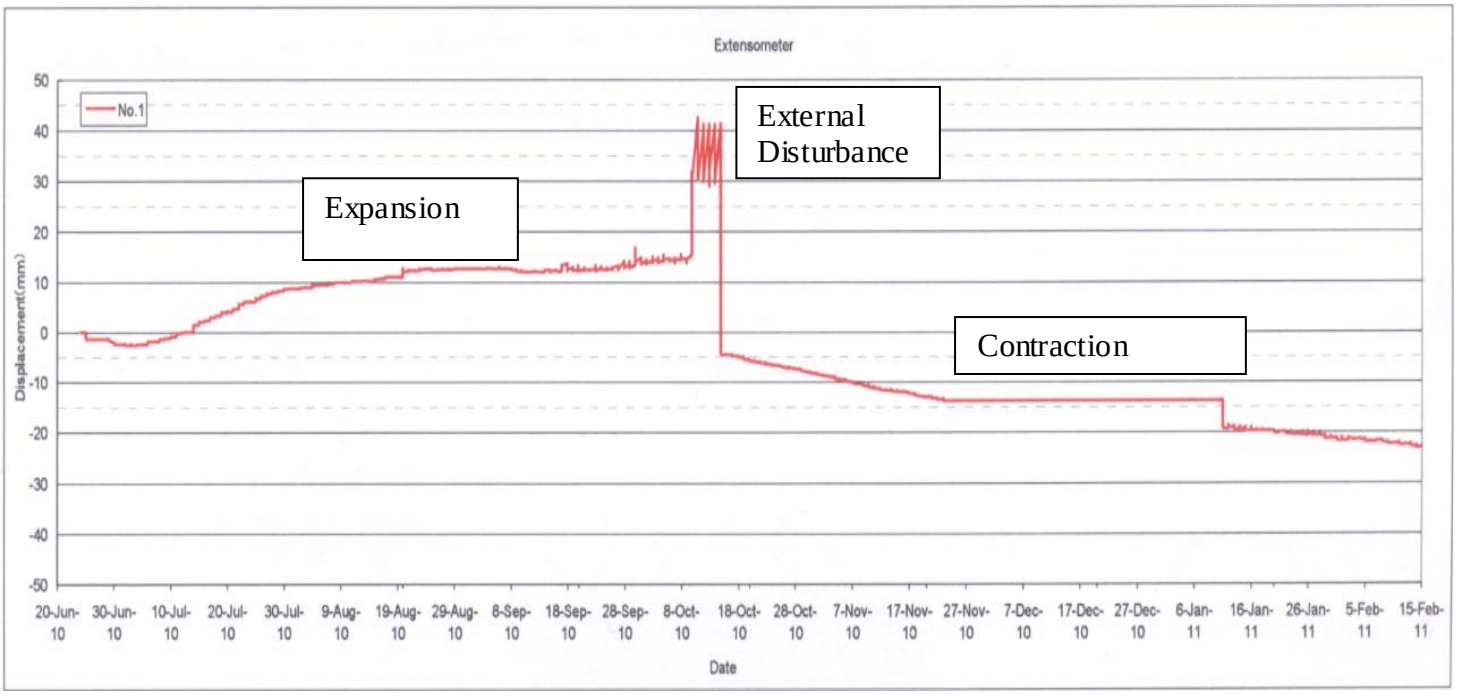

Figure 3-2 Horizontal Extensometer Reading at L/S00 (3)

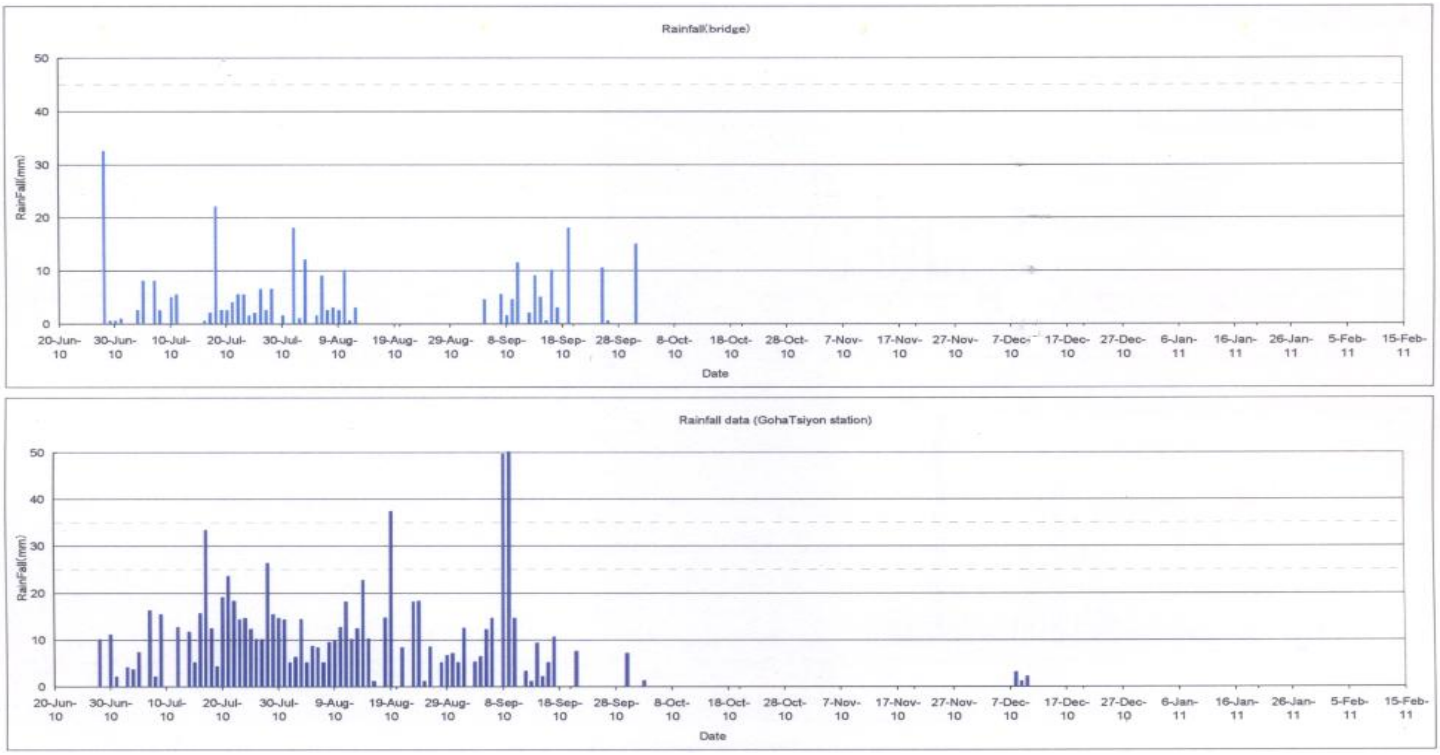

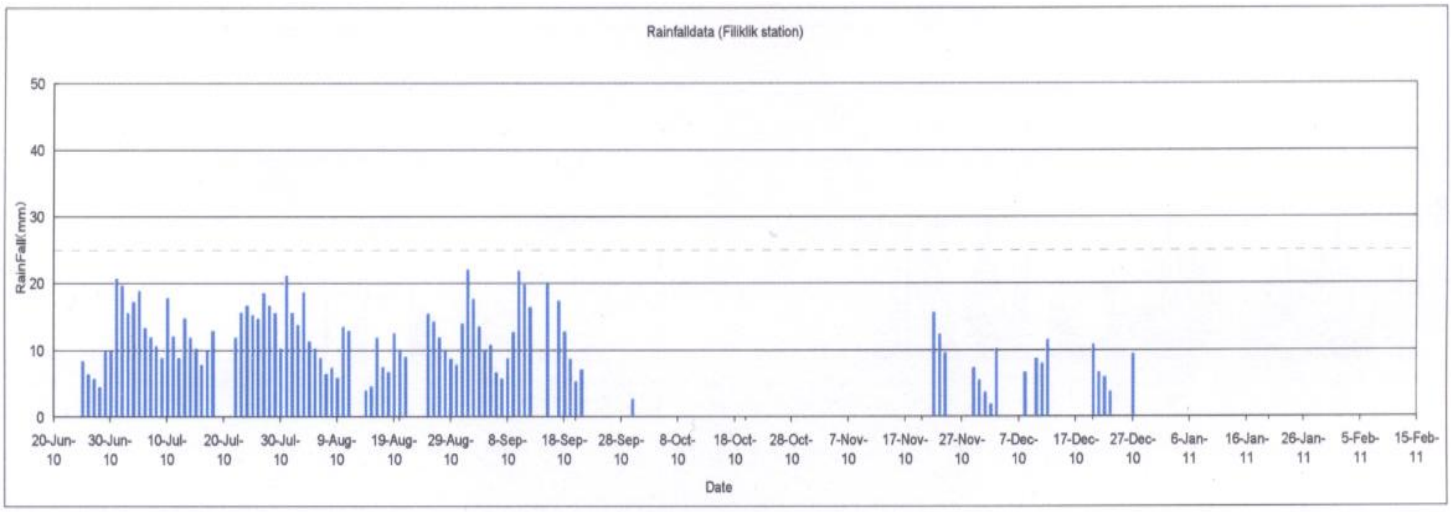

Figure 3-3 Rain fall Reading at Bridge station, Gohatsion station and Fliklik station (3)

From the Extensometer reading it has been observed that there is expansion in displacement around 15mm this also corresponds to the rainy season June to October as i have seen from rain fall data. At the middle of October it is observed that magnificent increment of displacement is recorded this is due to external disturbance of the Invar Line (wire) of the extensometer because there is no visible change in the cracks.

Table 3-3 Summary of Horizontal Extensometer Reading Data

Locations	Displacement Readings	Remark
L/S00	Up to 15mm	Expansion In Rainy season
	Up to -25 mm	Contraction in Dry season
L/S05	Up to 40mm	Expansion In Rainy season
L/S27	Up to 50mm	Expansion In Rainy season and continue to dry season also
L/S28	Up to 170mm	Expansion In Rainy season and continue to dry season also
	Up to 245mm	

3.2.2. Vertical Extensometer Survey

The purpose of vertical borehole extensometer is to measure the distance between the main part of the extensometer and the end of the wire that is installed in the borehole. When the wire is installed in an active landslide, the wire expands the length by movement of the landslide. The record of extensometer can be obtained in real time to compare with inducing factors, but it is difficult to identify the depth of the slip surface.

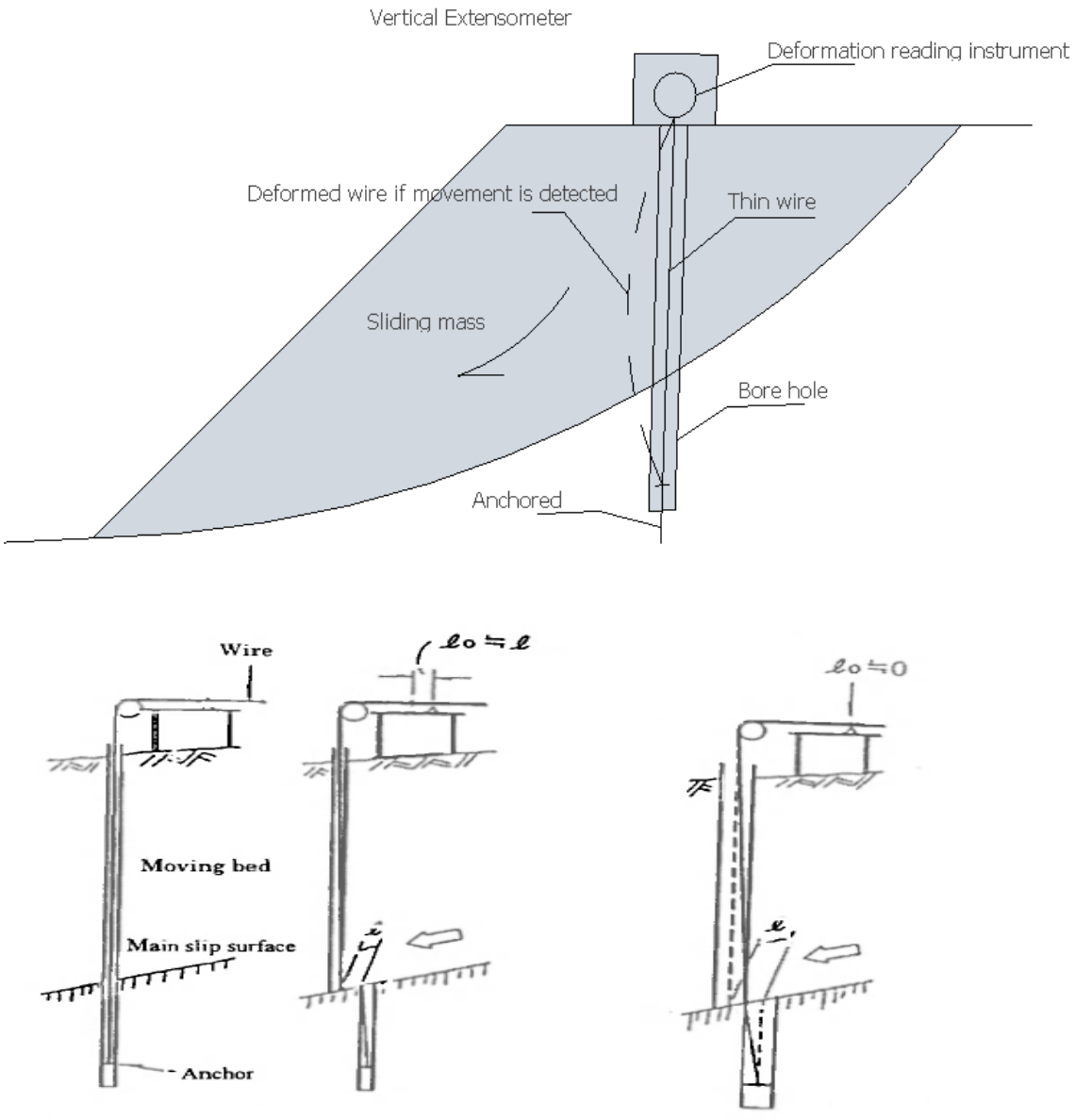

Figure 3-4 Conceptual diagram of Vertical Extensometer (3)

Typical Vertical extensometer reading at L/S05 is presented below for illustration the others reading is also summarized.

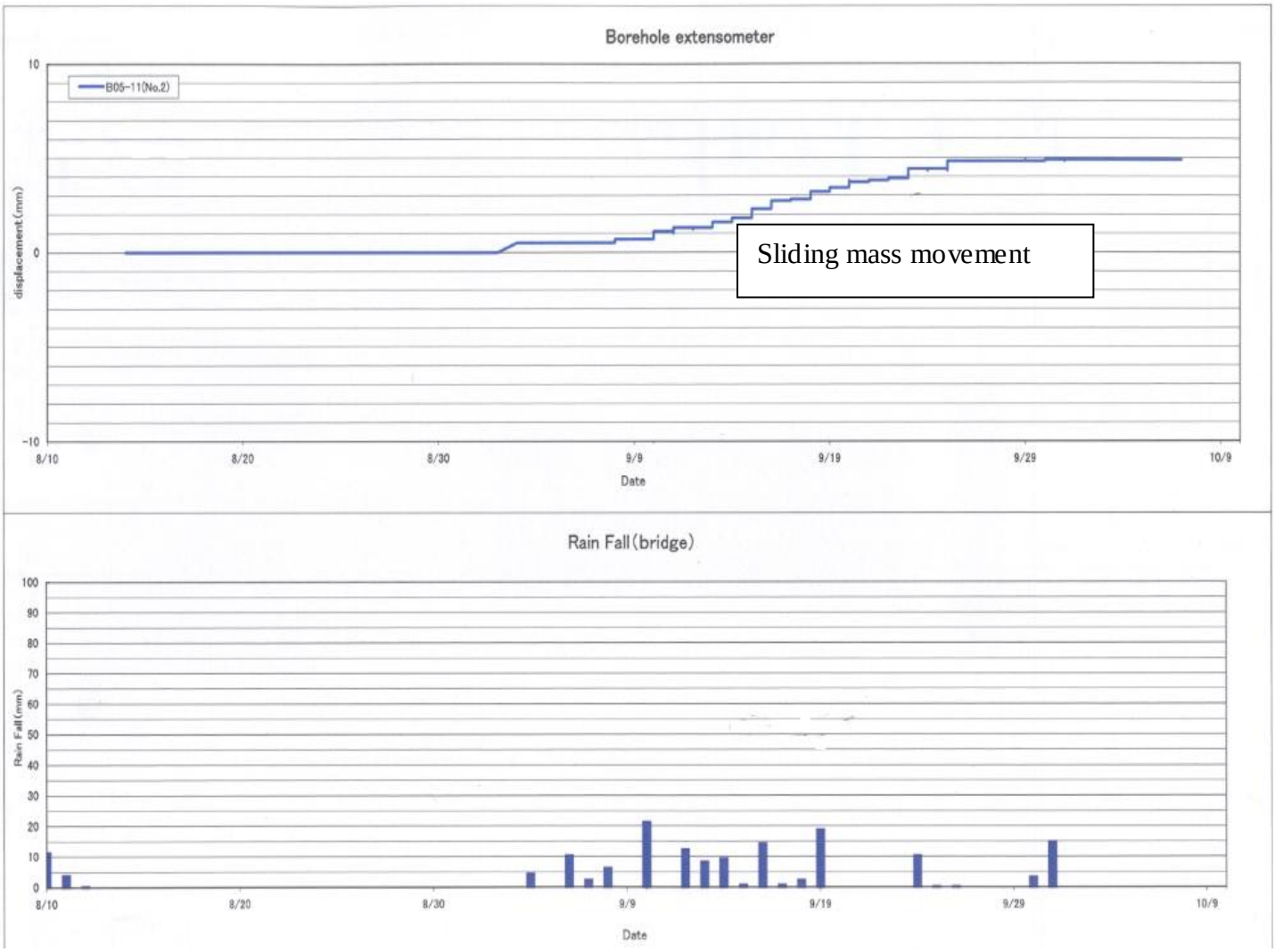

Figure 3-5 Vertical Extensometer Reading at L/S05 with Rain fall data at Bridge station (3)

The Vertical Extensometer reading shows displacement around 5mm corresponding to the rainy season. This implies the occurrence of sliding mass movement. In other vertical extensometers movement is not detected this is may be the installation of the instrument is late to the rainy season.

3.2.3. Inclinometer Survey

The purpose of borehole inclinometer is to measure the inclination of the guide pipe that is installed in the borehole. When the guide pipe is installed in an active landslide, the guide pipe is bent by movement of the landslide. The guide pipe is not straight at the initial state, initial value of inclination should be measured at the time of installation. If there is a great deal of landslide movement the inclinometer cannot be inserted at the point of the slip surface. The purpose of main slip surface survey is to determine the position of the slip surface. A borehole inclinometer

measurement is one of the most important factors to determine it, and also quantitatively grasp the displacement of a landslide.

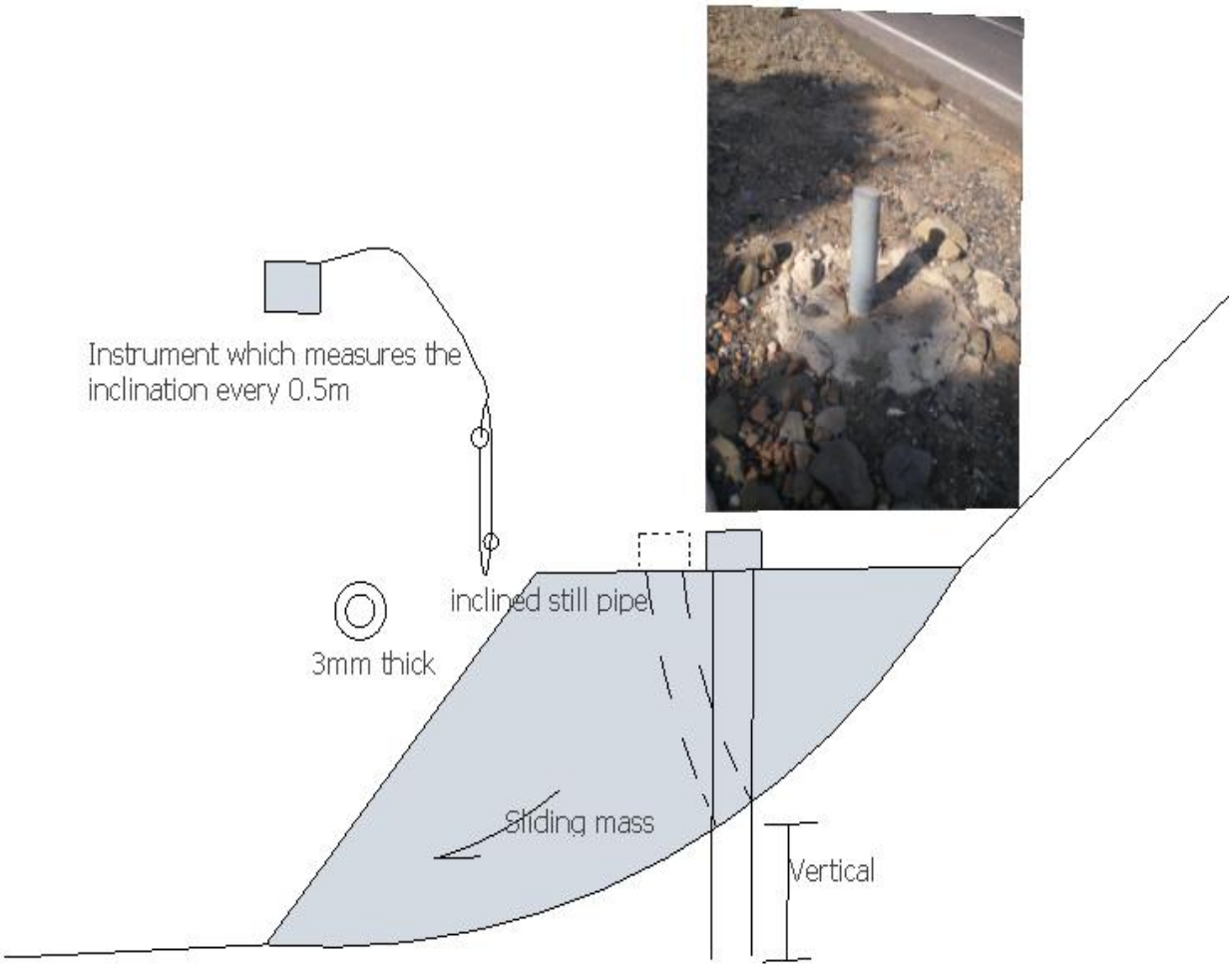

Figure 3-6 Conceptual diagram of Inclinometer

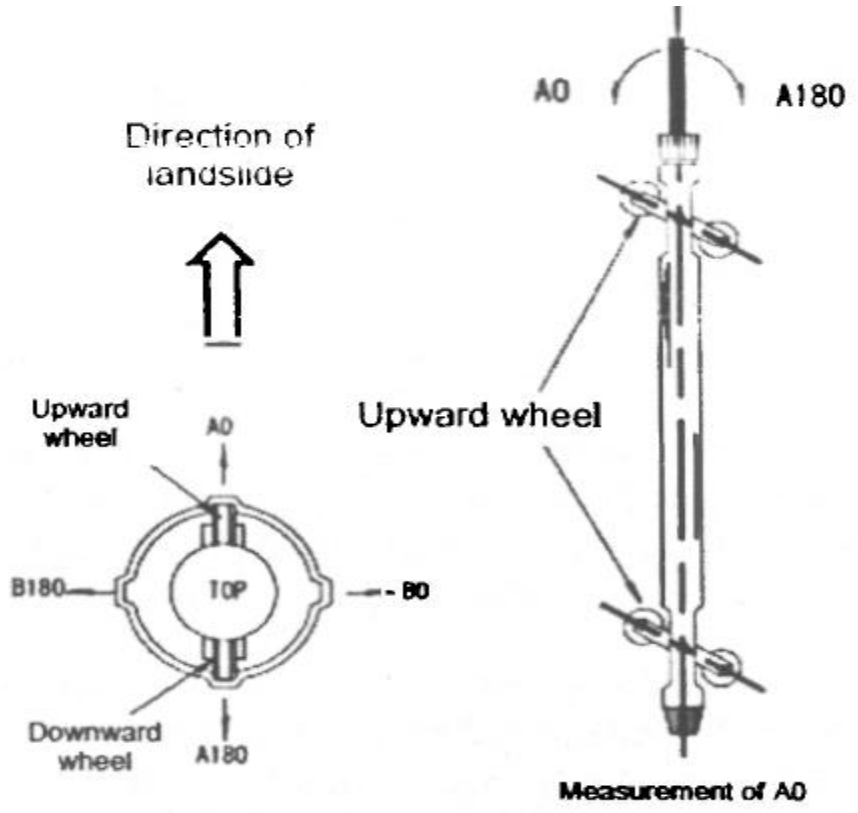

Figure 3-7 Conceptual diagram for measurement of borehole inclinometer (3)

Typical Vertical extensometer reading at L/S00 is presented below for illustration the others reading is also summarized.

As it has been seen from the reading below the impossibility of measurement at a depth of 16.6m is due to the collapse of inclinometer tube which is also the interface of Embankment and Basaltic layer. Similarly in other inclinometers also the interface of Colluvial deposit and Limestone, Colluvial deposit and Sand stone, Colluvial deposit and Tuff with Silt and Shale boundaries are mainly sliding interfaces.

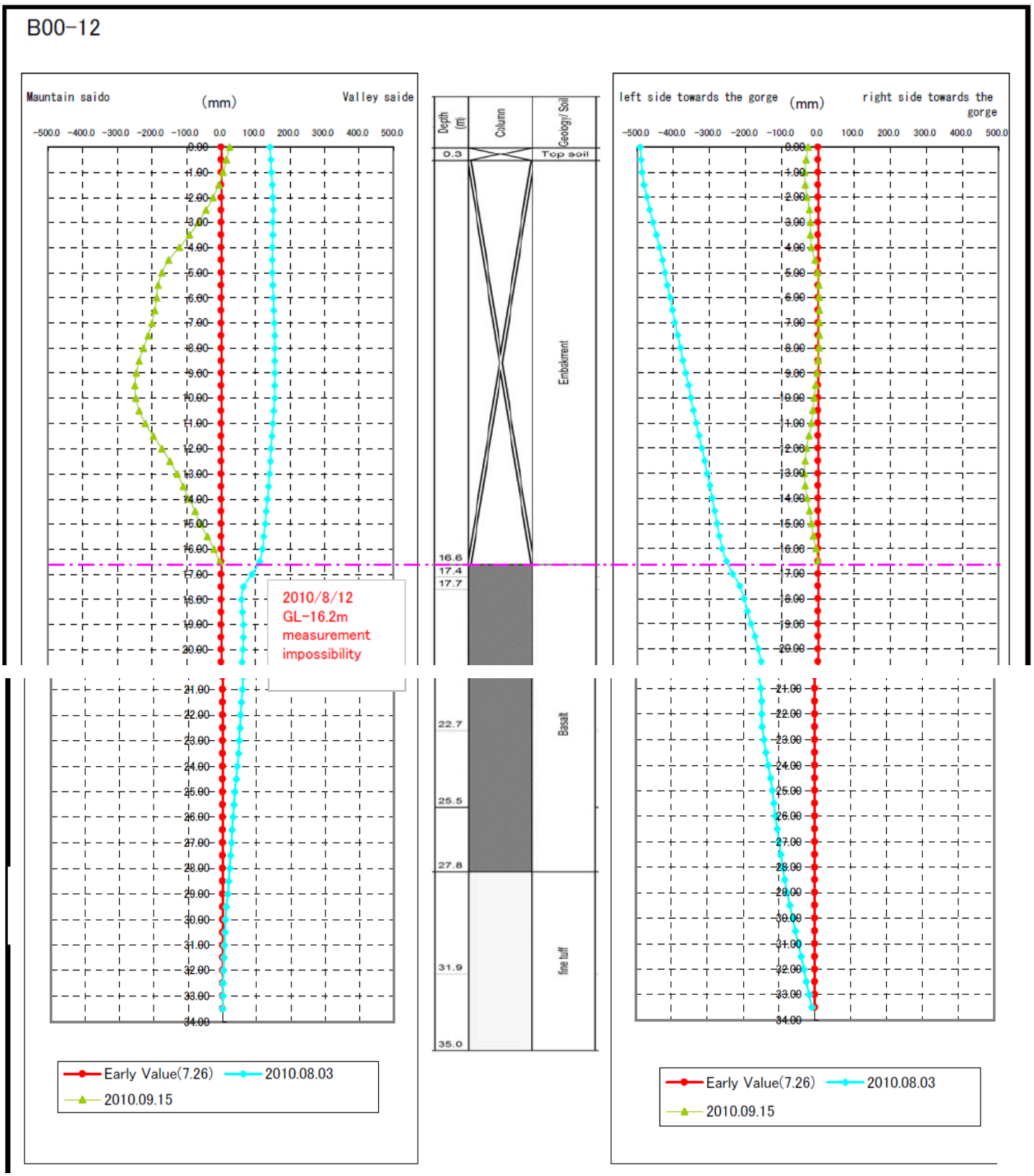

Figure 3-8 Vertical Extensometer Reading at L/S00 (3)

3.2.4. Groundwater Survey

The groundwater level in boreholes has been measured continuously, the correlation between groundwater level and precipitation is investigated, and also the relationship between groundwater level and landslide activity was considered. Frequency of data measurements was done from once to several times a month, while the frequency will be increased in the rainy season when there are more landslides.

Typical Readings taken from boreholes using automatic water level meter at L/S00 with the corresponding Rain fall data is presented below for illustration the others reading is also summarized.

From the reading it is observed that the rising of Ground water table (GW) is during the rainy season due to the percolation of surface water. This fluctuation of GW saturated the Interface of slip surface which increases sliding activity by developing pore water pressure that is driving force for sliding.

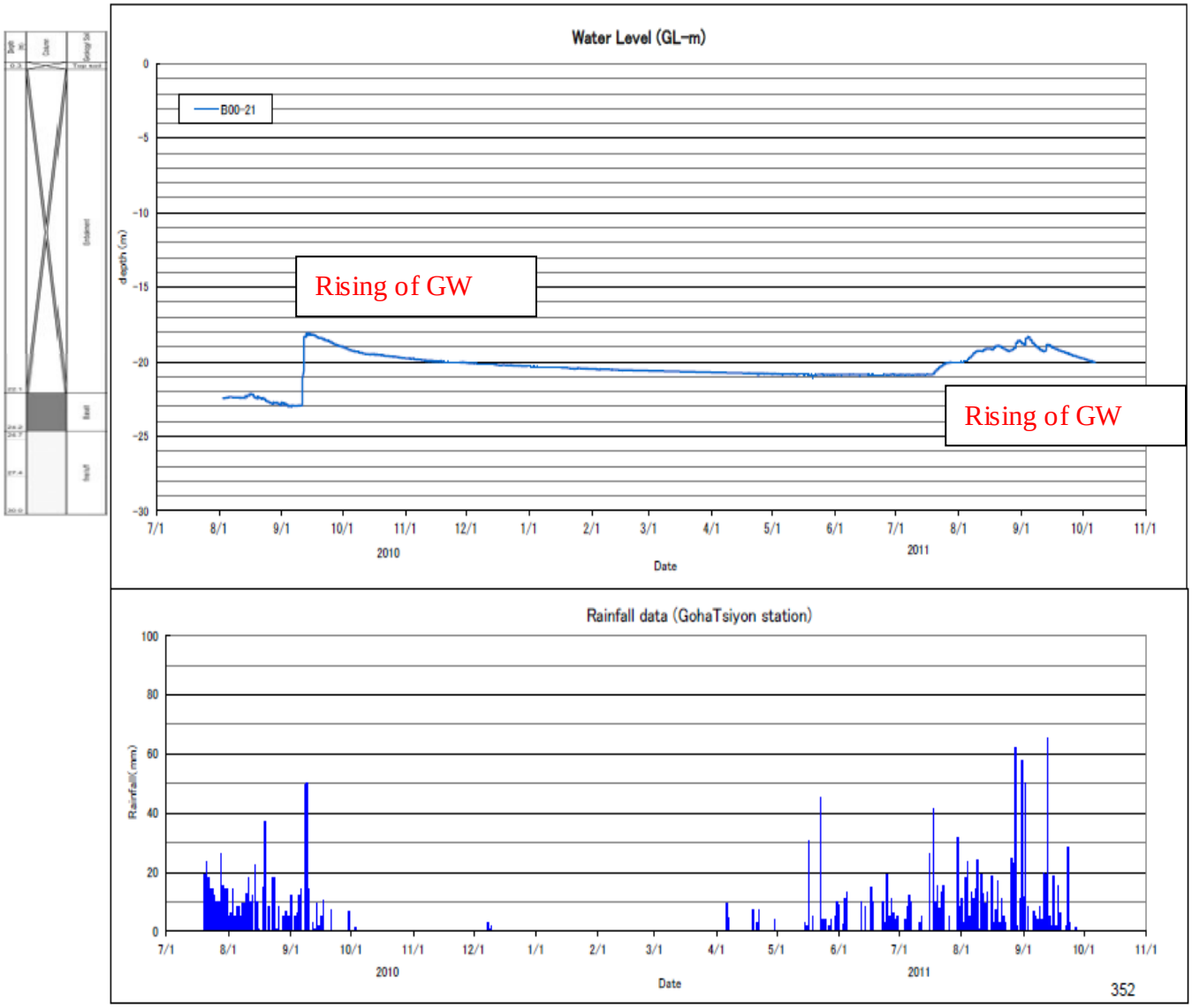

Figure 3-9 Automatic water level meter Reading at L/S00 with Rain fall data at Goha Tsiyon station (3)

3.2.5. Precipitation Survey

Inducing factors survey is necessary for determination of landslide mechanism and relation between landslide factors. In the study area, only precipitation observation has been conducted. Two precipitation observation stations (rain gauges) are installed at the Abay bridge and St. Gebrial Church site in addition to the existing stations at Gohatsiyon, Filiklik and Dejen stations. The reading of each station is presented in the above figures corresponding with the effect in the instrumentation readings.

3.3. Laboratory test results

Under laboratory investigation the JICA research team conducted different physical and chemical tests such as bulk density, sieve analysis, specific gravity, water absorption, porosity, pipette analysis and X-Ray diffraction (XRD) tests in the Geosciences laboratory center of the Geological Survey of Ethiopia (GSE) to identify the rock and soil properties with parallel to the drilling logo preparation.

For the analysis purpose in this thesis two representative sample areas L/S00 and L/S28 are selected from those five extremely damaged priority stations, so the adopted drilling Log data includes test results conducted for these two stations only.

Different Boreholes in L/S00 and L/S28 are used to determine the geological cross sections. Typical drilling log for BH00-11 is presented below for illustration.

Table 3-4 Typical Drilling Log for BH00-11 at L/S00 (3)

Drilling log

Name of Study : THE PROJECT FOR DEVELOPING COUNTERMEASURES AGAINST LANDSLIDESIN THE ABAY RIVER GORGE

Borehole name	BH00-11	Location	Around 1km from Goha Tsion, Abay Gorge area, National road 3	Latitude	10.01.267
Organization	Geological Survey of Ethiopia, JICA Study Team	Duration	9th/Jul/2010 to 15th/Jul/2010	Longitude	38.14.360
Surveyer	Makito NODA	Core appraiser	Takeshi KUWANO	Drilling operaters	Getnet Kassaye
Elevation (m)	2,435	Depth (m)	50.0	Drilling rig, Engine, Pump	Crysten Rig, Crystensen, Triplex
Angle	Vertical	Direction	Gradient	Remarks	Installation of borehole extensometer

Scale (m)	Elevation (m)	Thickness (m)	Depth (m)	Column	Geology/ Soil	Colour	Relative density	Hardness	Weathering	Size	Geological logs	Groundwater level (m)	Core recovery (%)	Maximum length (cm)	Rock Quality Designation	SPT N value	In-site test	Laboratory test
	2434.8	0.2	0.2		Top soil						Top soil (replaced by cement for drilling)							
1.0													90	13	13			
2.0													95	18	18			
3.0									relatively fresh	5-18 cm	Fresh massive basalt with weathered cracks. The crackes are red-brown in color by weathering.		90	14	42			
			3.1								3.1-4.5m: More fragmented. The cracks are dominantly red-brown							
4.0					Basalt	bluish grey	relatively high	hard	mode rately	-8cm			85	14	14			
	2430.5	4.3	4.5															
5.0													85	8	0			
6.0													95	15	15			
7.0	2428.1	2.4	6.9		Sandstone	white brown	moderately	relatively brittle, soft	relatively weathered	2-40cm	Tufficeous sandstone with weathered cracks. The crackes were red-brown in color by weathering. 6.7-6.9m: highly weathered, grey to black brown mud which is soft and brittle.		100	40	89			
8.0													100	35	60			
9.0													100	35	65			
10.0													95	25	47			
11.0													90	30	55			
12.0													100	33	63			
13.0													100	28	69			
14.0													100	35	90			
15.0													95	8	0			

Continued from Table 3.4

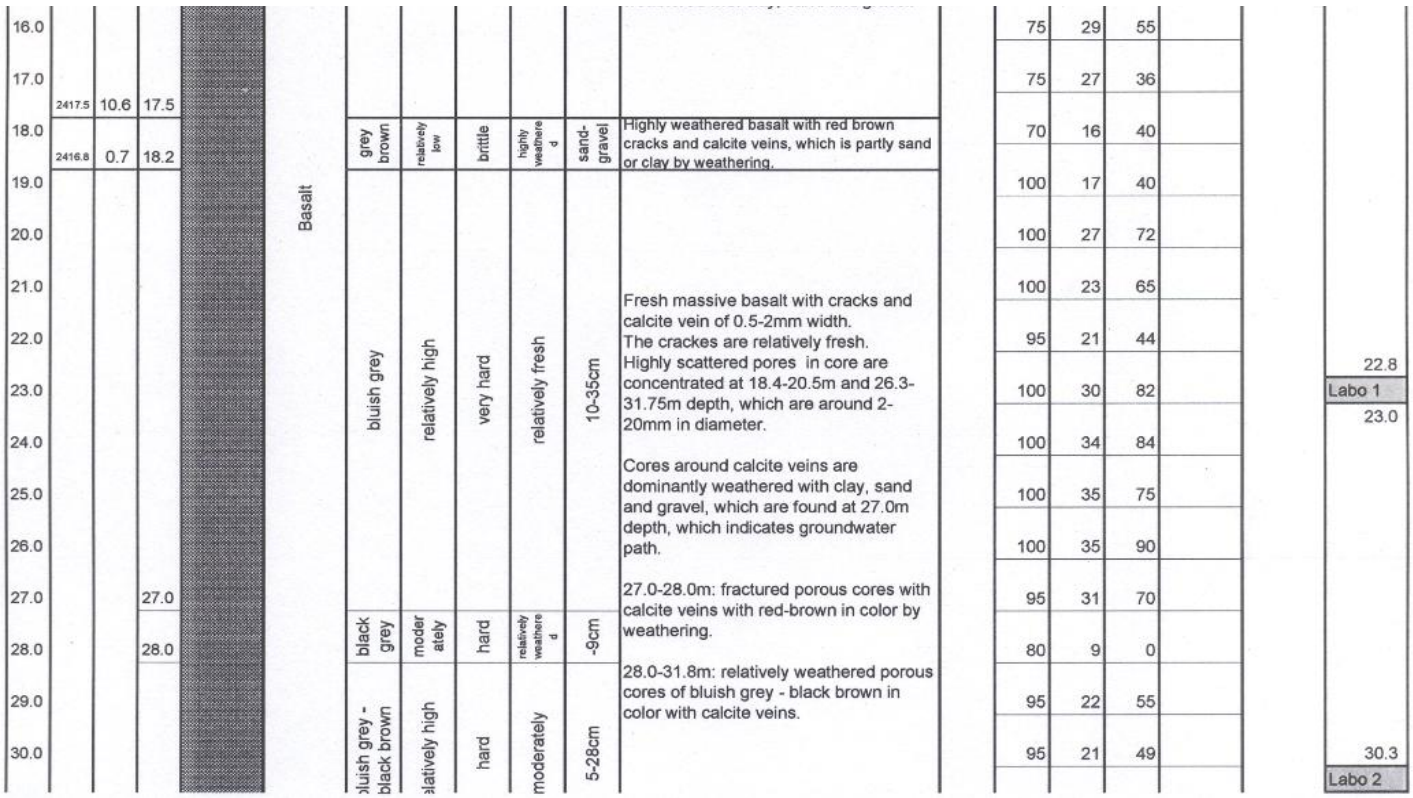

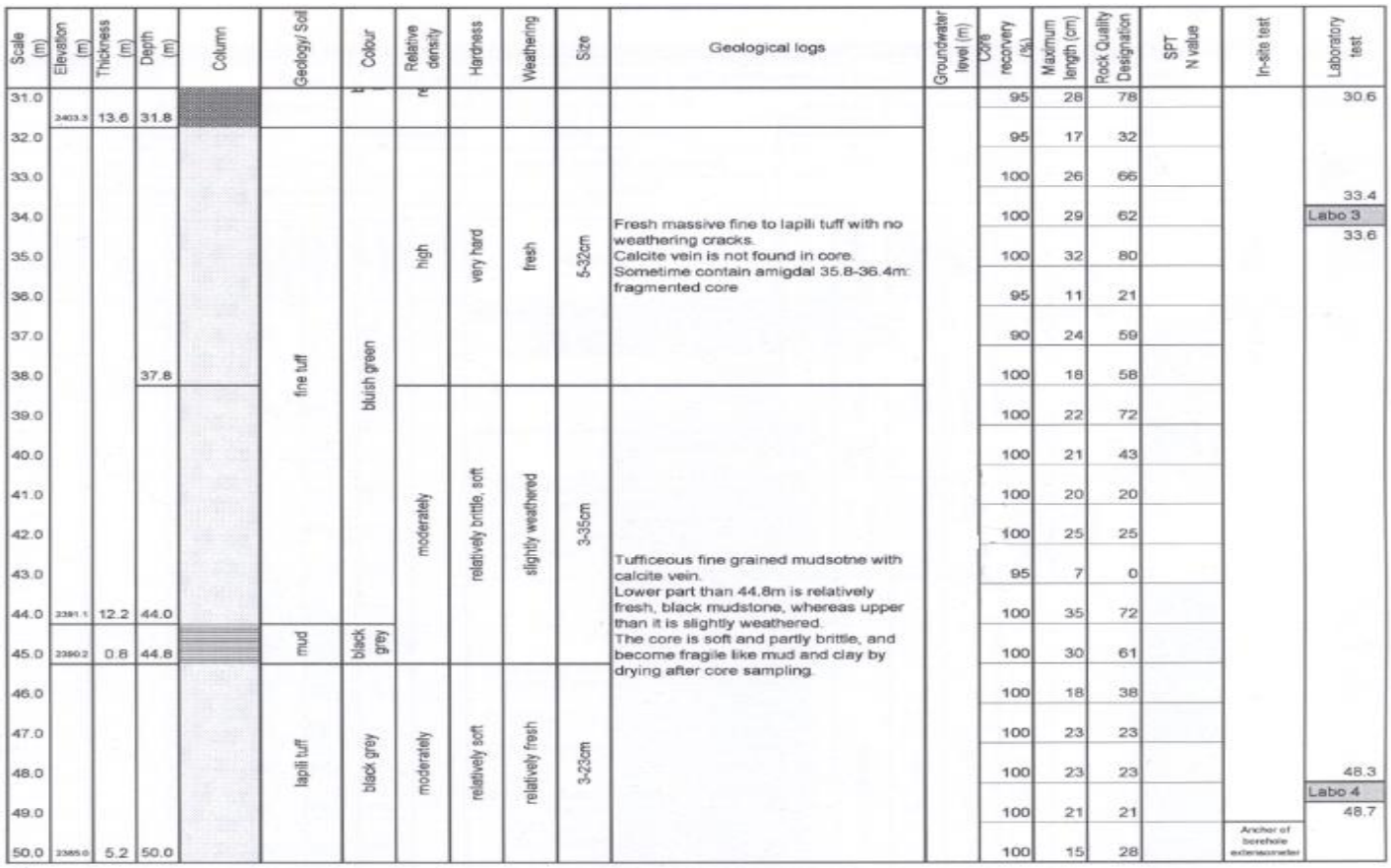

Figure 3-10 Core photographs for Bore Hole 11 at L/S00

Figure 3-10 Core photographs for Bore Hole 11 at L/S00

Figure 3-10 Core photographs for Bore Hole 11 at L/S00 (3)

4. ANALYSIS AND DISCUSSION

4.1. Landslide Block Interpretation

In this section, the geology of each landslide block is summarized based on the results of geological reconnaissance, the sample core photograph observation of the drilling operation with the drilling logs.

4.1.1. Geology of the landslide in L/SOO (ST.0+200 to 1+100)

The area is located in basalts and pyroclastic rocks. The main road was mainly constructed on the bedrocks, and the embankment runs through the boundary of the cliff and the flat plane. The presumed stratigraphic classification is described as follows.

Table 4-1 Schematic geological column in the landslide L/S00

Geology	Remarks	Borehole
Basalt(1)	Flat plane of Goha Tsiyon village.	BH00-11
Pyroclastic(1)	Sandy tuff to tuffaceous sandstone. 2-5 m Thickness. Flat plane on top of the basalt (2).	BH00-11
Basalt(2)	Massive with pillow lava. Cliffs on road side.	BH00-11
Pyroclastic(2)	Fine tuff to lapili tuff with mudstone-like tuff. Widely Exposed at the road side.	BH00-11
Basalt(3)	Highly weathered porous basalt. Very soft and Brittle.	BH00-12, BH00-21
Pyroclastic(3)	Fine tuff to lapili tuff. As deeper, Fresh rod-like Mudstone.	BH00-12, BH00-13, BH00-21
Basalt(4)	Escarpments over 100 m thick below the area. Developed columnar joints	

Each layers composition, thickness, water permeability and the intercalated materials detail description is presented below, from this it can be easily identify the most probable slipping interface during the saturation stage.

a.l Artificial embankment

Artificial backfill embankment is composed of basalt cobbles/boulders (5-60 cm), gravel, sand, mud land clay. The thickness of the layer is up to 22 m in this area. Water permeability of the layer is considered to be very high.

a.2 Colluvial deposit

Colluvial deposit is mainly composed of basalt cobbles/boulders (5-600 cm), gravel, sand, mud and clay including black and organic soil as "black cotton soil", which have come from the mountainous side cliff. The deposit overlies on the surface with 0-5 m thickness, and partly intercalated with around 20 m thickness under the artificial embankment. Water permeability of the deposit is considered to be very high.

a.3 Basalt (1)

Basaltic lava which is distributed on the uppermost layer of the area is purported as "basalt (1)" in this thesis. The basalt is widely exposed over 40 m thick. The unit is mainly black to dark grey and has clearly developed vertical columnar joints (20-50 cm). Small holes (3-10 mm) by foaming are scattered in the rock. Water permeability of the layer is controlled by the columnar joints and it is high. The top surface of the unit forms the flat plane of Gohatsion Village and it also shows steep escarpments at the beginning of the Abay Gorge.

a.4 Pyroclastic rock (1)

Pyroclastic rock (1) is intercalated between the upper basalt (1) and after-mentioned basalt (2). The unit is sandy tuff to tuffaceous sandstone with lenticular clayey mud layers. It is very soft and brittle, and is susceptible to weathering and erosion, resulting in a flat plane on top of the basalt (2). The color is mainly white to grey which is relatively fresh area and grey to black brown which is highly weathered. The layer is partly exposed at the area and at 4.5-6.6 m depth of BH00-11. The thickness is around 2-5 m. The strike of the bedding is EW with 10-60 north dipping. Water permeability of the layer is moderate, and the groundwater from the columnar joints of the upper basalt flows out from top of this tuff layer.

a.5 Basalt (2)

This layer is basalt lava. The structure is "massive" which means that columnar joint is little or nothing, and relatively fresh. Spherical structure like pillow lava is observed at top of the unit. The fresh part of the unit is bluish grey, whilst the weathered area is grey brown with red brown cracks. Small holes (1-4 mm) by foaming are sparsely scattered at the upper part in the rock. Water permeability of the layer is controlled by the joints and it is high. Basalt (2) is exposed on the mountainous side and at 6.9-31.8 m depth of BH00-11, and forms cliffs on the main road side. The boundary of the overlying pyroclastic rock (1) is unclear. The thickness is around 5-30 m.

a.6 Pyroclastic rocks (2)

Pyroclastic rock (2) is intercalated between the upper basalt (2) and after-mentioned basalt (3). The unit is fine tuff to lapili tuff with partly sandy tuff. Mudstone-like tuff with dark grey in color is partly observed as outcrops and the core samples. It is susceptible to weathering and erosion, resulting in overhung landform under the basalt (2). The top of the unit which is boundary to the basalt (2) is especially soft and brittle because of the contact of basalt lava, which results in rock fall and slope failure. The color is bluish green to black grey which is relatively fresh area and brownish grey to red brown which is highly weathered. The layer is widely exposed at the road side and below 31.8m depth of BH00-11. The thickness is estimated around 30-40 m and becomes thick toward the end point. The bedding plan is unclear in this area. Water permeability of the layer is moderate, and the groundwater from the upper basalt flows out from top of this layer.

a.7 Basalt (3)

Basalt (3) is obtained under the embankment as core samples of BH00-12 and BH00-21. The layer is considered to be distributed as almost horizontal sheet, which is 2-11 m thick. The core samples are highly weathered porous basalt with cracks which are red-brown or black in color by weathering. Fractured and weathered parts are mainly composed of clay, sand and gravel. It is very soft and brittle by weathering. Water permeability of the layer is controlled by the joints and the cracks and it is considered to be high.

a.8 Pyroclastic rocks (3)

Pyroclastic rock (3) is observed as core samples of BH00-12, BH00-13 and BH00-21. The unit is fine tuff to lapili tuff. The mudstone-like tuff with black in color is observed below 33.9 m depth of BH00-13. As deeper, the core sample gradually becomes fresh rod-like mudstone. Weathered

parts are clay, sand and gravel with cracks which are red-brown or black in color by weathering. The color is bluish green to grey which is relatively fresh area and brownish grey to brown which is highly weathered. It is soft and brittle, and is susceptible to weathering and erosion, resulting in a flat plane on top of the basalt (4).

a.9 Basalt (4)

The basalt is widely exposed as steep escarpments over 100 m thick below the area. The unit is mainly black to dark grey and has clearly developed columnar joints which are mainly horizontal direction (around 20-100 cm). The top surface of the unit forms flat plane under this area, and it is exposed on the river surface next to the landslide site. Water permeability of the layer is controlled by the columnar joints and it is considered to be high.

Representative geological cross section is prepared on the basis of the geological features of landslide block in the previous description.

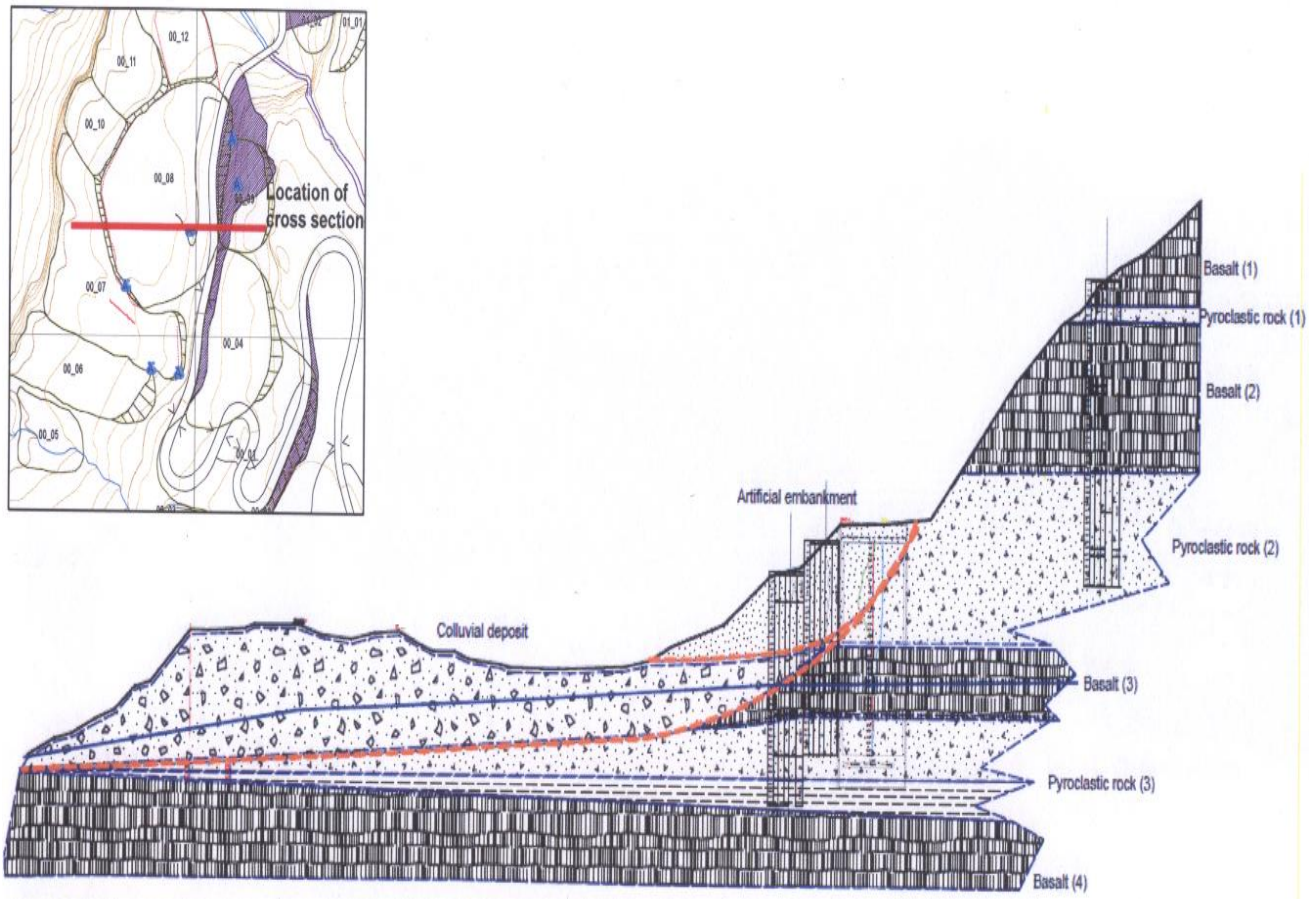

Figure 4-1 Geological cross section in L/S00 (3)

4.1.2. Geology of the landslide in L/S28 (ST. ST.28+100- ST.28+800)

The area is considered to be located on the siltstone, the shale and the limestone. Landslide activities are frequently observed in this area, especially in the rainy season. Hence the boundary of the base rock, which consists of the siltstone and so on, and the sliding soil mass cannot be clearly identified. The presumed stratigraphic classification is described as follows.

Table 4-2 Schematic geological column in the landslide L/S28 (3)

Geology	Remarks	Borehole
Limestone	Thick limestone beds and tuffaceous beds. Steep cliff including overhung. Grey white to white in color.	
Silt and shale	Siltstone and shale with limestone mixed with sliding soil mass. Gentle slope. Landslide forms.	BH28-11,21,31,32,41

For these layers also Composition, Thickness, Water permeability and the intercalated materials detail description is presented below, from this it can be easily identify the most probable slipping interface during the saturation stage.

b.l Colluvial deposit

Colluvial deposit is mainly composed of basaltic gravel, tuffaceous gravel, sandy gravel, mud and clay. The matrix is mixed with basalt, tuff, silt, shale and limestone. Most gravel is 2-6 cm in diameter, and is sub-angular and angular. The deposit is estimated to overly the "silt and shale" with a thickness of around 10-20 m on. There are several "basalt debris layers" in the colluvial deposit, which are mainly composed of basaltic gravel and basaltic tuff breccia in black grey in color. The layers are mainly observed at around 15 to 25m depth in the drilling core in the L/S28 block. The layers might be related with slip surface in the area. The colluvial deposit is mixed up with sliding soil mass in the area where landsides frequently happen, especially in the rainy season, therefore it is difficult to clearly classify the colluvial deposit and the sliding soil.

b.2 Limestone

The limestone which is fine grained overlies the "silt and shale" area. In general, it is horizontally bedded. The structure is "stratification" which means that it is composed dominantly of alternative layers of thick limestone beds and tuffaceous gravel or clay beds. It forms steep cliffs including overhangs. The surface of the outcrops has been highly weathered and become brittle. The color is slightly grey-white to white. Water permeability of the layer is relatively low.

b.3 Silt and shale

These units are mainly composed of siltstone and shale with minor limestone. These are mixed up with sliding soil mass in the area where landsides frequently happens, especially in the rainy season, therefore it is difficult to classify the sliding soil. The siltstone unit is composed of silt/clay particles cemented together. It is found intercalated with shale, mudstone and sandstone with calcite and/or gypsum veins in places. The color is white brown to reddish brown which have been weathered and yellowish green to brownish grey which are relatively fresh. The shale unit is argillaceous clastic sedimentary rock which contains a lot of clay minerals. A part of the shale is totally changed to clay by weathering, which is relatively soft and weak due to weathering.

The layers are susceptible to weathering and erosion, therefore the area shows an almost flat plane and/or gentle slope in the village area. In this area a gentle slope is formed by removed soil and has lots of landslide forms. Representative geological cross section is prepared on the basis of the geological features of landslide block in the previous description.

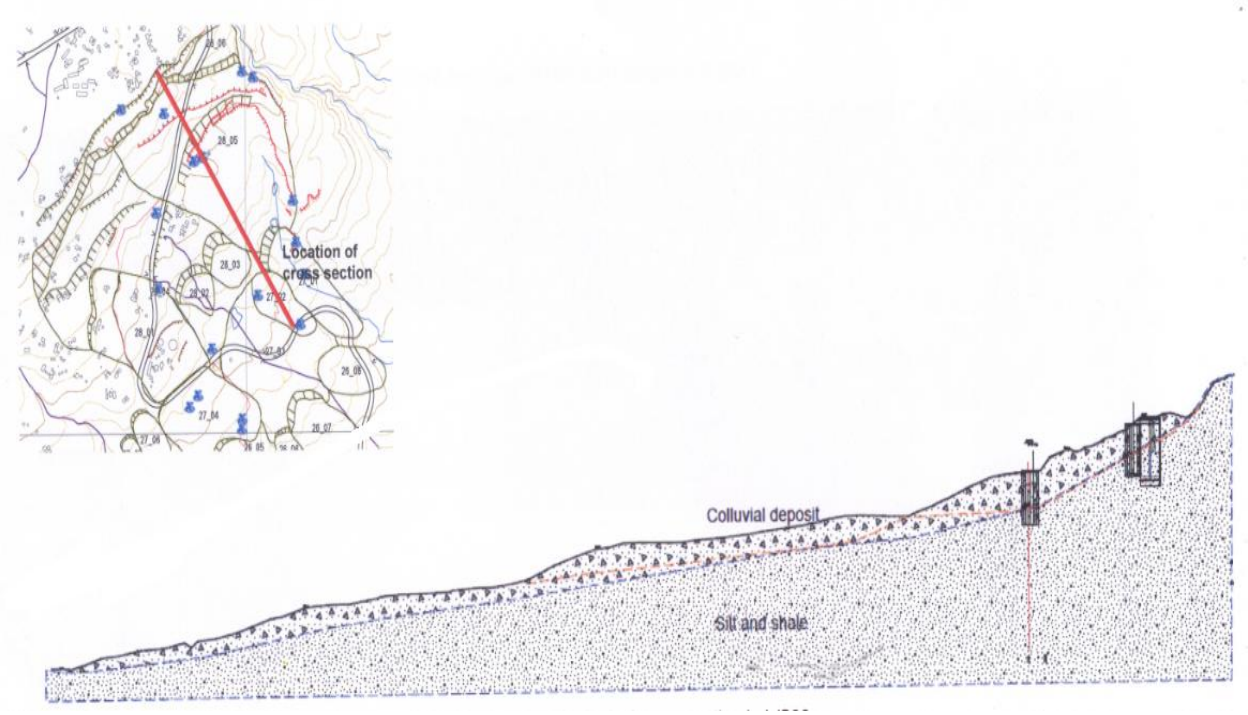

Figure 4-2 Geological cross section in L/S28 (3)

4.2. Discussion on Hydrological data

The record of landslide occurrence in the Abay Gorge shows that most landslides are concentrated mainly in July to September in the rainy season.

Table 4-3 Record of Landslide Occurrence

Station No.	Time	Others
ST.0+700- ST.1+100	2008 rainy season	Road settlements Every rainy season
	2009 rainy season	Ditto
	2010 rainy season	Ditto
ST.4+900- ST.5+200	2006 Aug ~Sep	Collapse of existing retaining wall
ST.21+850- ST.22+200	2008 rainy season	Collapse of retaining wall
	2009 rainy season	Landslide area expansion
ST.27+500- ST.27+800	2006 unknown	Old church destroyed New church under construction (cracks found)
	Every rainy season	Road subsidence
ST.28+100- ST.28+600	Every rainy season	Road subsidence and cracks
ST.32+250	2009	Road culvert is damaged

The presence of streams and spring waters greatly influences the stability by toe erosion or by saturating the slope material or both. It is clear that the water which flowed into the osmosis and the mountain streams of surface water by rain turned into groundwater, and has contributed to the rise of the groundwater level. In the area high drainage density is observed. The Drainage network prepared by the JICA project shows the river network of the section between Dejen and Gohatsion.

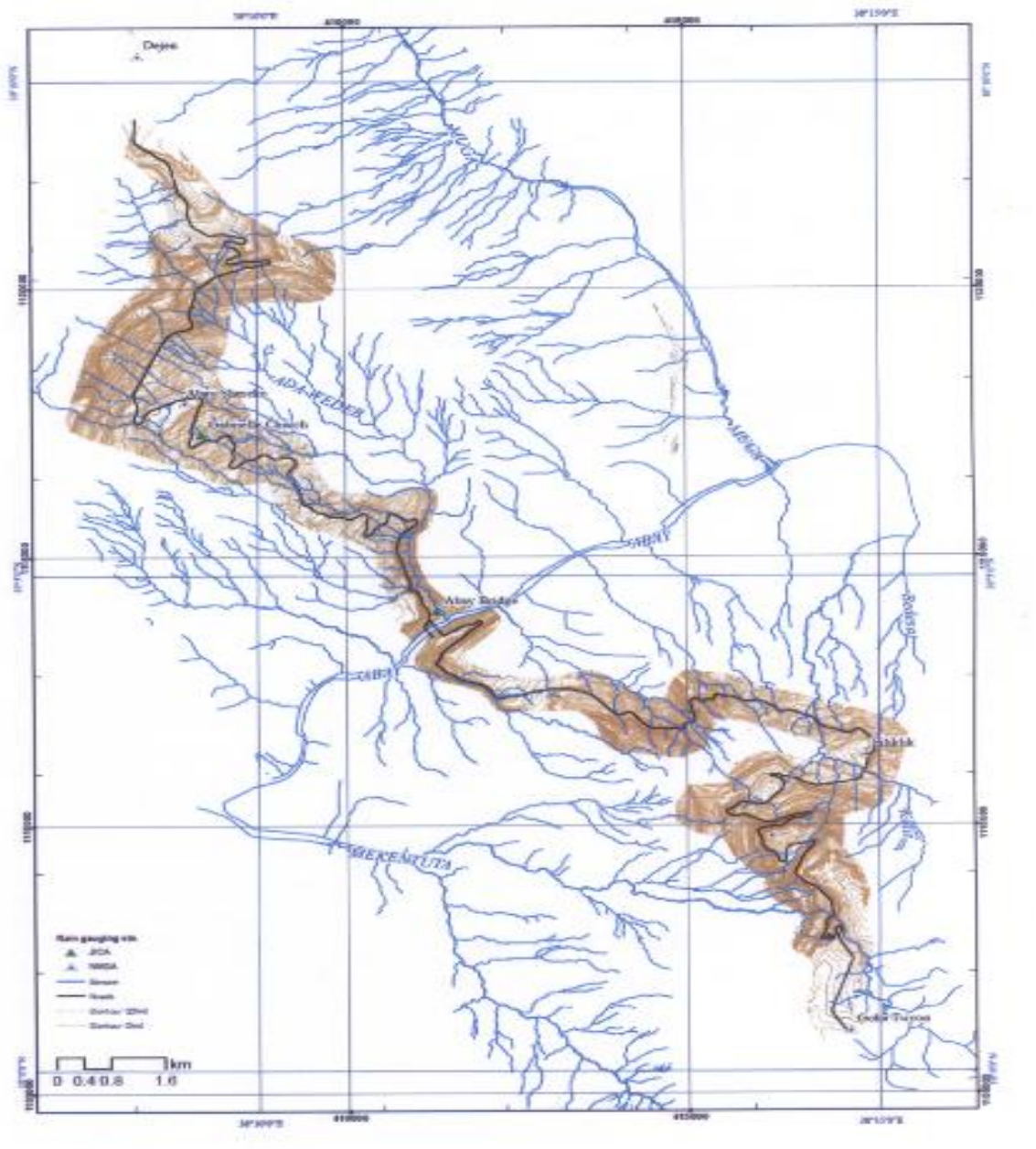

Figure 4-3 Drainage network (3)

4.3. Discussion on monitoring data

The results of the observation and monitoring with the equipment which were installed in the Rainy season in 2010 are summarized in table 4.4. The assumed activities of the landslides were examined but to accurately identify the movements of the landslides the monitoring is continuing in each rainy season. The monitoring data interpretation for L/S00 and L/S28 landslide block is described as followed.

Table 4-4 Outline of the monitoring results

Location	Extensometer		Borehole Extensometer		Borehole inclinometer		Water level meter	
L/S00	EX-1	17.0mm (Compression18.0mm)	B00-11	No movement	B00-12 B00-22	16.2m 10.5m (collapse of borehole:14 m)	B00-21	-20 to -23m Highest: -18.1m
L/S05	EX-2	46.5mm	B05-11	7.0mm	B05-21	6.6m (minute movement:2 9.8m)	B05-12	-31 to -32m Highest: -31.0m
	EX-3	40.5mm			B05-22	11.6m (minute movement:2 8.0m)	B05-31	-22 to -23m Highest: -22.2m
L/S22					B22-11	18.0m (minute movement:5. 5m)		
L/S27	EX-4	53.0mm	B27-12	No movement	B27-11	7.5m	B27-21	-22 to -24m Highest: -21.9m
	EX-5	167.5mm			B27-22	15.0m	B27-23	-20 to -21m Highest: -20.3m
L/S28	EX-6	246.2mm	B28-41	No movement	B28-11 B28-31 B28-32	14.7m 13.0m 24.5m	B28-21	-20.0m Highest: -20.0m

a. Location L/S 00

At extensometer EX-1 the movement which is opening in rainy season and closing in dry season of the cracks in this block is considered to be notably related with the precipitation (and/or the temperature). At borehole extensometer BOO-11(50m depth) there has been no movement even throughout the rainy season. It is considered, therefore, that there are no landslide activities below 50m depth in that area. At borehole inclinometer B00-12(35m depth) the casing pipe was

broken by the movement of the landslide at 16.2m depth and at borehole inclinometer B00-22(21m depth) the measurement has not been able to be implemented since the collapse of the borehole at 10.5m depth when the casing pipe was installed The broken pipe and the collapsed borehole is attributed to landslide movement. It is considered that there are slip surfaces around these depths accompanying active landslide movements.

At water level meter B00-21 (30m depth) installed on the roadside, the steady water level of -22 to -23m and the high water level of -18.1m from August to October 2010 were recorded. The steady water level keeps about -20m after October.

b. Location L/S 28

At extensometer EX-6 installed on the step of the head of the landslide, extension movement started in early July and was continuously occurring until late November 2010, and the extension movement reached 211.8mm. The movement re-started on January 2011, and it reached 246.2mm in the middle of February. It is considered, therefore, that the landslide intensively activates in the rainy season and is continuously moving even in the dry season.

At borehole extensometer B28-41(45m depth) installed on the roadside in September 2010, there has been no movement even throughout the rainy season. It is considered, therefore, that there is no landslide activity in that area. At borehole inclinometer B28-11(25m depth) installed on the roadside on September 2010, the Measurement has not been able to be implemented since October 2010 because the bending of pipe occurred at around 14.7m depth. At borehole inclinometer B28-31(25m depth) installed on the roadside in September 2010, a distinct slip surface was confirmed at around 13.0m depth, and the measurement has not been able to be implemented since December 2010 because of a deep bending of the pipe. At borehole inclinometer B28-32(40m depth) installed on the roadside in October 2010, the measurement has not been able to be implemented since November 2010 because the bending of pipe occurred at around 24.5m depth. It is considered, therefore, that there are slip surfaces around these depths accompanying active landslide movement.

At water level meter B28-21 (25m depth) installed on the roadside in September 2010, both the steady water level and the high water level keeps around -20m.

4.4 Discussions on the slip surface

The landslide blocks and cross sections of the slip surface developed based on the results of the geomorphological and geological analysis, the site reconnaissance, and the monitoring are used for the slip surface analysis. Based on the sampling data of the borehole core, it is considered that the geological boundary and heavily weathered and/or clayey thin layer are the slip surfaces. The landslide block activities are estimated by extensometers, which observe displacement corresponding to rainfall. The monitoring data of the borehole inclinometer is used for the depth of the slip surface and displacement of the landslide mass.

The monitoring data of the water level meter is utilized for the analysis the groundwater level. However, the results obtained for each borehole were different from the altitude of the spring water at the site, this is because the monitoring is started late to the rainy season. The landslide blocks and slip surface were examined by other information regarding surface anomalies on the road and locations of spring water by site reconnaissance.

Hereinafter, the characteristics of the movements of the landslide block and the probable slip surface will be described as follows.

a. L/S 00 area

The L/SOO area is composed of 12 landslide blocks. Block 00-08 is the major landslide block that directly damaged the road in 2009 and 2010. In view of the landslide situation, block 00-08 is assumed to be a "complex slide". The scarp zone is at the eastern end of the road, and the end zone is in the terrace located east-southeast of the road. Depression zone formed as a result of the horizontal movement of the soil mass in the middle slope. The block is assumed to have moved from the embankment of the road, due to the rising of the ground water level in the rainy season of 2009 and 2010. The extrusion is observed at the end zone. New cracks occurred in this extrusion, and landslide blocks 00-07, 00-10, and 00-11 are assumed to have been triggered by this extrusion. In view of the cracks on the ground surface, block 00-07 is divided into smaller blocks.

Spring water was observed at three points in the rainy season of 2010: just above the slope of the road (altitude 2,390m), at the slope toe of the embankment (altitude 2,365m), and near the scarp zone of block 00-06 (altitude 2,375m). The spring water level is analyzed to draw the landslide cross section. The ground water level in B00-21 is different from the altitude of spring water at

the site. Therefore, the observed data of ground water in B00-21is not adopted for stability analysis. Multi-tuff layers existed at 27.8 to 28.4m depth and 31.5m depth for BOO-12, and a multi-tuff layer or a clay layer existed in another borehole. A tuff layer existed on the line connected at 25m depth in the embankment and 15m depth in the middle to lower slope. It is assumed that the tuff layer forms the slip surface because the layer has low shear strength.

Displacement of block 00-08 was detected at a depth of 17.0m depth by a borehole inclinometer in 2010. This displacement is assumed to have occurred at the inner embankment of the road; however, it could also extend to the entire block 00-08. In consideration of above mentioned results of the investigation and the monitoring, slip surfaces were discussed. The thick red line in Figure 4.4 denotes the possibility of the slip surface. Slip surface (1) is a landslide of the embankment which is the smallest volume in the area; slip surface (2) is a landslide continuing from the road to the end of the field plane; and slip surface (3), which is few possible, is a landslide continuing from the upper part of the basalt slope to the end of the field plane.

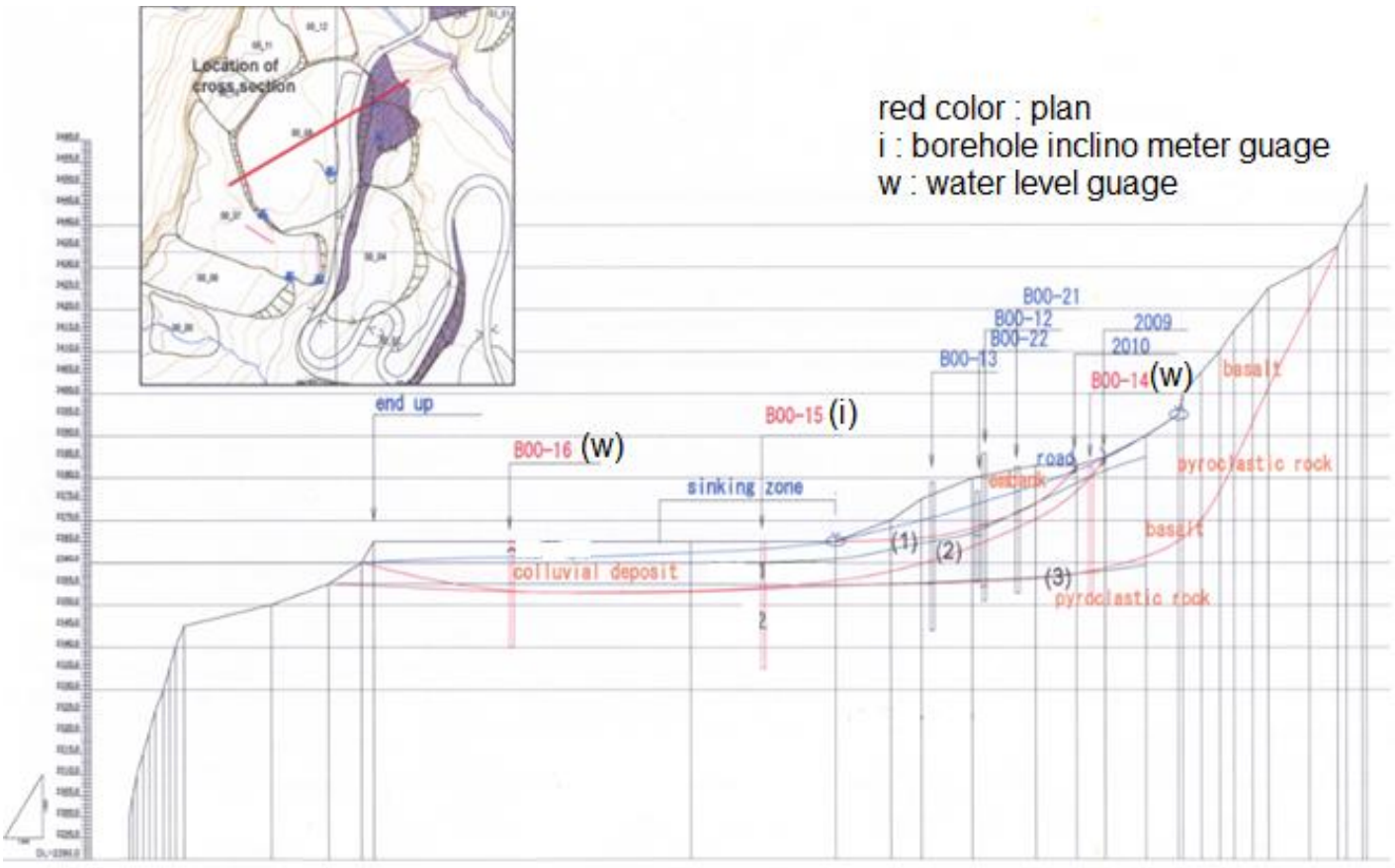

Figure 4-4 Landslide cross-section of L/S00 (3)

b. L/S 28 area

The landslide block in the L/S28 area continues from the upper slope to the lower slope. The large cracks of the scarp zone extend over the L/S27 area and the L/S28 area at an altitude of 1,810m. The depression zone, which is just below the scarp zone, is a source of water supply. While the colluvial deposit in the L/S27 area is composed of siltstone and shale, the one in the L/S28 area is different for each borehole. The colluvial deposit in B28-11 is composed of siltstone and shale, which in B28-21 is gravel of basalt and tuff, and that in B28-31 is limestone.

In the past, a large landslide occurred in the L/S27 and L/S28 areas. That the colluvial deposit of L/S27 is silt stone and shale shows the possibility of a deep landslide exists. Because the colluvial deposit of B28-21, B28-31 and B28-32 are different from each other, geological differences between B28-31 and B28-32 may exist, and the landslide blocks in them may differ. Blocks 28-03 and 27-02 exist under the landslide which length is 400m from middle to upper part of the slope. Block 27-02, which has a scarp located at an altitude of 1,715m, damages the road in the end zone.

Spring water is observed at three points in the rainy season of 2010: the depression zone (altitude 1,790m), the slope toe under the road (altitude 1,755m), and the end zone (altitude 1,725m). There are ponds in the slope toe on the valley side of the road and in the end zone of the dry season. Ponds form in the depression zone, and rain infiltrates from the zone. Therefore, infiltration water becomes spring water and oozes. The spring water level analyzed by the landslide cross section in Figure 4.5. The ground water level in B28-21 is different from the altitude of the spring water at the site. Therefore, the observed water level is not adopted in the stability analysis.

In consideration of above mentioned investigation and the monitoring, slip surfaces were discussed. The thick red line in Figure 4.5 denotes the possibility of the slip surface. Slip surface (1), which was identified by drilling survey, is a landslide from the upper slope to the end of the field; slip surface (2), which is needed to be identified on additional surveys, is a large landslide deeper than (1); and slip surface (3) is a landslide on the lower slope

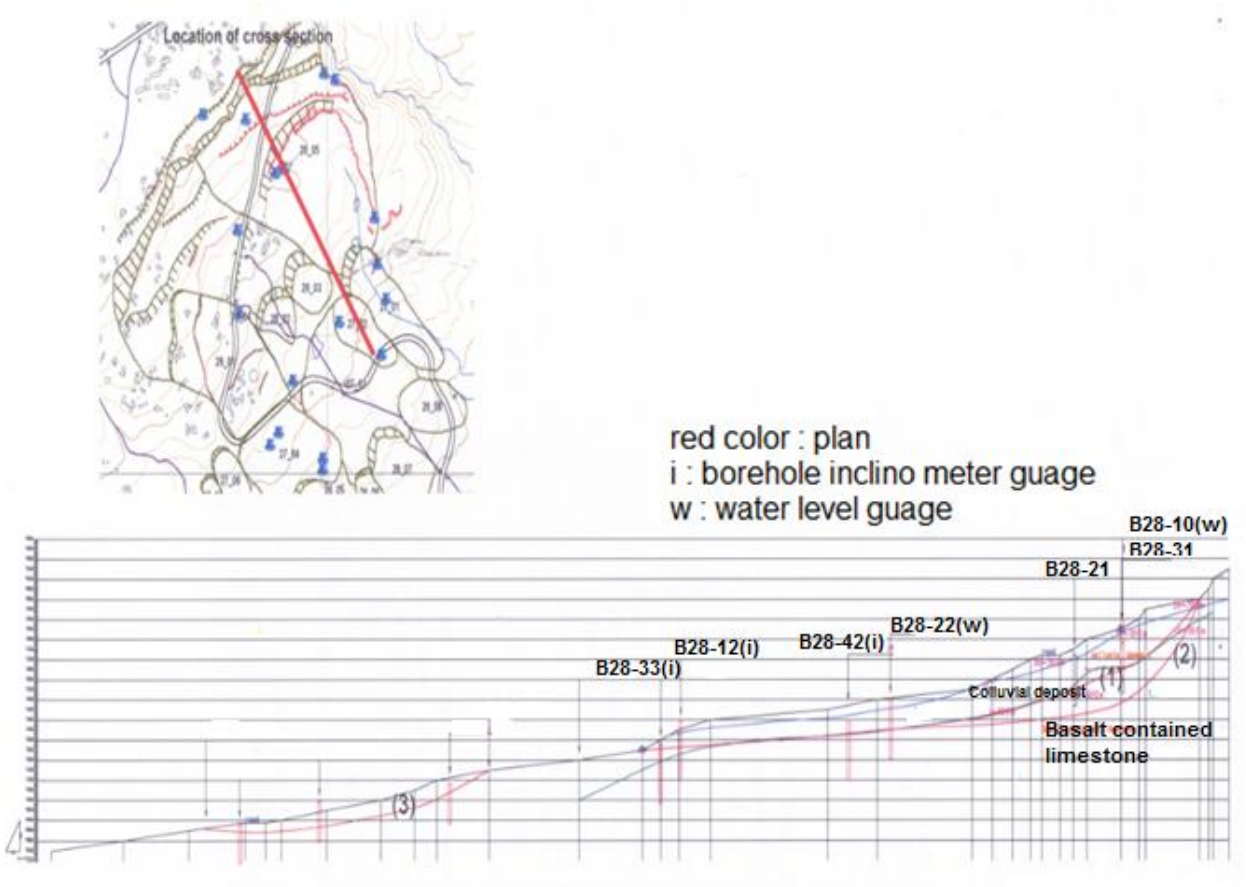

Figure 4-5 Landslide cross-section of L/S28 (3)

4.4. Stability analysis of landslides

The objectives of stability analysis are as follows;

• To calculate a safety factor and restraint stress to be needed for design of countermeasure

• To get soil parameters (c, φ) for back calculation

For this case obtaining the soil shear parameters(c, φ) for the rock/colluvial soil samples from Geotechnical laboratory test only and calculating directly safety factor is difficult so inverse stability analysis is performed to obtain the shear parameters and also to evaluate how much the factor of safety has been improved.

4.4.1. Safety factor in landslide analysis

Safety factor Fs is defined as the ratio of resistance force against landslide soil mass to force when landslide soil mass starts sliding along the slip surface.

$$Fs = \frac{\text{Resistance force against landslide soil mass}}{\text{Force when landslide soil mass starts sliding along the slip surface}}$$

If the slip surface and the distribution of pore water pressure are decided, Fs is obtained from cohesion c' and shear resistance angle Ø', which are constants for soil strength along slip surface, using the stability analysis formula.

Since Fs =1 when the land mass starts sliding, Fs is decided by considering the active state of the landslide for 0.95 < Fs< 1 if a landslide occurs.

Safety factor is defined for each landslide condition from Disaster Notebook edited by Japan Construction Engineer's Association (2010). In this Study this safety factor is used.

Table 4-5 Definition of safety factor for landslide

Safety factor	Landslide condition
Fs =0.95	Case in moving continuously anytime
Fs =0.98	Case in moving continuously for corresponding to rainfall etc.
Fs =1.00	Case in settling down of the landslide

4.4.2. Selecting parameters

The parameters for landslide stability analysis are as follows;

- γ_t : wet unit weight (wet density)
- u : pore water pressure
- c' : effective cohesion (as soil strength constant)
- ϕ' : effective shear resistance angle (as soil strength constant)

The volume and configuration of the landslide mass is determined by investigating and monitoring the landslide. Pore water pressure is derived from the critical pore water pressure when the land starts sliding with water level monitoring, cohesion and shear resistance angle (particularly shear resistance angle) are obtained from the shear test of the slip surface soil.

In the current investigation in Abay Gorge, the volume and configuration of the landslide and the wet unit weight γ_t are identified. The unidentified parameters are the pore water pressure u (particularly the critical pore water pressure), cohesion **c'** and shear resistance angle ϕ'. Because landslides frequently occur in the rainy season in the Abay area, cohesion c' is considered to be relatively small. Critical pore water pressure when the land mass starts' sliding in the rainy

season is necessary parameter because it is indispensable for ensuring accuracy of stability analysis and determining landslide countermeasures.

4.4.3. Stability analysis method

The landslide stability can be analyzed using different methods such as "Fellenius method", "Bishop method", "Spencer method", "Janbu method", "Morgenstern & Price method" etc. In this case the slip surfaces of both L/S00 and L/S28 landslide areas are non-circular (complex) slide. So the stability analysis is implemented by using Janbu's simplified method.

Janbu's simplified method

The Janbu's simplified method (1956) is applicable to noncircular slip surfaces as shown in figure below. In this method, the interslice forces are assumed to be horizontal and thus the shear forces are zero. Therefore, the expression obtained for the total normal force on the base of each slice is the same as that obtained by Bishop's method.

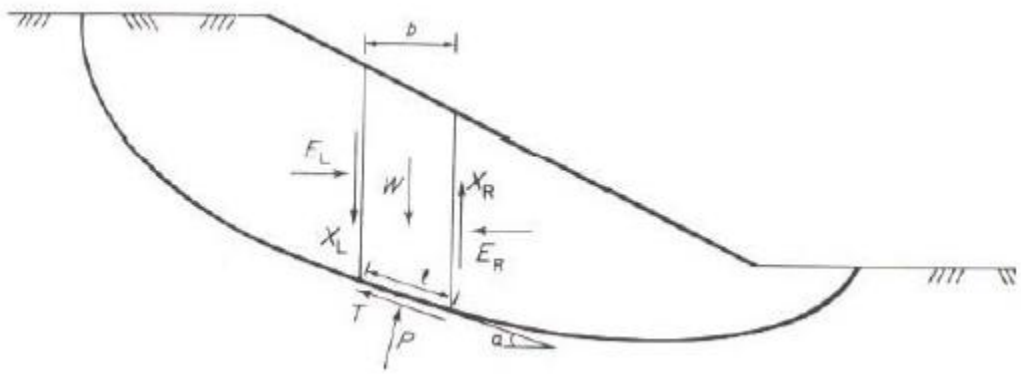

Resolving forces in the vertical direction gives

l = b secα
N' = N-ul

$$W = N' \cos a + ul \cos a + \frac{C'l}{Fs} \sin a + \frac{N'}{Fs} \tan \emptyset' \sin a$$

Therefore $$N' = \frac{W - ul \cos a - \frac{C'l}{Fs} \sin a}{\cos a + \frac{\tan \emptyset'}{Fs} \sin a}$$

By examining overall horizontal force equilibrium, a value of the factor of safety F_0 is obtained:

$$Fo = \frac{\sum (C'b + (N - ub) \tan \emptyset') ma}{\sum W \tan a} \quad \ldots\ldots\ldots\ldots (1)$$

Where

$$ma = \frac{\sec 2a}{1 + \tan \emptyset' \tan a / Fo}$$

Here, Fo: safety factor, c': cohesion, ϕ': shear resistance angle,

W: soil weight, u: pore water pressure, b: slice width,

$W = \gamma_t hb$, γ_t : soil unit weight, h : slice height,

l: slice length of slip surface, α: inclination angle of slip surface.

Using this method the back analysis Iteration is performed by assuming the shear strength parameters until the computed factor of safety (F_o) is equal to the safety factor at which the land slide moves ($F_{o=0.98}$).The computational flow chart is shown below.

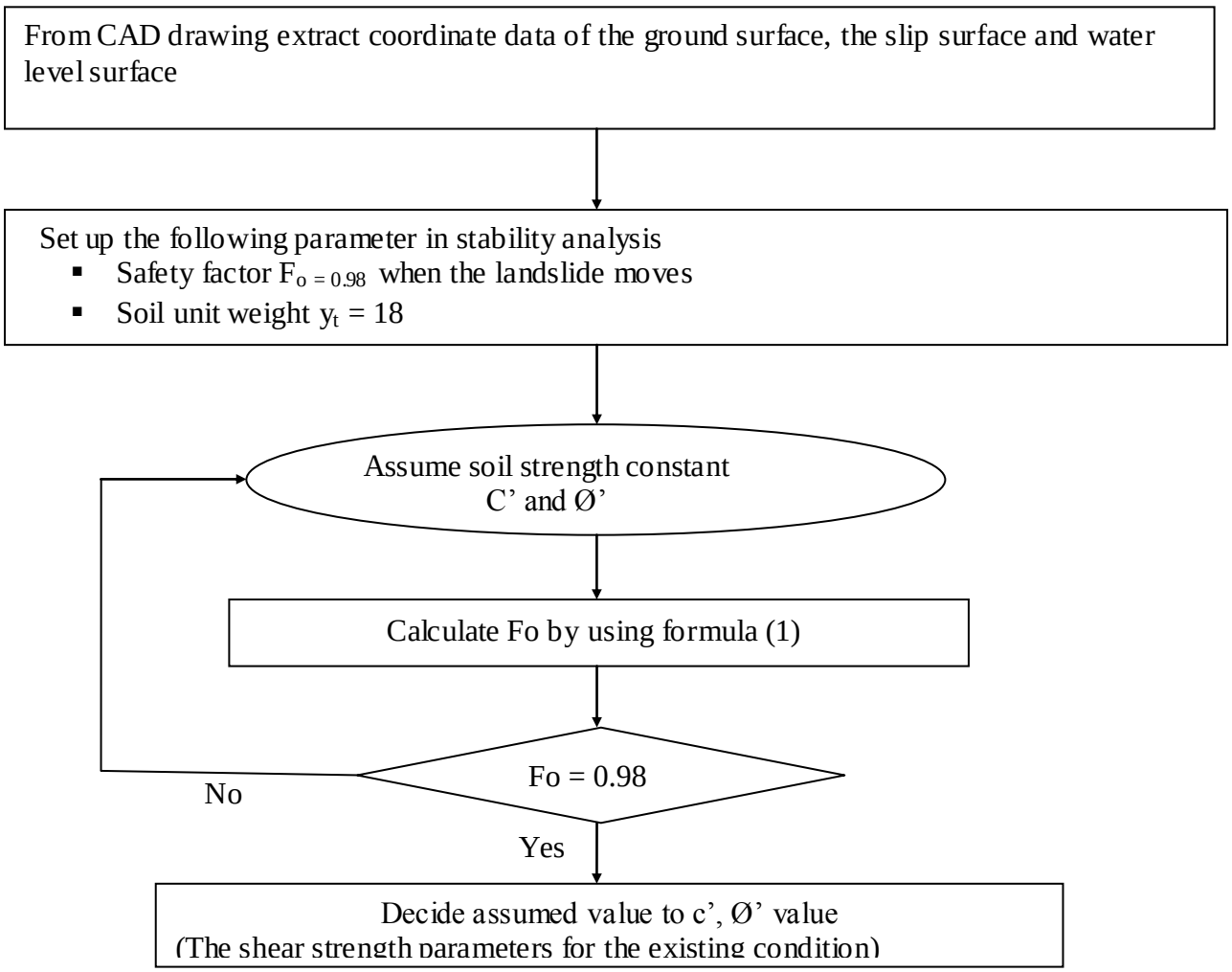

Figure 4-6 Shows back analysis procedure using Janbu's simplified method

The landslide block in each area is move, and the landslide activates when ground water rises during the rainy season. Therefore; it assigned c'≈0. Although there are damages on the road due to cracks and subsidence, the landslide is not moving so much. Therefore, the safety factor Fo

should be less than 1.0, it is reasonable to adopt 0.98 from Table 4.5 for the area. Soil in investigation area is silt with gravels, which is Cohesionless soil or loose gravel. From different literatures the average values of Unit weight of soils and rocks are given as follow:

Unit weight (γ) (recall that γ = ρg)	
"Rock"	26.5 kN/m3
Gravel soil	19 kN/m3
Sandy soil	16 kN/m3
Silty soil	15 kN/m3
Clay soil	18 kN/m3

Even if the mineralogy of soils and rocks are site dependent a more detail studied values of Unit weight from Japan Road Association is adopted from Table 4.6.for the Landslide Analysis. Therefore wet unit weight of a moving soil mass is determined as 18kN/m3 in the stability analysis in this study.

Table 4-6 Design value of soil constant in Japan (Japan Road Association (2010))

Classification		Soil state		Wet unit weight [kN/m3]
Embankment	Gravel and Sand with Gravel	Compacted		20
	Sand	Compacted	Wide grain size	20
			Sorted	19
	Sandy soil	Compacted		19
	Cohesive soil	Compacted		18
	Kanto Loam	Compacted		14
Natural	Gravel	Dense or wide grain size		20
		Not dense or sorted		18
	Sand with Gravel	Dense		21
		Not dense		19
	Sand	Dense or wide grain size		20
		Not dense or sorted		18
		Dense		19

Ground	Sandy soil	Not dense	17
	Cohesive soil	Hard (yield under strong pressure of a finger)	18
		A little soft (penetrate under pressure of a finger)	17
		Soft (penetrate under pressure of a finger easily)	16
	Clay and silt	Hard (yield under strong pressure of a finger)	17
		A little soft (penetrate under pressure of a finger)	16
		Soft (penetrate under pressure of a finger easily)	14
	Kanto Loam		14

For the Back Analysis of L/S00 in the CAD drawing below any necessary data for analysis is taken from the drawing such as slice length li(m) , average height of slice hav (m) , inclination angle of slip surface $\alpha i(o)$, starting slice height hi(m) , ending slice height hi+1(m) then using the formula (1) Fo is calculated by using the following spread sheet and assuming different value of ϕ ' till calculated Fo is equal to Fo=0.98 (Case in moving continuously for corresponding to rainfall).

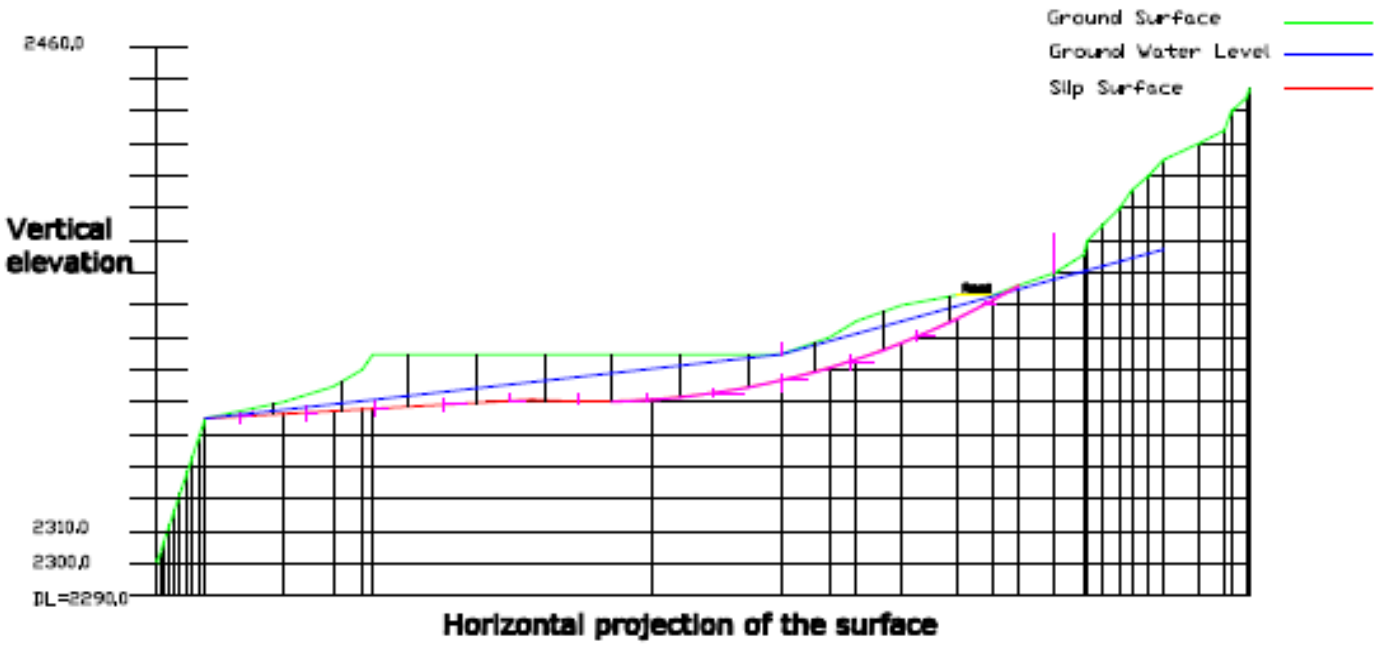

Figure 4-7 Shows Land slide block with Slice at L/S00

Table 4-7 Trial Back Analysis for L/S00

$$Fo = \frac{\sum(C'b + (N - ub)\tan \emptyset')ma}{\sum W \tan a}$$

$$ma = \frac{\sec 2a}{1 + \tan \emptyset' \tan a / Fo}$$

$$N' = \frac{W - ul\cos a - \frac{C'l}{Fs}\sin a}{\cos a + \frac{\tan \emptyset'}{Fs}\sin a}$$

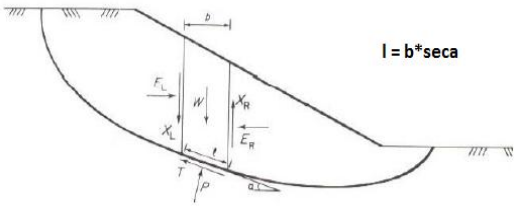

Assume	c'=	0
	Ø'=	19
	Fso=	0.98

Slice No.	c'	bi(m)	γt (KN/m3)	hav (m)	Wi=γt *havi*bi	αi(o)	αi(rad)	cosαi	secαi	$\sec^2\alpha i$	l (m)	tanαi	sinαi	Ø'(°)	Ø'(rad)
1	0	20	18	1.59	572.4	3	0.05236	0.99863	1.001372	1.002747	20.02745	0.052408	0.052336	19	0.331613
2	0	20	18	5.97	2149.2	3	0.05236	0.99863	1.001372	1.002747	20.02745	0.052408	0.052336	19	0.331613
3	0	20	18	12.465	4487.4	3	0.05236	0.99863	1.001372	1.002747	20.02745	0.052408	0.052336	19	0.331613
4	0	20	18	15.565	5603.4	3	0.05236	0.99863	1.001372	1.002747	20.02745	0.052408	0.052336	19	0.331613
5	0	20	18	14.585	5250.6	2.5	0.043633	0.999048	1.000953	1.001906	20.01905	0.043661	0.043619	19	0.331613
6	0	20	18	14.385	5178.6	0	0	1	1	1	20	0	0	19	0.331613
7	0	20	18	13.895	5002.2	4	0.069813	0.997564	1.002442	1.00489	20.04884	0.069927	0.069756	19	0.331613
8	0	20	18	11.705	4213.8	9	0.15708	0.987688	1.012465	1.025086	20.2493	0.158384	0.156434	19	0.331613
9	0	20	18	9.625	3465	14	0.244346	0.970296	1.030614	1.062164	20.61227	0.249328	0.241922	19	0.331613
10	0	20	18	10.44	3758.4	19	0.331613	0.945519	1.057621	1.118562	21.15241	0.344328	0.325568	19	0.331613
11	0	20	18	9.78	3520.8	24	0.418879	0.913545	1.094636	1.198229	21.89273	0.445229	0.406737	19	0.331613
12	0	20	18	3.875	1395	29	0.506145	0.87462	1.143354	1.307259	22.86708	0.554309	0.48481	19	0.331613

Cont..

tanØ'	hi(m)	hi+1(m)	Yw(KN/m3)	Ui=γw*hi	Ui+1=γw*hi+1	U=(Ui+Ui+1)/2	N = (w-ulcosα)/(cosα+(tanøsinα/0.98))	mα = $\sec^2\alpha/(1+(\tan\emptyset*\tan\alpha/0.98))$	W*tanα	((N-ub)tanøm$_a$)
0.344328	0	1.12	9.81	0	10.9872	5.4936	454.7884022	0.98461613	29.99821	116.9371879
0.344328	1.12	2.24	9.81	10.9872	21.9744	16.4808	1789.136441	0.98461613	112.6348	494.821977
0.344328	2.24	3.36	9.81	21.9744	32.9616	27.468	3872.143782	0.98461613	235.1747	1126.52512
0.344328	3.36	4.48	9.81	32.9616	43.9488	38.4552	4753.402504	0.98461613	293.6618	1350.798801
0.344328	4.48	6.07	9.81	43.9488	59.5467	51.74775	4155.907574	0.986768773	229.2461	1060.411476
0.344328	6.07	8.76	9.81	59.5467	85.9356	72.74115	3723.777	1	0	781.2635155
0.344328	8.76	9.75	9.81	85.9356	95.6475	90.79155	3117.554241	0.980792554	349.7879	439.6101098
0.344328	9.75	9.04	9.81	95.6475	88.6824	92.16495	2273.529671	0.971047683	667.4004	143.8512951
0.344328	9.04	8.28	9.81	88.6824	81.2268	84.9546	1673.376753	0.976610836	863.9215	-8.647370976
0.344328	8.28	7.3	9.81	81.2268	71.613	76.4199	2103.957128	0.997841514	1294.121	197.7531301
0.344328	7.3	4.23	9.81	71.613	41.4963	56.55465	2262.006997	1.036141636	1567.561	403.4786482
0.344328	4.23	0	9.81	41.4963	0	20.74815	937.8704842	1.094160765	773.2611	197.0052716
								Sum =	6416.769	6303.809162
								Fs0 =		**0.98239622**

Finally from this calculation Fso=0.98 at $\phi' = 19^{o}$ which implies the angle of friction of the site; for the rainy season at which c' is assumed to be zero.

In the above analysis the Colluvial deposit and Artificial backfill embankment is mainly composed of similar materials therefore the two units are assumed to be having similar unit weight and angle of internal friction.

For the Back Analysis of L/S28 in the CAD drawing below any necessary data for analysis is taken from the drawing such as slice length li(m) , average height of slice hav (m) , inclination angle of slip surface αi(o) , starting slice height hi(m) , ending slice height hi+1(m) then using the formula (1) Fo is calculated by using the following spread sheet and assuming different value of ϕ ' till calculated Fo is equal to Fo=0.98 (Case in moving continuously for corresponding to rainfall).

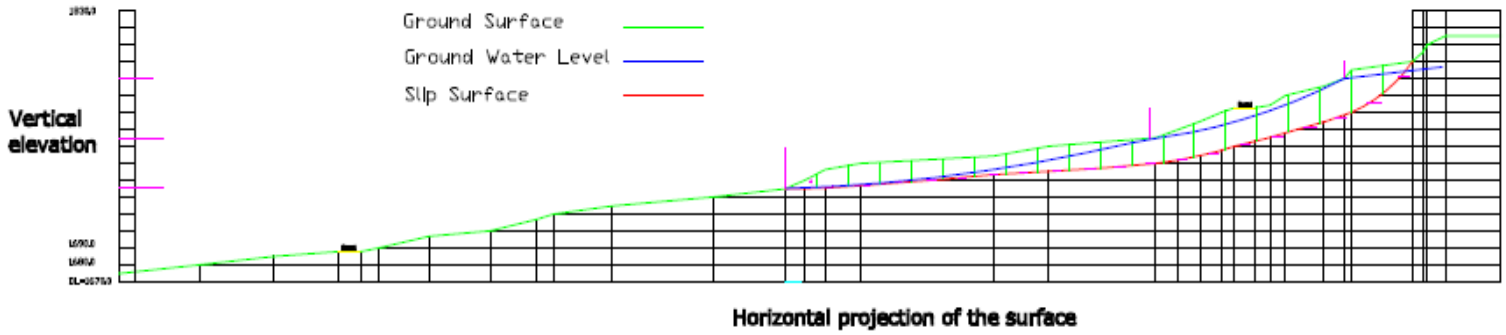

Figure 4-8 Shows Land slide block with Slice at L/S28

Table 4-8 Trial Back Analysis for L/S28

$$Fo = \frac{\sum(C'b + (N - ub)\tan \emptyset')ma}{\sum W \tan a}$$

$$ma = \frac{\sec 2a}{1 + \tan \emptyset' \tan a / Fo}$$

$$N' = \frac{W - ul\cos a - \frac{C'l}{Fs}\sin a}{\cos a + \frac{\tan \emptyset'}{Fs}\sin a}$$

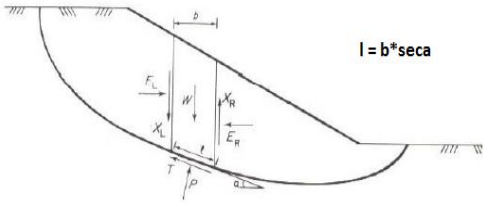

Assume	c'=	0														
	Ø'=	34.5														
	Fso=	0.98														
Slice No.	c'	bi(m)	γt (KN/m3)	hav (m)	Wi=γt *havi*bi	αi(o)	αi(rad)	cosαi	secαi	sec²αi	l (m)	tanαi	sinαi	Ø'(°)	Ø'(rad)	
1	0	20	18	3.65	1314	3	0.05236	0.99863	1.00137	1.00275	20.0274	0.05241	0.05234	34.5	0.60214	
2	0	20	18	10.83	3898.8	3	0.05236	0.99863	1.00137	1.00275	20.0274	0.05241	0.05234	34.5	0.60214	
3	0	20	18	13.1	4716	4	0.06981	0.99756	1.00244	1.00489	20.0488	0.06993	0.06976	34.5	0.60214	
4	0	20	18	12.56	4521.6	4	0.06981	0.99756	1.00244	1.00489	20.0488	0.06993	0.06976	34.5	0.60214	
5	0	20	18	12	4320	5	0.08727	0.99619	1.00382	1.00765	20.0764	0.08749	0.08716	34.5	0.60214	
6	0	20	18	11.46	4125.6	4	0.06981	0.99756	1.00244	1.00489	20.0488	0.06993	0.06976	34.5	0.60214	
7	0	20	18	10.9	3924	4	0.06981	0.99756	1.00244	1.00489	20.0488	0.06993	0.06976	34.5	0.60214	
8	0	20	18	12.8	4608	3	0.05236	0.99863	1.00137	1.00275	20.0274	0.05241	0.05234	34.5	0.60214	
9	0	20	18	14.76	5313.6	4	0.06981	0.99756	1.00244	1.00489	20.0488	0.06993	0.06976	34.5	0.60214	
10	0	20	18	14.82	5335.2	4	0.06981	0.99756	1.00244	1.00489	20.0488	0.06993	0.06976	34.5	0.60214	
11	0	20	18	14.88	5356.8	4	0.06981	0.99756	1.00244	1.00489	20.0488	0.06993	0.06976	34.5	0.60214	
12	0	20	18	14.94	5378.4	5	0.08727	0.99619	1.00382	1.00765	20.0764	0.08749	0.08716	34.5	0.60214	
13	0	20	18	17.7	6372	9	0.15708	0.98769	1.01247	1.02509	20.2493	0.15838	0.15643	34.5	0.60214	
14	0	20	18	21.1	7596	13	0.22689	0.97437	1.0263	1.0533	20.5261	0.23087	0.22495	34.5	0.60214	
15	0	20	18	21.4	7704	14	0.24435	0.9703	1.03061	1.06216	20.6123	0.24933	0.24192	34.5	0.60214	
16	0	20	18	19.25	6930	14	0.24435	0.9703	1.03061	1.06216	20.6123	0.24933	0.24192	34.5	0.60214	
17	0	20	18	21.36	7689.6	16	0.27925	0.96126	1.0403	1.08222	20.806	0.28675	0.27564	34.5	0.60214	
18	0	20	18	21.12	7603.2	16	0.27925	0.96126	1.0403	1.08222	20.806	0.28675	0.27564	34.5	0.60214	
19	0	20	18	20.46	7365.6	30	0.5236	0.86603	1.1547	1.33333	23.094	0.57735	0.5	34.5	0.60214	
20	0	20	18	7.48	2692.8	45	0.7854	0.70711	1.41421	2	28.2843	1	0.70711	34.5	0.60214	

Cont..

tanØ'	hi(m)	hi+1(m)	Yw(KN/m3)	Ui=Yw*hi	Ui+1=Yw*hi+1	U=(Ui+Ui+1)/2	N = (w-ulcosα)/(cosα+(tanøsinα/0.98))	mα = sec²α/(1+(tanø*tanα/0.98))	W*tanα	((N-ub)tanømα)
0.68728	0	0.69	9.81	0	6.7689	3.38445	1203.777784	0.967198222	68.8638	755.2001609
0.68728	0.69	0.65	9.81	6.7689	6.3765	6.5727	3638.776694	0.967198222	204.327	2331.44689
0.68728	0.65	0.61	9.81	6.3765	5.9841	6.1803	4388.400264	0.957913518	329.775	2807.751701
0.68728	0.61	0.94	9.81	5.9841	9.2214	7.60275	4175.450197	0.957913518	316.181	2648.825244
0.68728	0.94	1.52	9.81	9.2214	14.9112	12.0663	3857.567346	0.949402337	377.951	2359.619712
0.68728	1.52	2.3	9.81	14.9112	22.563	18.7371	3584.245219	0.957913518	288.49	2112.994804
0.68728	2.3	3.56	9.81	22.563	34.9236	28.7433	3200.365764	0.957913518	274.393	1728.512789
0.68728	3.56	5.58	9.81	34.9236	54.7398	44.8317	3584.707139	0.967198222	241.495	1786.861463
0.68728	5.58	8.16	9.81	54.7398	80.0496	67.3947	3789.54969	0.957913518	371.563	1607.477991
0.68728	8.16	10.77	9.81	80.0496	105.6537	92.85165	3323.667129	0.957913518	373.074	965.5669689
0.68728	10.77	13.45	9.81	105.654	131.9445	118.7991	2848.410328	0.957913518	374.584	311.0258922
0.68728	13.45	14.92	9.81	131.945	146.3652	139.15485	2454.61052	0.949402337	470.549	-214.3394481
0.68728	14.92	14.94	9.81	146.365	146.5614	146.4633	3137.182062	0.922606112	1009.23	131.8374151
0.68728	14.94	14.69	9.81	146.561	144.1089	145.33515	4142.013441	0.906525095	1753.67	769.6446505
0.68728	14.69	15.24	9.81	144.109	149.5044	146.80665	4182.496246	0.904080931	1920.82	774.4372862
0.68728	15.24	16.72	9.81	149.504	164.0232	156.7638	3328.830037	0.904080931	1727.84	120.2662739
0.68728	16.72	19.56	9.81	164.023	191.8836	177.9534	3577.555876	0.901029059	2204.96	11.44880397
0.68728	19.56	20.5	9.81	191.884	201.105	196.4943	3181.548063	0.901029059	2180.18	-463.415837
0.68728	20.5	11.15	9.81	201.105	109.3815	155.24325	3501.938606	0.949059351	4252.53	258.9993677
0.68728	11.15	0	9.81	109.382	0	54.69075	1329.158194	1.175566715	2692.8	190.1442671
								Sum =	21433.3	20994.3064
								Fs0 =		**0.979518922**

Finally from this calculation Fso = at $\phi' = 34.5^{o}$ which implies the angle of friction of the site; for the rainy season at which c' is assumed to be zero.

In this analysis the computed shear strength parameters (Ø') are under the interval of a Literature value of the geology so Pore pressure is responsible for initiation of land slide this can be assessed by controlling the effect of groundwater by assuming effective surface and subsurface drainage work so c'=0 since material in the slip surface is Cohesion less Soil and Pore water pressure (U=0) by effective utilization of surface and subsurface drainage work, Ground water table is blow slip surface then improved FS can be calculated as:-

$$Fo = \frac{\sum(\cancel{C}\cancel{b} + (N - \cancel{u}\cancel{b})\tan\emptyset')ma}{\sum W \tan a}$$

$$ma = \frac{\sec 2a}{1 + \tan\emptyset' \tan a / Fo}$$

$$N' = \frac{W - ul\cos a - \frac{C'l}{Fs}\sin a}{\cos a + \frac{\tan\emptyset'}{Fs}\sin a}$$

Table 4-9 Assessment Analysis for L/S00 to know the improvement of FS by the proposed Countermeasure.

Assum	c'=	0														
	Ø'=	19														
	Improved Fso=	2.44														
Slice No.	c'	bi(m)	γt (KN/m3)	hav (m)	Wi=γt *havi*bi	αi(o)	αi(rad)	cosαi	secαi	sec²αi	l (m)	tanαi	sinαi	Ø'(°)	Ø'(rad)	
1	0	20	18	1.59	572.4	3	0.05236	0.99863	1.001372	1.002747	20.02745	0.052408	0.052336	19	0.331613	
2	0	20	18	5.97	2149.2	3	0.05236	0.99863	1.001372	1.002747	20.02745	0.052408	0.052336	19	0.331613	
3	0	20	18	12.465	4487.4	3	0.05236	0.99863	1.001372	1.002747	20.02745	0.052408	0.052336	19	0.331613	
4	0	20	18	15.565	5603.4	3	0.05236	0.99863	1.001372	1.002747	20.02745	0.052408	0.052336	19	0.331613	
5	0	20	18	14.585	5250.6	2.5	0.043633	0.999048	1.000953	1.001906	20.01905	0.043661	0.043619	19	0.331613	
6	0	20	18	14.385	5178.6	0	0	1	1	1	20	0	0	19	0.331613	
7	0	20	18	13.895	5002.2	4	0.069813	0.997564	1.002442	1.00489	20.04884	0.069927	0.069756	19	0.331613	
8	0	20	18	11.705	4213.8	9	0.15708	0.987688	1.012465	1.025086	20.2493	0.158384	0.156434	19	0.331613	
9	0	20	18	9.625	3465	14	0.244346	0.970296	1.030614	1.062164	20.61227	0.249328	0.241922	19	0.331613	
10	0	20	18	10.44	3758.4	19	0.331613	0.945519	1.057621	1.118562	21.15241	0.344328	0.325568	19	0.331613	
11	0	20	18	9.78	3520.8	24	0.418879	0.913545	1.094636	1.198229	21.89273	0.445229	0.406737	19	0.331613	
12	0	20	18	3.875	1395	29	0.506145	0.87462	1.143354	1.307259	22.86708	0.554309	0.48481	19	0.331613	

Cont..

tanØ'	hi(m)	hi+1(m)	Yw(KN/m3)	Ui=Yw*hi	Ui+1=Yw*hi+1	U=(Ui+Ui+1)/2	N = (w-ulcosα)/(cosα+(tanøsinα/Fso))	mα = sec²α/(1+(tanø*tanα/Fso))	W*tanα	((N-ub)tanøm$_a$)
0.344328	0	0	9.81	0	0	0	568.9775581	0.995385032	29.99821	195.0105445
0.344328	0	0	9.81	0	0	0	2136.349699	0.995385032	112.6348	732.2094031
0.344328	0	0	9.81	0	0	0	4460.569347	0.995385032	235.1747	1528.80908
0.344328	0	0	9.81	0	0	0	5569.896661	0.995385032	293.6618	1909.018318
0.344328	0	0	9.81	0	0	0	5223.418912	0.995770995	229.2461	1790.961216
0.344328	0	0	9.81	0	0	0	5178.6	1	0	1783.134978
0.344328	0	0	9.81	0	0	0	4965.416514	0.99507048	349.7879	1701.301869
0.344328	0	0	9.81	0	0	0	4173.054133	1.002674968	667.4004	1440.741425
0.344328	0	0	9.81	0	0	0	3449.699788	1.026062805	863.9215	1218.784995
0.344328	0	0	9.81	0	0	0	3790.765321	1.066728342	1294.121	1392.363357
0.344328	0	0	9.81	0	0	0	3626.164489	1.127394684	1567.561	1407.652109
0.344328	0	0	9.81	0	0	0	1479.266395	1.212419534	773.2611	617.5486387
								Sum =	6416.769	15717.53593
								Fs0 =		2.449447229

Since the improved Fs >1 for L/S00 the proposed counter measure which is controlling the ground water table blow the slip surface by using different surface and sub surface drainage mechanisms will be effective to improve the stability.

Table 4-10 Assessment Analysis for L/S28 to know the improvement of FS by the proposed Countermeasure.

Assum	c'=	0													
	Ø'=	34.5													
	Improved Fso=	3.52													
Slice No.	c'	bi(m)	Yt (KN/m3)	hav (m)	Wi=Yt *havi*bi	αi(o)	αi(rad)	cosαi	secαi	sec²αi	l (m)	tanαi	sinαi	Ø'(°)	Ø'(rad)
1	0	20	18	3.65	1314	3	0.05236	0.99863	1.001372	1.002747	20.02745	0.052408	0.052336	34.5	0.602139
2	0	20	18	10.83	3898.8	3	0.05236	0.99863	1.001372	1.002747	20.02745	0.052408	0.052336	34.5	0.602139
3	0	20	18	13.1	4716	4	0.069813	0.997564	1.002442	1.00489	20.04884	0.069927	0.069756	34.5	0.602139
4	0	20	18	12.56	4521.6	4	0.069813	0.997564	1.002442	1.00489	20.04884	0.069927	0.069756	34.5	0.602139
5	0	20	18	12	4320	5	0.087266	0.996195	1.00382	1.007654	20.0764	0.087489	0.087156	34.5	0.602139
6	0	20	18	11.46	4125.6	4	0.069813	0.997564	1.002442	1.00489	20.04884	0.069927	0.069756	34.5	0.602139
7	0	20	18	10.9	3924	4	0.069813	0.997564	1.002442	1.00489	20.04884	0.069927	0.069756	34.5	0.602139
8	0	20	18	12.8	4608	3	0.05236	0.99863	1.001372	1.002747	20.02745	0.052408	0.052336	34.5	0.602139
9	0	20	18	14.76	5313.6	4	0.069813	0.997564	1.002442	1.00489	20.04884	0.069927	0.069756	34.5	0.602139
10	0	20	18	14.82	5335.2	4	0.069813	0.997564	1.002442	1.00489	20.04884	0.069927	0.069756	34.5	0.602139
11	0	20	18	14.88	5356.8	4	0.069813	0.997564	1.002442	1.00489	20.04884	0.069927	0.069756	34.5	0.602139
12	0	20	18	14.94	5378.4	5	0.087266	0.996195	1.00382	1.007654	20.0764	0.087489	0.087156	34.5	0.602139
13	0	20	18	17.7	6372	9	0.15708	0.987688	1.012465	1.025086	20.2493	0.158384	0.156434	34.5	0.602139
14	0	20	18	21.1	7596	13	0.226893	0.97437	1.026304	1.0533	20.52608	0.230868	0.224951	34.5	0.602139
15	0	20	18	21.4	7704	14	0.244346	0.970296	1.030614	1.062164	20.61227	0.249328	0.241922	34.5	0.602139
16	0	20	18	19.25	6930	14	0.244346	0.970296	1.030614	1.062164	20.61227	0.249328	0.241922	34.5	0.602139
17	0	20	18	21.36	7689.6	16	0.279253	0.961262	1.040299	1.082223	20.80599	0.286745	0.275637	34.5	0.602139
18	0	20	18	21.12	7603.2	16	0.279253	0.961262	1.040299	1.082223	20.80599	0.286745	0.275637	34.5	0.602139
19	0	20	18	20.46	7365.6	30	0.523599	0.866025	1.154701	1.333333	23.09401	0.57735	0.5	34.5	0.602139
20	0	20	18	7.48	2692.8	45	0.785398	0.707107	1.414214	2	28.28427	1	0.707107	34.5	0.602139

Cont..

tanØ'	hi(m)	hi+1(m)	ϒw(KN/m3)	Ui=ϒw*hi	Ui+1=ϒw*hi+1	U=(Ui+Ui+1)/2	N = (w-ulcosα)/(cosα+(tanøsinα/Fso))	mα = $sec^2α/(1+(tanø*tanα/Fso))$	W*tanα	((N-ub)tanøm$_s$)
0.687281	0	0	9.81	0	0	0	1302.475509	0.992589768	68.86382	888.5332241
0.687281	0	0	9.81	0	0	0	3864.605413	0.992589768	204.3274	2636.387621
0.687281	0	0	9.81	0	0	0	4663.839522	0.991354568	329.7748	3177.656306
0.687281	0	0	9.81	0	0	0	4471.589649	0.991354568	316.1811	3046.668946
0.687281	0	0	9.81	0	0	0	4263.668915	0.990730425	377.951	2903.175469
0.687281	0	0	9.81	0	0	0	4079.969536	0.991354568	288.4901	2779.842844
0.687281	0	0	9.81	0	0	0	3880.599297	0.991354568	274.3928	2644.004102
0.687281	0	0	9.81	0	0	0	4567.585345	0.992589768	241.495	3115.952128
0.687281	0	0	9.81	0	0	0	5254.829874	0.991354568	371.5631	3580.32115
0.687281	0	0	9.81	0	0	0	5276.190971	0.991354568	373.0735	3594.875301
0.687281	0	0	9.81	0	0	0	5297.552068	0.991354568	374.5839	3609.429452
0.687281	0	0	9.81	0	0	0	5308.2678	0.990730425	470.549	3614.453458
0.687281	0	0	9.81	0	0	0	6257.904554	0.994336177	1009.226	4276.578887
0.687281	0	0	9.81	0	0	0	7459.551236	1.007868362	1753.675	5167.1471
0.687281	0	0	9.81	0	0	0	7571.267784	1.012857187	1920.823	5270.491688
0.687281	0	0	9.81	0	0	0	6810.60303	1.012857187	1727.843	4740.979673
0.687281	0	0	9.81	0	0	0	7575.363781	1.024844812	2204.957	5335.755393
0.687281	0	0	9.81	0	0	0	7490.247334	1.024844812	2180.183	5275.803086
0.687281	0	0	9.81	0	0	0	7643.434725	1.198256516	4252.531	6294.665725
0.687281	0	0	9.81	0	0	0	3186.106181	1.673289725	2692.8	3664.086361
								Sum =	21433.28	75616.80792
								Fs0 =		3.528008631

Similarly the improved Fs >1 for L/S28 the proposed counter measure which is controlling the ground water table blow the slip surface by using different surface and sub surface drainage mechanisms will be effective to improve the stability.

5. CONCLUSION AND RECOMMENDATION

5.1. Conclusion

From the findings of this study the following conclusions are drawn

1. The record of landslide occurrence in the Abay Gorge shows that most landslides are concentrated mainly in July to September during the rainy season. In all investigated landslide areas, landslides are triggered by rising ground water in the rainy season. The rising of ground water table is due to infiltration of surface run off, so controlling of the infiltration process using different remedial techniques will minimize the sub surface problem. In addition geographical features, geology, or natural conditions are also causes of landslide in the Abay Gorge.
2. Even if shear strength parameters of a soil is directly determine from the shear test; for this case the stratum is composed of Rocks and Colluvial deposits so it is difficult to obtain shear parameters from direct test under the scope of this study. rather the indirect approach is followed to obtain angle of friction of the presumed slip surface by using inverse analysis of stability using Janbu's simplified method as Ø'=19 for L/S00 and Ø'=34.5 for L/S28 this soil constants can be used in countermeasures design as primary input data.
3. Since the slope failure in the study area is morphological using remedial works such as Retaining walls, Sheet Piles, Gabions …etc could not be feasible to control the problem. Rather using different surface and subsurface Ground water control mechanism such as drainage well, drainage tunnel, horizontal drain by drilling and using network of ditches are capable to handle the slide.
4. The stability analysis is used to evaluate the effectiveness of the proposed countermeasure by calculating the factor of safety (FS). until FS >1 additional remedial should be performed, for L/S00 and L/S28 surface and subsurface drainage work to control Ground water fluctuation is the effective method since the computed FS after the drawdown of phreatic line below slip surface is FS=2.44 for L/S00 and FS=3.52 for L/S28 which is stable.

5.2. Recommendation

- For the future development and strengthening of this study additional factor such as; Morphological mode of failure which is more hazardous than localized failure may also be considered.
- The presumed slip surface in this study is determine from borehole investigations tracking along the route of the road only but in future study taking additional borehole investigation by offsetting left and right to the road is also give a more clear slip surface for the sliding area.

LIST OF REFERENCES

1. Almaz,G.& etal,1994, "A report on Engineering Geological studies of part of Blue nile gorge (Gohatsion-Dejen)", Addis Ababa.

2. Awoke,S.,2006, " Further investigation of road failures constructed on expansive soils of central Ethiopia Addis Ababa-Jimma road as a case study", Thesis for Master of Science Degree, Addis Ababa University.

3. Japan International Cooperation Agency & Geological Survey of Ethiopia, 2011, "The project for developing countermeasures against Landslide in the Abay River Gorge."

4. Lulseged, A & etal, 2009, "Geotechnical Aspects and Stability of Road Cuts in the Blue Nile Basin, Ethiopia", Springer Science+Business Media B.V.

5. Ministry of Water Resources, 2010, "River Basins of Ethiopia."

6. Shiferaw,A., 2009, "Slope instability and hazard zonation mapping using Remote Sensing and GIS technique in Abay gorge (Gohatsion- Dejen), central Ethiopia", Thesis for Master of Science Degree, Addis Ababa University.

7. The Japan Society of Landslide, 1969-2002, "National Conference of Landslide Control."

8. Lulseged,A.& Hiromitsu. , 2003, "Slope failures in the Blue Nile basin, as seen from landscape evolution perspective", Elsevier Science B.V.

DECLARATION

I, the undersigned, declare that this thesis is my original work performed under the supervision of my research advisor Messele Haile (Assist.Prof) and has not been presented as a thesis for a degree in any other university. All sources of materials used for this thesis have also been duly acknowledged.

Name: Adane Amare Bitew
Signature

Place: Addis Ababa institute of Technology
School of Graduate Studies,
Department of Civil Engineering,
Addis Ababa.
July, 2013